

Experimental research project on bolted connections in bearing for high strength steel

Stevin: 6-05-03

June 2005

S. Teixeira de Freitas



Stevin: 6-05-03

**Experimental research project on bolted
connections in bearing for high strength steel**

June 2005

S. Teixeira de Freitas

c1253743 - Exchange Student

PRINCIPAL:

Delft University of Technology

Projectnr.:

Date 07-02-05/01-07-05

KEYWORDS:

Bolted connections, Bearing, High Strength Steel

TU-DELFT

Delft University of Technology

Faculty of Civil Engineering and Geosciences

Stevin II Laboratory, Section Steel- en Timber Structures

P.O. Box 5049; 2600 GA DELFT

tel. +31 15 278 4005 / + 31 15 278 2329

fax +31 15 278 2308

Preface

This research has been carried out during five months in the framework of the Socrates-Erasmus program in the Research Group of Steel and Timber Structures of the Section on Buildings and Civil Engineering Structures at the Faculty of Civil Engineering and Geosciences of the Delft University of Technology.

I am a civil engineering student from Portugal, where the whole civil engineering course of study lasts for five years. This project was carried out in my last semester of the course of study.

Being an exchange student is a way to get different experience and study in the areas we enjoy the most, fulfilling any possible gaps and capturing a whole new experience in our formation process. The use of steel in Portugal is far less common than in the northern countries of Europe. The Portuguese course of study is more orientated to stability, paying less attention to the study of connections. Making this research project gave me knowledge about connections, experimental programmes and also helped me to discover a little more about scientific research.

I would like to express my gratitude to Prof. Ir. Frans S. K. Bijlaard and Ir. Peter de Vries for their support and knowledge.

The daily support of Edwin Scharp and Gerrit van der Ende is most appreciated. I would like also to thank John Hermsen, Peter Stolle and Liesbeth Eekhout for their support whenever necessary.

A special word of gratitude to Prof. Dinar Camotim, from Instituto Superior Técnico, without whom this marvellous experience would not have been possible.

Finally, I would like to thank my father Manuel Freitas and my mother Conceição Freitas for their love and daily support. To the friendship of my very special friend Joana Pragosa and for the love, support and patience of João Fernandes.

Delft, 27 June 2005
Sofia Teixeira de Freitas

Table of Contents

Abstract

List of symbols

1 – Aim of the study	1
2 – Introduction	2
3 – Literature review	5
4 – Design rules for bearing type connections – EC3 Part 1.8.....	8
4.1 – Test specimen design resistance	15
5 – Test specimens	17
5.1 One bolt test specimens	19
5.1.1 Bearing of the plate – Series A	19
5.1.2 Bearing of the bolt – Series B	21
5.2 Two bolts tests specimens – Series D	22
6 – Materials, Specimens and Experimental Programme.....	25
6.1 – Materials	25
6.1.1 – Tension tests on the bolts.....	25
6.1.2 – Tension test of the steel plates	27
6.2 – Geometrical properties of the specimens	27
6.3 – Experimental Procedure	29
7 – Results	32
7.1 – Test Results and Observations	32
7.2 – Comparison with EC3	37
8 – Statistical evaluation	41
8.1 – Standard Procedure	41
8.3 – Proposed correction for the k_t factor.....	46
9 - Conclusions.....	48
10 - References.....	49
11 - Bibliography	51
ANNEX A – Design calculation procedure of test specimens.....	52
A.1 – Series A	52
A.2 – Series B	55
A.3 – Series D	59
ANNEX B: Material Tests	64
B.1 - Tension test on the bolts	64
B.1.1 – Group 1: M24 10.9.....	64
B.1.2 – Group 2: M27 8.8.....	66

B.1.3 – Group 3: M27 10.9.....	67
B.2 – Tension tests of the steel plates	68
ANNEX C: Actual properties of the test specimens	69
ANNEX D: Test results	70
D.1 – Test specimen A1010.....	70
D.2 – Test specimen A1210.....	72
D.3 – Test specimen A1012.....	74
D.4 – Test specimen A1212.....	76
D.5 – Test specimen A1015.....	78
D.6 – Test specimen A1215.....	80
D.7 – Test specimen A1020.....	82
D.8 – Test specimen A1220.....	84
D.9 – Test specimen A2020.....	86
D.10 – Test specimen B3025	88
ANNEX E: Statistical evaluation.....	91
E.1 – Two groups of tests results: Group I $e_2 \leq 1.2d_0$ and Group II $e_2 \geq 1.5d_0$	91
E.2 – One group of tests results	93

List of Figures

Figure 2.1 – Force components in the bearing bolts (1) and preloaded bolts (2) [2].	2
Figure 2.2 – Possible failure mechanism of bolted joint loaded in shear [3].	3
Figure 2.3 – Stress –strain curve of mild steel and high strength steel.	4
Figure 3.1 – Reduction factor for bearing resistance in relation to the bolt spacing and edge distance.	5
Figure 4.1 – Symbols for spacing in a joint.	9
Figure 4.2 – Shear-out of the plate.	9
Figure 4.3 – Reduction factors for bearing design load in relation to the bolt spacing ($p_1 - \alpha d$ and $p_2 - k_1$), end distance ($e_1 - \alpha d$) and edge distance ($e_2 - k_1$).	10
Figure 4.4 – Net-section failure mechanism.	11
Figure 4.5 – Stress distribution in the neighbourhood of the hole [17].	11
Figure 4.6 – Values for the <i>theoretical stress-concentration factor</i> in the net cross section [17].	12
Figure 4.7 – Application example of the design resistance of a group of fasteners given in clause 3.7(1) of Part 1.8, EC3 [1].	13
Figure 4.8 – Distribution of bolt shear loads in a long joint (elastic range – full line; plastic range – dashed line).	14
Figure 4.9 – Distance L_j .	14
Figure 5.1 – One bolt test specimens of double lap joints.	17
Figure 5.2 – Functions to be validated for high strength steels.	18
Figure 5.3 – Values of the reduction factor α_b where the bearing of the bolt is the failure mode – red line.	18
Figure 5.4 – Graph of the reduction factor α_b where the red cross symbolises the test specimen of series B.	21
Figure 5.5 – Graph which gives the number of cases in each failure mechanism with different edge distances (e_2).	23
Figure 6.1 – Bolt specimen before testing.	25
Figure 6.2 – Test device for the tension test on the bolts.	25
Figure 6.3 – Graph of the tension test on bolt M24 10.9.	26
Figure 6.4 – Bolts specimens.	26
Figure 6.5 – Comparison of the necking on the three groups of specimens (from the left to the right: M24 10.9, M27 8.8, and M27 10.9).	27
Figure 6.6 – Specimen geometry and notification.	28
Figure 6.7 – Specimen and measuring devices.	30
Figure 6.8 – Illustration of the test set-up.	31
Figure 7.1 – Load-displacement curves for the two different failure mechanisms occurred in the test.	32
Figure 7.2 – Failure of the inner plates of the test joint of specimens A1212_2 and A1210_2.	33
Figure 7.3 – Load-displacement curves of specimens with the same edge distance and different end distance.	33

Figure 7.4 – Load-displacement curves of specimens with the same end distance and different edge distance.....	34
Figure 7.5 – Bearing and shear deformations of the inner plate after failure (A1220_3).....	35
Figure 7.6 – Yield lined in the end of the inner plate of specimen A1015_2.	35
Figure 7.7 – Shear fracture with splitting and without splitting present on test specimens A1010_1 and A1220_1, respectively.	36
Figure 7.8 – Shear and tensile fracture present on test specimen A2020_1.....	36
Figure 7.9 – Bearing deformations on B3025_1 test specimen.....	37
Figure 7.10 – Load-displacement curves for A1010_2 test specimen with high distance between the predicted value and experimental value for the maximum bearing load of the connection.	39
Figure 7.11 – Load-displacement curves for A1020_2 test specimen with low distance between the predicted value and experimental value for the maximum bearing load of the connection.	39
Figure 7.12 – Load-displacement curves for A1210_2 test specimen.	40
Figure 8.1 – re - rt diagram.	42
Figure 8.2 – re - rt diagram with the mean value correction line $r_e = \bar{b}_{(r)} r_t$	43
Figure 8.3 – Values for the factor k_l	47
Figure 8.4 – Comparison with previous corrections available in literature.	47

List of Tables

Table 5.1 – Nominal values of the yield strength f_y and the lower and the higher ultimate tensile strength f_u for steel grade S690 [18].	19
Table 5.2 – Nominal values of the yield strength f_{yb} and the ultimate tensile strength f_{ub} for bolts [1].	19
Table 5.3 – Diameters and areas of bolts used in this investigation.	19
Table 5.4 – Resistance and failure mechanism of test joint (blue) and strongest joint (yellow) in series A.	20
Table 5.5 - Resistance and failure mechanism of test joint (blue) in the series B.	22
Table 5.6 – Resistance of each end and inner bolt varying the end and pitch distance in the joint (yellow – test specimens chose).	23
Table 5.7 – Resistance and failure mechanism of test joint (blue) and strongest joint (yellow) in the series D.	24
Table 6.1 - Average characteristics values for the bolts.	26
Table 6.2 - Average characteristics values for the steel plates.	27
Table 6.3 – Geometrical characteristics of the specimens (nominal values).	28
Table 6.4 – Actual properties of Series B test specimens (yellow cells – the design value was $0.85 < 1.0$).	28
Table 7.1 – Average values of the test results for each specimen type.	32
Table 7.2 – Steel grades used in this investigation (S690).and in Kim and Yura investigation (~S235 and ~S460).	34
Table 7.3 – Displacement at the maximum force of two test specimens using different steel grades.	35
Table 7.4 – Test results for specimens with bearing failure.	37
Table 7.5 – Test results for the specimen with net section failure.	37
Table 8.1 – Mean correction factor and number of test results used.	42
Table 8.2 - Coefficient of variation V_δ for each group.	43
Table 8.3 – Values for the calculation of r_k .	44
Table 8.4 – Initial estimative for the partial safety factor.	45
Table 8.5 – Values of k_c , γ_R^* , γ_{M2}/γ_R^* obtained for each Group I and II.	45
Table 8.6 – Comparison between the present rules in EC3 and the proposed ones.	46

Abstract

The rules described in Eurocode 3 for bolts in bearing are dependent on end-distance, edge-distance and pitch for 8.8 and 10.9 bolt classes and are allowed to be used in plates of steel grade up to S700. However, these rules are based on test data of steel plates in mild steel and not for high strength steel, 8.8 and 10.9 steel classes in plates of steel grade up to S460. In fact "strong" bolts in "weak" steel plates. Steel grades of S690, S960 and even higher are being used in civil engineering structures more and more. So, in these cases "weak" bolts in "strong" steel plates.

In this study, a series of tests were carried out using specimens designed according to the rules of Eurocode 3 Part 1-8 "Design of Joints", in order to investigate whether or not those rules are adequate to high strength steels.

The experimental programme consisted in ten different types of specimens of one bolt joints made with steel grade S690. The end and edge distance varied. In total, thirty test were performed (three tests per each different type of specimens).

The test results showed that the rules given by Eurocode 3 are conservative using steel grade S690, mainly when edge distance is smaller than $1.5 d_0$. Therefore, a corrected function for the k_1 factor of the bearing resistance formula given by EC3 is proposed based on a statistical evaluation according to Annex D of EN1990: Basis of Design (formerly Annex Z of Eurocode 3: Design of Steel Structures).

This correction was made in the k_1 factor, since the main differences between experimental values and theoretical values were found in tests specimens with different edge distances. The minimum values for the edge and end distances can also be reduced from $1.2d_0$ to $1.0d_0$ in case of steel grade S690.

Further investigations are necessary to see if this also holds to mild steels (from S235 to S700) as well.

List of symbols

d	nominal bolt diameter;
d_0	hole diameter for a bolt;
e_1	end distance from the centre of a fastener hole to the adjacent end of any part, measured in the direction of load transfer;
e_2	edge distance from the centre of a fastener hole to the adjacent edge of any part, measured in the perpendicular direction of load transfer;
p_1	spacing between centres of fasteners in a line in the direction of load transfer;
p_2	spacing measured perpendicular to the load transfer direction between centres of fasteners;
C_1	clear end distance;
C_2	clear edge distance;
t	thickness of the plate;
A	gross cross-section area of a bolt;
A_s	tensile stress area of the bolt;
f_y	yield stress of a plate;
f_y^H	higher yield stress of a plate;
f_y^L	lower yield stress of a plate;
f_u	ultimate or tensile stress of a plate;
f_{yb}	yield stress of a bolt;
f_{ub}	ultimate or tensile stress of a bolt;
$F_{v,Rd}$	design shear resistance per bolt;
$F_{b,Rd}$	design bearing resistance per bolt;
γ_{M2}	partial safety factor for resistance of bolts and resistance of plates in bearing;
A_u	percentage elongation after fracture;
Z	percentage reduction of area;
F_u	maximum load of the connection;
δ_u	displacement at the maximum load.

1 – Aim of the study

The rules described in EC3 for bolts in bearing dependent on end-distance, edge-distance and pitch for 8.8 and 10.9 bolt classes are allowed to be used in plates of steel grade up to S700. However, these rules are based on data of steel plates in mild steel and not for high strength steel, 8.8 and 10.9 steel classes in plates of steel grade up to S460. In fact "strong" bolts in "weak" steel plates. Steel grades of S690, S960 and even higher are being used in civil engineering structures more and more. So, in these cases "weak" bolts in "strong" steel plates. The question is now if the rules for bearing of bolts as they are in EC3 are adequate in case of bolts in bearing with these strong plates.

In order to answer this question an experimental program was carried out.

Two kinds of specimens were designed: one bolt and two bolts joints.

1. One bolt joints: Ten different test specimens were designed to validate the maximum bearing resistance for each fastener as well as the minimum distances in a bolted joint with high strength steels- chapter 3, Part 1.8 EC3 [1]. The question is, if on the one hand the high strength steels has less deformation capacity, they would need a larger end distance to get the same deformation. On the other hand the plates have more strength, so it can handle a lower end distance to get the same resistance for each fastener.
2. Two bolts joints: in a row, in order to get the resistance of a group of fasteners in high strength steel, if it can be added or not with the rule that is given in clause 3.7 (1) of EC3 Part 1.8 [1]. The question remains the same, if the high strength steel is less ductile, it will have less deformation capacity, but more strength. These test specimens weren't tested due to lack of time.

All the specimens were designed to have bearing failure mechanism with the design rules give in table 3.4 of EC3 Part 1.8 [1].

2 – Introduction

Connections are important parts of every steel structure. The mechanical properties of the connections are of great influence on the strength, stiffness and stability of the whole structure.

Connections are used to transfer the forces from one member to another. Although both welded and bolted connections can be used in steel structures, bolted connections are commonly used because of their ease fabrication, buildability and ability to accommodate minor site adjustments.

Depending on the shape of the connection and the location of the bolts, they can be loaded in tension, shear or combination of tension and shear.

In shear connections, considering the load transfer, bolts may behave as either:

- 1) Bearing type bolts: the non-preloaded bolt. This means that the plates joined are restricted from moving primarily by the bolt shank.
- 2) Pre-loaded bolts: friction-grip connection made with high strength bolts. This means that the plates are clamped together by the tension induced in the bolts by tightening them.

The internal forces in these two types of connections are shown in Figure 2.1.

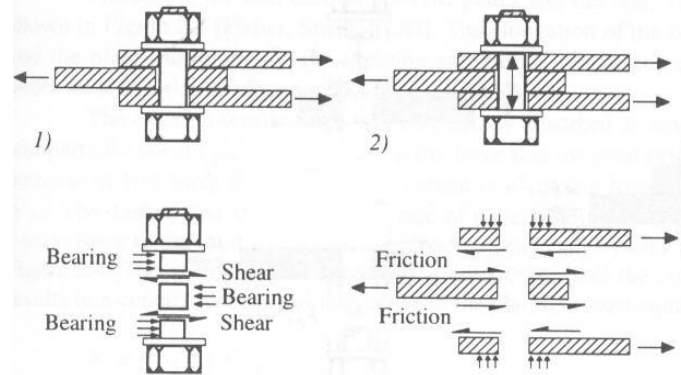


Figure 2.1 – Force components in the bearing bolts (1) and preloaded bolts (2) [2].

Where a joint loaded in shear is subjected to reversible loads, or where slip is not allowed in the shear joint, preloaded bolts in a slip resistance connection should be used. In all other situations, non-preloaded bolts are an efficient and satisfactory solution.

In this work, the performance of non-preloaded bolts in shear connections is studied – Bearing type.

Bearing type joints

In bearing-type joints, the shear strength of the fasteners and the local bearing stresses in the plate around the fasteners are the critical parameters. It is assumed that the loads are transferred by bearing and shear only and the unintentionally present frictional resistance caused by uncontrolled tightening of the bolts is ignored.

These bolts are hand-tightened. The tightness is obtained by the effort of a person using an ordinary spanner such that the bolt cannot be untightened by hand. This tightness is sufficient to produce a small friction between the plates that is overcome with the increasing of the load. A little slippage occurs due to the clearance between the bolt and the hole. The slipping stops when the shank of the bolt comes into contact with the plate. When further load is applied, there is an elastic response until plastic deformation starts either on the shank of the bolt or on the connected plate.

The maximum resistance of a joint loaded in shear is determined by one of the four possible failures mechanism:

- 1) Shear failure of the bolt: relatively brittle and based on the pure shear strength of the bolt material – Figure 2.2 (a)
- 2) Bearing failure, that covers two different failure modes:
 - 2.1) Hole elongation: bearing between the bolt and/or the plate will cause ovalization of the hole. It is the most ductile mode of failure – Figure 2.2 (b).
 - 2.2) Shear failure of the plate: shearing out occurs in the case of a smaller end distance – Figure 2.2 (c). It can also occur when the pitch distance between two bolts in a row is relatively small.
- 3) Tension failure of the plate at the net-cross section – Figure 2.2 (d).

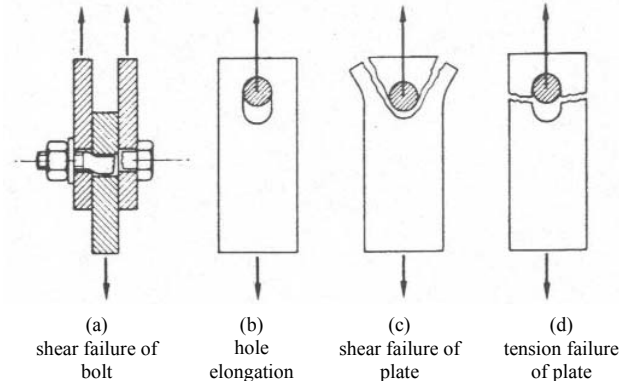


Figure 2.2 – Possible failure mechanism of bolted joint loaded in shear [3].

Each different failure mechanism has specific load resistance. This resistance is not easy to predict by calculation due to complicated stress distribution in the connection and forces in the bolts. Consequently, the design of a bolted connection is semi-empirical, based on past experience, custom and practice, and validated with the statistical evaluation of test results.

Concerning the deformation capacity of each joint, if the failure mechanism is bearing, the deformation capacity of the connection is very large. The joint has a ductile behaviour. However, when the failure is due to shear of the bolts, the deformation capacity of the connection is smaller and the joint has a brittle behaviour. Finally, if net section rupture governs the failure load of the connection, the deformation capacity is also small.

The design rules for joints followed in this study are the European Standard Eurocode 3 Part 1.8, June 2004 [1].

High strength-steel

The use of high-strength steel has increased in the last few years. Although the prices of the steel increases with the increasing yield stress, the percentage of price does not keep up with the percentage of yield-stress increase [4]. The result is that the use of stronger steels will quite frequently be economical for tension members, beams and columns. The use of high-strength steels carries some advantages: superior corrosion resistance; possible saving in erection and foundation costs; use of lower beams permitting smaller floor depths and possible saving in fire proofing because smaller members can be used [4].

The problem with using the high-strength steel is due to its different properties when compared with mild steel. With the treatments and processes that are known so far, the increase of the strength causes a decrease of the ultimate deformation. High-strength steels are less ductile than mild steels. These differences can not be ignored when using the design rules. Figure 2.3 shows the typical stress-strain curves of mild steel and high strength steel.

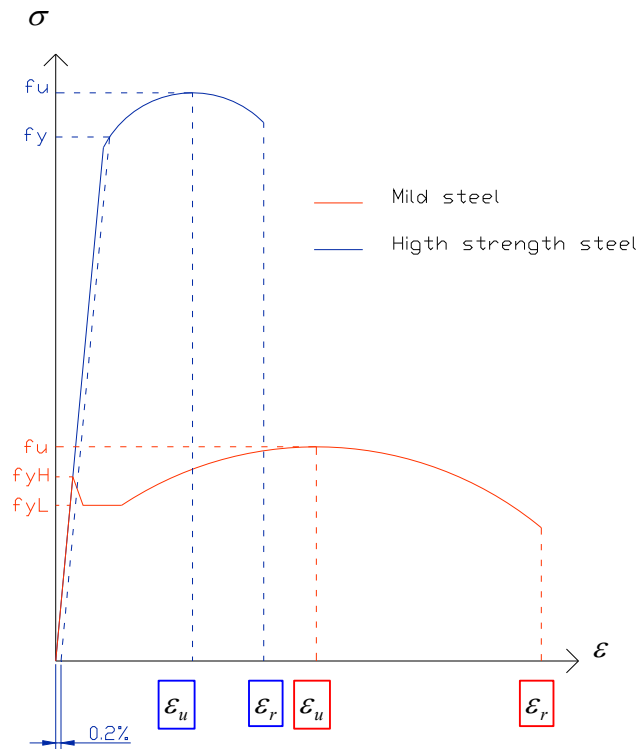


Figure 2.3 – Stress –strain curve of mild steel and high strength steel.

The use of high strength-steel plates in bearing type connections will bring differences in the bearing and net section failure. The shear failure of the bolt depends on the material resistance of the bolt and whether the shank or threaded portion is in the shear plane, so different properties in the steel plate will not influence the maximum load of this failure mechanism.

The design rules for joints given in EC3 [1] can be used for steel grades up to S700 as it is described in part 1.12 of Eurocode 3 [5]. The aim of this investigation was to confirm the design rules for bearing type connections with bearing failure using high strength steel.

3 – Literature review

As the use of high strength steel increases, the influence of its different properties from mild steel on the behaviour of structural steel is often questioned. Many kinds of studies were made concerning the influence on bearing resistance of a connection when using high strength steels. Experimental tests were carried out as well as models in finite element methods, in order to predict the bearing resistance. In this part of the report, some studies concerning these topics are mentioned.

Puthli and Fleischer (2000) [6] carried out 25 bolted connections with the web of a HE 800 B high-strength steel beam. The aim of this investigation was to confirm that the design rules of EC3 concerning the edge and bolt spacing for steel grades S235, S355 were also valid for S460. All the connections had been provided with different spacing to observe the influence of bolt spacing and edge distance and designed to have bearing failure mechanism. EC3 requires a reduction of the design bearing resistance of bolted connections loaded in shear when the edge distance $e_2 < 1.5d_0$ or bolt spacing $p_2 < 3.0d_0$, where d_0 is the hole diameter. For $e_2 = 1.2d_0$ or $p_2 = 2.4d_0$, the design resistance has to be reduced 2/3. Intermediate values can be interpolated. For values lower than $e_2 = 1.2d_0$ or $p_2 = 2.4d_0$, no calculations are possible. The test results showed that this reduction does not need to be so large. For the investigated tests, it is observed that a reduction of the design bearing is not required for edge distances $e_2 \geq 1.2d_0$ or bolt spacing $p_2 \geq 2.4d_0$. The minimum edge distance and minimum bolt spacing may be reduced to $e_2 = 1.0d_0$ and $p_2 = 2.4d_0$, respectively. However, a reduction of the design bearing resistance of 3/4 is then necessary for these minimum distances. The intermediate values may be interpolated. The results and the comparison of the proposal reduction factor and the one given by EC3 are shown in Figure 3.1.

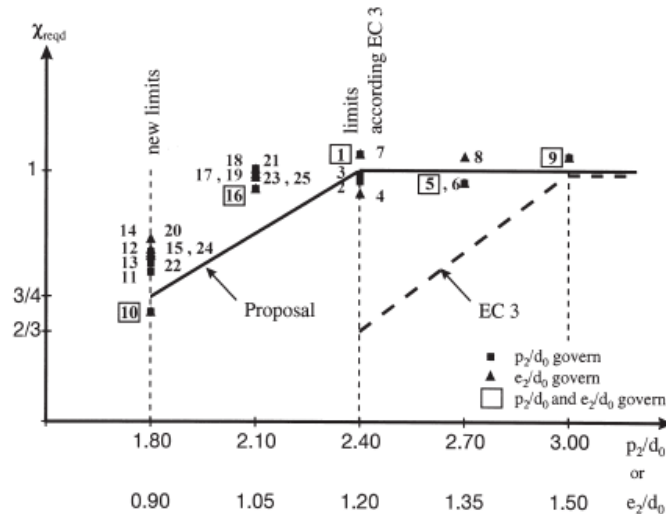


Figure 3.1 – Reduction factor for bearing resistance in relation to the bolt spacing and edge distance.

The yield-tensile ratio typically increases with the increasing levels in the strength. The influence of this increasing in tension members was studied and discussed by Kato (1990) [7], Ohashi et al (1990) [8], and Kulak et al (1987) [9]. In bolt members the section is reduced (net section), and the behaviour will depend on the ratio on the net section area to the gross section area and the yield-tensile ratio. These investigations focus the influence of these parameters. The increasing of the yield-tensile ratio leads to decreasing elongation. If the yield-tensile ratio is 1.0 and if the member is subjected to increasing loads, the length of the member that yields approaches zero and total elongation is limited. At smaller yield-tensile ratios, a zone of increasing length is able to reach the yield strength while the minimum section is reaching the tensile strength, and thus the total elongation before rupture increases. At higher yield-tensile

ratio, if the member is design in proportion so that it yields in the gross section before the tensile strength in the net section is reached, the elongation will be high. However, if the product of the net section area times the tensile strength of the material is less than the gross section area times the yield strength, the member deformation will be limited.

Kim and Yura (1997) [10] investigated the effect of the ultimate-to-yield stress ratio on the bearing strength. The tests were provided with different end distance and bolt spacing. One steel had F_u/F_y ratio of 1.61 and the other had a F_u/F_y ratio of 1.13. Contrary to what was expected, specimens made by steel of a low ultimate-to-yield stress ratio have deformations capacities similar to those with a high ultimate-to-yield stress ratio with the corresponding end distance. As the end distance increased, the deformation at ultimate strength increased, therefore more deformation capacity can be achieved by increasing the end distance. The end distance is a more significant factor on deformation capacity than the ratio F_u/F_y . It was then concluded that steels with an ultimate-to-yield stress ratio equal to or greater than 1.13 do not influence the bearing resistance of a joint. The test results were also compared with the design rules of EC3 and it is reported that EC3 recommendations are conservative by approximately 25%.

Ju et al (2003) [11] used a three-dimensional (3D) elasto-plastic finite element method to study the structural behaviour of the butt-type steel bolted joints. It is very difficult to simulate a complete bearing failure since the large plastic region near the contact region causes the numerical difficulty. The analysis results confirm that for the linear elastic behaviour, each bolt in the connection can resist different loads, and the bolt adjacent to the applied force (the first bolt) will support the maximum force. For the non linear behaviour, the nominal forces obtained from the finite element analyses are almost linearly proportional to the bolt number arranged in the connection. This is because the plastic deformation of the more highly stressed first bolt caused redistribution of load to interior bolt until the load carried by each bolt is about the same. For very long connections, such as 5 or more bolt rows in the load direction, the first bolt may reach a critical shear deformation and fail before the full strength of each bolt can be utilized.

Aceti *et al* (2003) [12] investigated a numerical study concerning the role played by transverse plastic deformations, the restraining effect of the nut and the contact between the bolt and the metal plate in a bolted joint loaded in shear, focused in bearing and net section failure. They reported that at failure, transverse dissipation in the plate plays a major role for bolted connections, the increased resistance of bolted joints with respect to pinned connections, which codes assume to be significant is mainly due to restraining effect of the nut and the presence of washers is independent from the essential response of the joint. They also discuss the important role of contact between the bolt and the hole boundary when bearing failure occurs. The aim of their research was also to define a numerical model to represent some aspects influencing the joint behaviour with respect to failure. They propose a simplified numerical procedure by the definition of a solid (3D) finite element with planar symmetry to model metal plates and the computation of the limit load by rigid-plastic limit analysis.

Rogers and Hancock (1998) [13] summarised test results concerning the behaviour of bolted connections tested in shear, which were composed of 0.42 m G550 and 0.60 mm G300 sheet steels. Test specimens size and shape, as well as type and number of bolts, were varied to cause three distinct modes of failure: end pull-out, bearing and net section fracture. G300 sheet steels possess a greater ability to elongate than G550 sheet steels. Bolted connections composed of G550 sheet steels were able to elongate to at least 90% of the distance measured for nominally identical G300 test specimens. The limited elongation ability exhibited by G550 sheet steels did not translate into a small displacement capacity for bolted connections failures by end pull-out and bearing on the test specimens. To determine the degree of anisotropy and its effect on the connection resistance and failure type, test specimens were milled from the longitudinal, transverse and diagonal directions of the sheet. The results showed that the displacement of bolted connections, regardless of failure mode, is not dependent on the

direction of the material in the plane of the sheet. A limit number of eccentrically loaded tests were included in this study to determine the influence of load position on the behaviour of bolted connections. No significant changes in failure mode, load-carrying resistance, or connection displacement occurred with eccentric loading. Concerning design rules, the results indicated that Eurocode cannot be used to accurately predict the failure mode of bolted connections fabricated from G550 and G300 sheet steels. Furthermore, these design rules cannot be used to accurately determine the bearing resistance. The same authors later on (2000) [14] reports recommendation concerning the procedure that should be used to identify the net section fracture and bearing-failure modes in the same bolted connections with sheet steels.

Chung and Ip (2000) [15] established a finite element model with three-dimensional solid elements to investigate the bearing failure of cold-formed steel bolted connections under shear. A parametric study on bolted connections with different configurations is performed to provide bearing resistances for practical design, and the results of the finite element modelling are also compared with the design rules. In order to quantify the effect of the yield patterns and thus the ductility of the steels to the bearing resistances of the connections, a strength coefficient, α , is established – $F_b = \alpha d t f_u$, where F_b is the bearing resistance of bolted connections at 3 mm extension, d , t are the bolt diameter and the thickness, respectively, and f_u is the tensile strength of the steel strip. Tests were performed with G300 and G550. For all the connections the strength coefficient, α , is larger than unity. For low strength steels (G300), the strength coefficients are roughly 3.5 showing their large ductility. However, for high strength steels (G500), the strength coefficients are roughly 2.5, showing the reduced ductility of these steels. Consequently, it is demonstrated that any reduction in the ductility of the steels will have significant adverse effect on the bearing resistance of bolted connections. It is found that the design rules are not applicable for bolted connections with high strength steel due to reduced ductility. Consequently, a semi-empirical design formula for bearing resistance of bolted connections in cold-formed steel is proposed after calibrating against finite element results. The proposed design rule relates the bearing resistance with the design yield and tensile strengths of steel strips through a strength coefficient. It is also demonstrated that the design rule is applicable for bolted connections of both low strength and high strength steels with different ductility limits.

For what was described before, some important conclusions should be mentioned.

Previous experimental programs proved that the rules described in EC3 for bearing resistance are conservative to steel plates S460, which can already predict some behaviour of the high strength steels. The reductions in the design bearing resistance concerning the distance between the bolts doesn't need to so large. Also the minimum distances can be reduced. Although the steel grade used in this study is higher than S460, these preliminary conclusions led our experimental program to include distances between the bolts smaller than the minimum required as well as previous warning of the big difference between the predicted values and experimental values on the bearing resistance. That is one of the reasons that in the design of the test specimens some cautions were made to increase the difference between the values of the bearing resistance and the others resistances in order to guarantee the bearing as failure mechanism.

Another important idea to keep in mind it's related to the end distance seems to be a more significant factor on deformation capacity than the steel grade. Some tests were made that describe almost no difference on the deformation capacity of the joint in bearing for different steel grade (mild steel and high strength steel), i.e. a joint in bearing with steel plates of high strength steel has the same deformation capacity as with steel plates with mild steel. This is contrary to what was expected and warn us to a deformation capacity larger than the expected for high strength steel. This is also a relevant statement to provide the necessary cautions on the experimental program, for example on the preparation and calibration of the deformation measurement devices.

4 – Design rules for bearing type connections – EC3 Part 1.8

The studied joints are shear connections from bearing type. They are included on Category A defined on clause 3.4 in EC3, Part 1.8 [1].

The design resistance of the joint belonging to this category should exceed neither the design shear resistance nor the design bearing resistance. The bolt classes from 4.6 up to and including 10.9 may be used.

The following text shows the design resistance rules for each individual fastener subjected to shear described in clause 3.6.1 (1) in EC 3, Part 1.8 [1].

Shear resistance – $F_{v,Rd}$

The design shear resistance of a bolt ($F_{v,Rd}$), per shear plane, is:

$$F_{v,Rd} = \frac{\alpha_v f_{ub} A}{\gamma_{M2}} \quad (4.1)$$

- Where the shear plane passes through the threaded portion of the bolt (A is the tensile stress area of the bolt A_s):
 - For classes 4.6, 5.6 and 8.8:
 $\alpha_v = 0.6$
 - For classes 4.8, 5.8, 6.8 and 10.9:
 $\alpha_v = 0.5$
- Where the shear plane passes through the unthreaded portion of the bolt (A is the gross section area of the bolt):
 $\alpha_v = 0.6$

The described design resistance for shear through the threaded portion of a bolt should only be used for bolts with rolled and cut thread according with EN 1090. For bolts with cut threads not according with EN 1090, the design resistance for shear through the threaded portion of a bolt should be multiplied by a factor of 0.85.

Shear tests on bolts show the shear strength to be about 60% of the tensile strength. This reduction is caused by secondary bending actions on the bolt due to excessive hole clearance or even by bearing of the plates. This reduction is reflected on the reduction factor α_v .

The reduction factor α_v varies in the case that shear plane is in the threaded portion of the bolt. In this case, the value depends on the ductility of the bolt. Due to the threads, the surface of the plane failure is irregular and the behaviour next to failure depends on the ductility of the material. For bolts less ductile, α_v is smaller (classes 4.8, 5.8, 6.8, and 10.9) which is logical because the failure is brittle and gets the ultimate deformation faster, due to less plastic deformation.

When the shear plane is in the unthreaded portion of the bolt, α_v is independent of the bolt grade because the failure plane is a regular surface (smooth bar).

Bearing resistance – $F_{b,Rd}$

The design bearing resistance of a bolt is given by:

$$F_{b,Rd} = \frac{k_1 \alpha_b f_u d t}{\gamma_{M2}} \quad (4.2)$$

where:

- $\alpha_b = \min\{\alpha_d; \frac{f_{ub}}{f_u}; 1.0\}$
 - where α_d , in the direction of the load transfer:
 - for end bolts: $\alpha_d = \frac{e_1}{3 d_0}$

- for inner bolts: $\alpha_d = \frac{p_1}{3 d_0} - \frac{1}{4}$
- perpendicular to the direction of the load transfer:
 - for edge bolts: $k_1 = \min \left\{ 2.8 \frac{e_2}{d_0} - 1.7; 2.5 \right\}$
 - for inner bolts: $k_1 = \min \left\{ 1.4 \frac{p_2}{d_0} - 1.7; 2.5 \right\}$

The symbols for spacing of fasteners are represented in Figure 4.1.

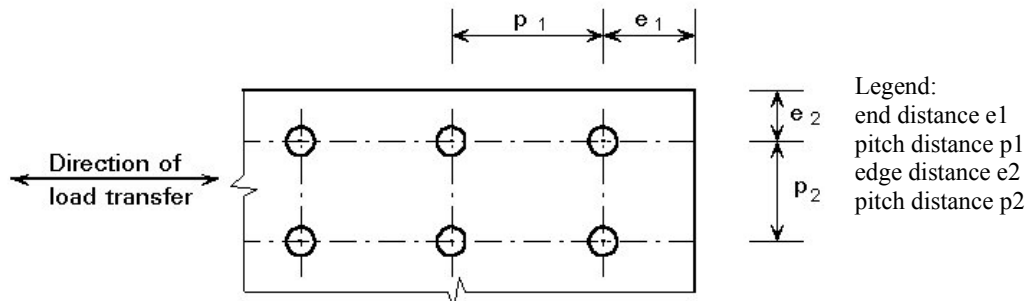


Figure 4.1 – Symbols for spacing in a joint.

The reduction factor α_d is necessary because, a smaller end/pitch distance will cause a reduction in the resistance of the joint.

When the end distance is short, the capacity of deformation is small and the resistance to the shear out of the plate decreases - Figure 4.2.

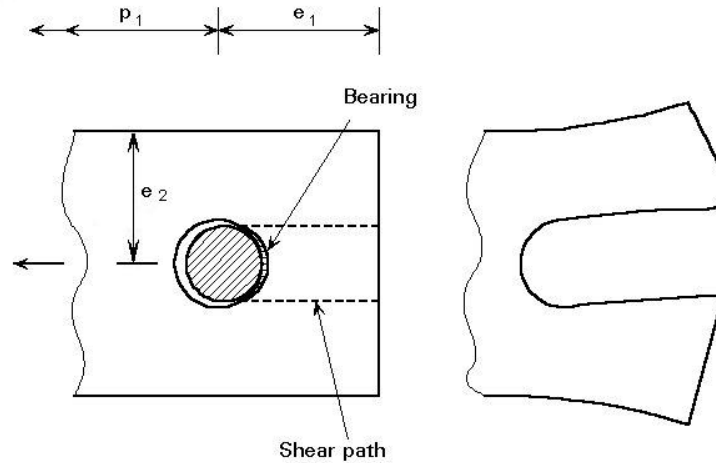


Figure 4.2 – Shear-out of the plate.

The factor α_b refers to the reduction associated with spacing (α_d) and also concerns the possibility of, instead of having bearing of the plate, having bearing of the bolt (f_{ub}/f_u). In this case the tensile strength of the bolt material is decisive instead of the plate material.

The factor k_1 concerns the fact that a smaller edge/pitch distance will reduce the resistance of the joint. Equation (4.2) can be simplified giving the value 2,5 to k_1 and turn to be the design bearing resistance given by the test results where the edge distance e_2 is $1,5 d_0$ and the pitch distance p_2 is $3 d_0$. If e_2 and/or p_2 is reduced then the bearing resistance $F_{b,Rd}$ should be reduced with the linear functions given for k_1 .

Besides the design bearing resistance - equation (4.2), EC 3 applies also for minimum spacing between the joints. In clause 3.5 of EC3: Part 1.8 [1] the following minimums are required:

- Minimum end distance: $e_1 \leq 1.2 d_0$
For smaller end distances the resistance is almost none due to the tearing out of the fastener through the material.
- Minimum edge distance: $e_2 \leq 1.2 d_0$
The punching of holes too close to the edges may cause the steel opposite the hole to bulge out or even crack.
- Minimum pitch distance: $p_1 \leq 2.2 d_0$ and $p_2 \leq 2.4 d_0$
Bolts should be placed in a sufficient distance apart to permit efficient installation and to prevent bearing failures of the members between fasteners.

Note: Maximum distances are also required in clause 3.5 of EC3: Part 1.8 [1] but won't be mentioned in this study. Those rules are related with corrosion phenomena, which is not an issue in this investigation.

Summarizing the reduction factors of equation (4.2) and the minimum distances, the following linear functions can be draw - Figure 4.3:

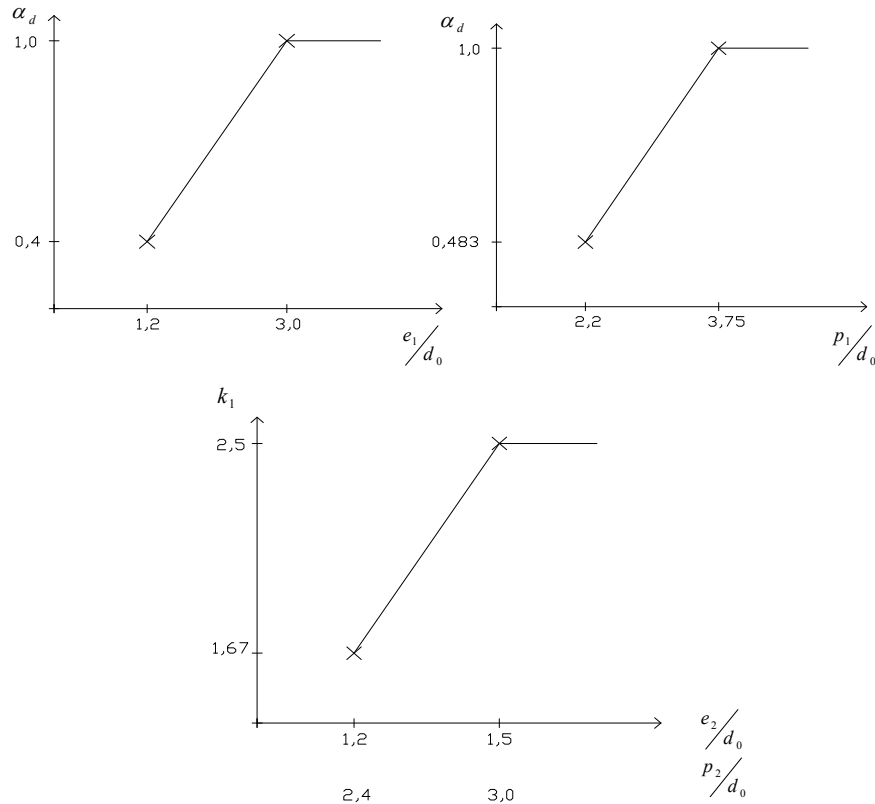


Figure 4.3 – Reduction factors for bearing design load in relation to the bolt spacing ($p_1 - \alpha_d$ and $p_2 - k_1$), end distance ($e_1 - \alpha_d$) and edge distance ($e_2 - k_1$).

Besides the bearing and shear resistance, the joint should neither exceed the design ultimate tension of the net section nor the design plastic tension resistance of the gross section. The following rules are given in clause 5.4.3 (1) of EC3: Part 1.1 [16].

Design ultimate tension resistance of the net cross-section at holes for fasteners – $N_{u,Rd}$

Failure of the cross section at bolt holes occurs when the edge distance e_2 and/or pitch distance p_2 is too small in relation with end distance e_1 and/or pitch distance p_1 . Necking of the cross-section in this area occurs, causing subsequent failure of the connections – Figure 4.4.

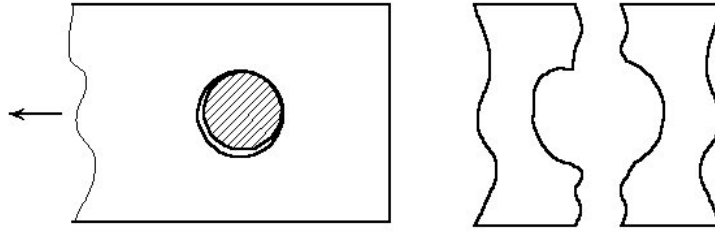


Figure 4.4 – Net-section failure mechanism.

The design ultimate resistance of the net section is:

$$N_{u,Rd} = \frac{0.9 A_{net} f_u}{\gamma_{M2}} \quad (4.3)$$

Failure in the net section starts with the plasticity but is hardly noticeable because the yielding takes place over a relative short length. So the prediction of the ultimate failure load is described in the formula using the tensile strength f_u .

Any discontinuity alters the stress distribution in the neighbourhood of the discontinuity so that the elementary stress equations no longer describe the state of stress. The presence of a hole obviously increases the unit stress in a tension member, even if the hole is occupied by a bolt. There is less area of steel which the load can be distributed and there will be some concentrations stress along the hole – Figure 4.5.

A *theoretical stress-concentration factor* K_t is used to relate the actual maximum stress at the discontinuity to the nominal stress. Using the methods of the theory of elasticity it is possible to determine the values of stress-concentration factors. The value for K_t is dependent on the ratio d/b , where d is the diameter of the hole and b is the width of the plate [17]. Figure 4.6 plots a graph where the K_t values can be obtained by the ratio b/d . This concentration factor is the ratio of the maximum tensile stress in the net section and the tensile stress at a point remote from the hole – gross section.

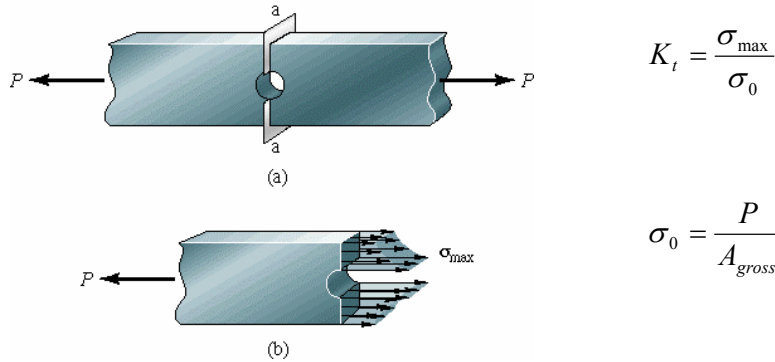


Figure 4.5 – Stress distribution in the neighbourhood of the hole [17].

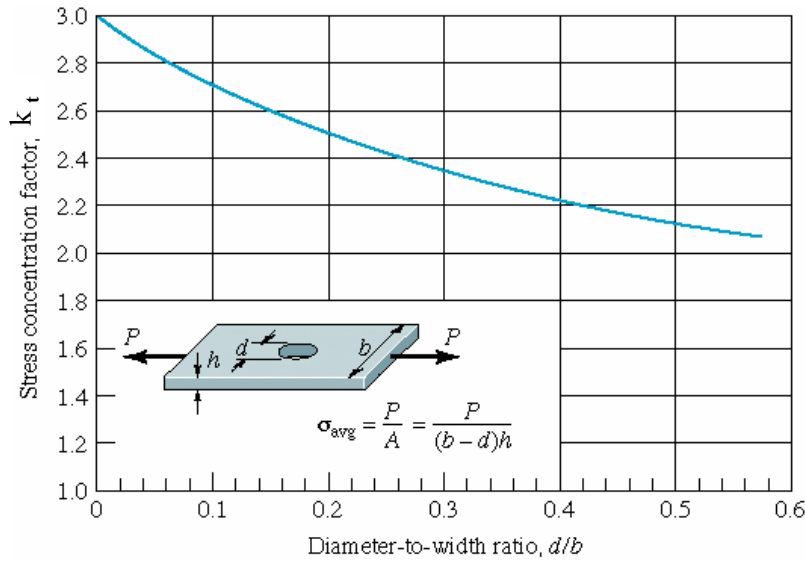


Figure 4.6 – Values for the *theoretical stress-concentration factor* in the net cross section [17].
(σ_{avg} , average tensile stress in the net section)

This concentrations factor only applies in the elastic range, and its value depends only on the geometry of the hole. The particular material used has no effect on the value of stress concentrations factor, that's why it is called a theoretical factor.

When the material reaches the plastic range, this concentration factor decreases. If the fibres around the hole are stressed to their yield stress, they will yield without further stress increase, with the result of redistribution of stresses and the ovalization of the hole will occur due to plastic deformation [4]. The theoretical stress concentration factors in plastic behaviour are then substituted for experimental factors.

In this case, as we are limiting the maximum load to tensile strength, an experimental concentration factor is used and its value is 0.9. This value results from a statistical evaluation of the test result.

Design plastic resistance of the gross cross section – $N_{pl,Rd}$

The design check for the gross section is also necessary. The design resistance is determined as follows:

$$N_{pl,Rd} = \frac{A_{gross} f_y}{\gamma_{M0}} \quad (4.4)$$

Design resistance of a group of fasteners – clause 3.7(1) of Part 1.8 of EC3 [1]

Concluded the design resistance of each fastener, the next question is the resistance of a group of fasteners in a joint, in order to design the test pieces with two bolts in a row.

Concerning the behaviour of a group of fasteners in a bearing type connection, two extremes should be described:

- Non deforming plates:
Plates: perfectly rigid behaviour
→ the loads applied will be equally divided between the bolts.
- Deforming plates:
Plates: perfectly elastic behaviour
→ the plate stresses and its deformation will decrease from the ends of the connection to the middle; the highest stressed element will be at the end of the plate.

The real behaviour is somewhere between the two extremes. Both plates and bolts have elastic behaviour and deformations that will affect the bolt stresses. The effect of this deformation is to cause a very complex distribution of load in the elastic range [4]. Actually, in the elastic range the loads resisted by the bolts of a group are never equal and the bolts at the ends have stresses much greater than those in the inside bolts.

The calculation of the theoretical correct elastic stresses in a bolt group based on plate deformations is a tedious problem and is rarely handle in the design office.

The analysis of a bolted joint based in the plastic theory is a very simple problem. In this theory, the end bolt is assumed to be stressed to their yield point and when the load increases, the end bolt will deform without any increasing of the load. The next bolts in the line will have their stresses increases until is also at the yield point, and so on.

When the plates and/or the bolt have enough deformation capacity in the plastic range, the plastic theory seems to be sufficient. But when there is one fastener in the joint that has a more brittle failure mechanism (small plastic deformation), the situation changes and reductions in the resistance of the group of fasteners must be made.

This theory is the background of the design rules given in EC3 for a group of fasteners.

The design resistance of a group of fasteners can be taken as the sum of the design bearing resistances $F_{b,Rd}$ of each individual fastener provided that the design shear resistance $F_{v,Rd}$ of each individual fastener is greater than or equal to its design bearing resistance $F_{b,Rd}$. This means that, the individual resistances of each fastener can be added if all the fasteners have its resistance equals to its bearing resistance $F_{b,Rd}$ (Figure 4.7 (a)).

Otherwise, if any individual fastener has its resistance equals to its shear resistance, the design resistance of a group of fasteners shall be taken as the number of fasteners multiplied by the smallest design resistance of all the fasteners (Figure 4.7 (b)).

An application example of this rule is shown in Figure 4.7.

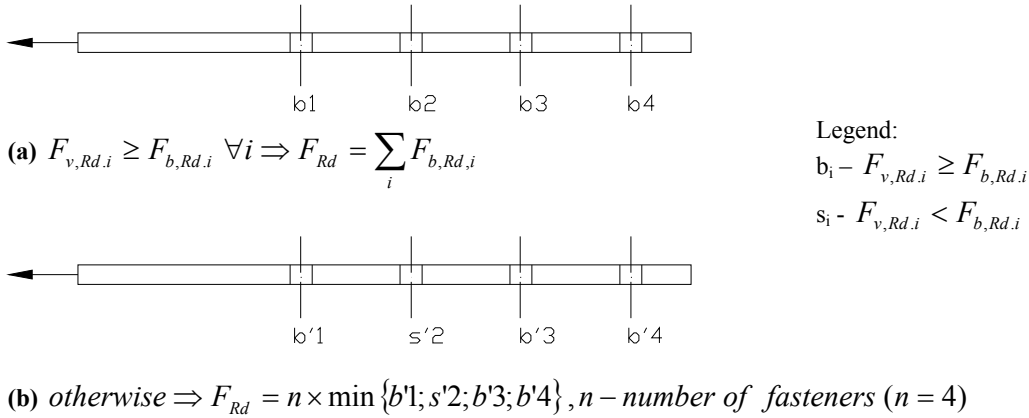


Figure 4.7 – Application example of the design resistance of a group of fasteners given in clause 3.7(1) of Part1.8, EC3 [1].

The background of this rule is related with the fact that the shear failure is much less ductile than the bearing failure.

If all the fasteners have a ductile failure mechanism – bearing, there will be a large plastic deformation, so that the inner bolts can be activated even when all the others, specially the end bolt, are already in the plastic range.

However, if one of the fasteners has a small plastic deformation - shear failure, it will fail quickly after reaching the yield strength. Consequently, the other bolts which are less stressed, will never reach the yield strength when the joint fails. The design resistance of the joint can't depend on the maximum resistance of these bolts. That is why the resistance is calculated by the number of bolts multiplied by the smallest resistance of each fastener.

Practical experience shows that this rule may be too conservative in a lot of cases. For instance, if the only fastener with shear failure is one of the inner bolts, maybe all the others

before it will reach their yielding stress. All these fasteners will contribute to the resistance of the joint, although if we apply the design rule of EC3 the lower resistance of each fastener will command the final load, ignoring the extra resistance that the other bolts could add to the total resistance of the joint. This is also an aim question in this investigation, reformulate the design rule so it could be more economical and less conservative.

The amount of deformation capacity that is needed is also greatly influenced by the length of the connections, especially when concerns shear resistance ($F_{v,Rd}$). In the bearing resistance ($F_{b,Rd}$), as it is a ductile failure mechanism, is assumed that the plates have always enough plastic deformation to activate the rest of the bolts.

The EC3 gives a reduction factor β_{Lf} for long joints that applies only for the design shear resistance, $F_{v,Rd}$ – clause 3.8, EC3:Part 1.8 [1].

Long joints - β_{Lf}

When one of the bolts yields, their flexibility increases causing a more uniform sharing of the load (Figure 4.8). However, for long joints this behaviour will be insufficient to produce an equal load distribution. The end bolt will reach its deformation limit and fail before the remaining ones have been fully loaded.

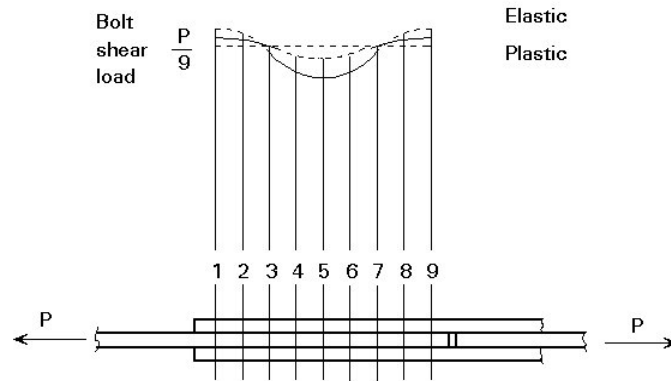


Figure 4.8 – Distribution of bolt shear loads in a long joint (elastic range – full line; plastic range – dashed line).

When the distance L_j between the centres of the end fasteners in a joint, measured in the direction of a transfer of a force (Figure 4.9), is more than $15d$ (d is the nominal diameter of the bolt) the design shear resistance of all fasteners shall be reduced by multiplying it by a reduction factor β_{Lf} , given by:

$$\beta_{Lf} = 1 - \frac{L_j - 15d}{200d} \quad (4.5)$$

but $\beta_{Lf} \geq 0.75$ and $\beta_{Lf} \leq 1.0$

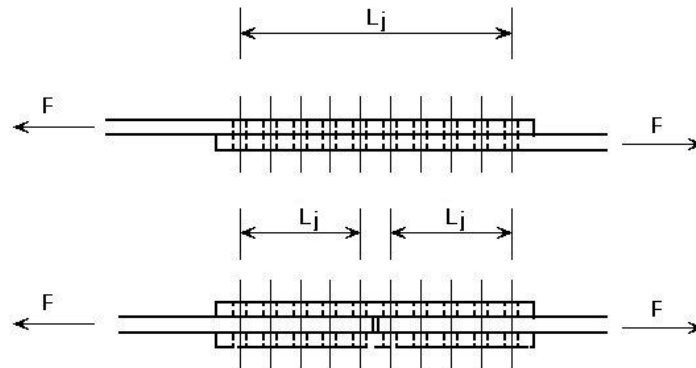


Figure 4.9 – Distance L_j .

4.1 – Test specimen design resistance

The phenomenon studied in this investigation is bearing failure mechanism. Bolt shear failure, net section failure and gross section failure have to be avoided since bearing resistance is to be investigated.

Some assumptions were taken, concerning the design resistance before starting with the design of the test specimens.

Shear resistance – $F_{v,R}$

$$F_{v,Rd} = \frac{\alpha_v f_{ub} A}{\gamma_{M2}}$$

It was decided to avoid the threaded portion of the bolt shank. This option simplifies the design rule and as the shear bolt isn't the aim of this investigation, it wouldn't give any extra information.

The value that was given to the safety factor on the shear design resistance γ_{M2} was 1.0. Considering that it is an experimental program and not a practical design, we must calculate the exact resistance of each bolt, and not reduced by a safety factor.

The nominal value was used for the ultimate tensile strength f_{ub} of the bolts.

To sum up:

$$\left\{ \begin{array}{l} - \text{for any bolt class chose, } \alpha_v = 0.6 \\ - A \text{ is the gross section area of the bolt} \\ - \gamma_{M2} = 1.0 \end{array} \right. \Rightarrow F_{v,R} = 0.6 f_{ub} A \quad (4.6)$$

Bearing Resistance – $F_{b,R}$

$$F_{b,Rd} = \frac{k_1 \alpha_b f_u d t}{\gamma_{M2}}$$

For the same reasons as used in the shear resistance, the safety factor γ_{M2} was reduced to 1.0.

The higher value for the ultimate tensile strength of the plates was taken to obtain the maximum value of the bearing resistance. This assumption was made in order to be shore that the failure mechanism of the test specimens would be bearing, for all the resistance range of plates tested.

$$\underbrace{F_{b,R}}_{\text{maximum}} \ll \underbrace{\{F_{s,R}, N_{u,R}, N_{pl,R}\}}_{\text{minimum}}$$

The value for the ultimate tensile strength of the bolts was also the nominal value.

To sum up:

$$\left\{ \begin{array}{l} - f_u = f_u^{higher} \\ - \gamma_{M2} = 1.0 \end{array} \right. \Rightarrow F_{b,R} = k_1 \alpha_b f_u^h d t \quad (4.7)$$

Net cross section resistance – $N_{u,R}$

$$N_{u,Rd} = \frac{0.9 A_{net} f_u}{\gamma_{M2}}$$

In this case, it was decided to keep the safety factor equal to $\gamma_{M2}=1.25$, in order to reach sufficient safety. On one hand, a simple formula does not describe the real behaviour good enough of this kind of mechanism, due to complicated behaviour before failure. On the other hand, the failure of the net section should not happen in the test specimens.

Following the same rule that is described in the bearing resistance, the lower value of the ultimate tensile strength f_u was used in order to minimize the resistance of the net section.

To sum up:

$$\begin{cases} - f_u = f_u^{lower} \\ - \gamma_{M2} = 1.25 \end{cases} \Rightarrow N_{u,R} = \frac{0,9 A_{net} f_u^l}{1.25} \quad (4.8)$$

Gross section resistance – $N_{pl,R}$

The failure of the gross section is also to be avoided. But, in this case as it is a much simple mechanism, it was decided to reduce the $\gamma_{M0}=1.1$ to the 1.0.

It was used the nominal value for the yield strength f_y .

$$N_{pl,Rd} = \frac{A_{gross} f_y}{\gamma_{M0}} \Rightarrow N_{pl,R} = \frac{A_{gross} f_y}{1.0} \quad (4.9)$$

5 – Test specimens

The experimental programme included two types of test specimens: one bolt joints and two bolts joints in one row.

Tests specimens are double lap joints, they have cover plates on both sides – Figure 5.1. This option was taken to avoid eccentricities. The eccentricities in the load path would cause moments that will produce additional stresses on the connection. Those extra stresses may influence the behaviour. The influence of eccentricity is out of our main subject so it should not be present in our tests specimens. Also concerning this subject, the test specimens have equal edge distance, i.e. the test specimen is symmetric relatively to the axes of the load.

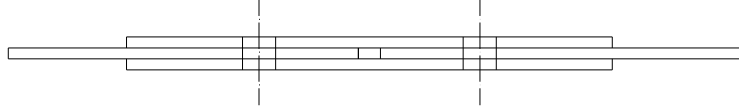


Figure 5.1 – One bolt test specimens of double lap joints.

Each test specimen has two joints. In order to focus the test in only one joint, one of the joints was deliberately designed with higher resistance capacity – strongest joint. The performance of the test specimen is only analysed in the other joint which of course will fail first – test joint.

The specimens were chosen to have bearing of the inner plate as failure mode. The choice of the inner plate has advantages and disadvantages. On the one hand the failure of the inner plate cannot be seen during the test. But on the other hand, as it is double lap joints, the inner plate is twice loaded than the outer plates, so it is easier to reach the failure first on the inner plate.

To study the equation given in EC3 for bearing resistance – equation (4.2), on high strength steel, first we have to ask which parameters could vary in this case.

$$F_{b,Rd} = \frac{k_1 \alpha_b f_u d t}{\gamma_{M2}}$$

Among others, the bearing strength of a joint depends on the ultimate tensile strength f_u of the steel plate and its thickness and also on the nominal bolt diameter, d . These values can't be calibrated because they aren't experimental factors, they are fixed for each steel class and each bolt class. On the opposite, the reduction factors k_1 and α_b are based on experimental data with mild steels and don't vary with the properties of steel. This wasn't a problem if mild steel had the same behaviour as the high strength steel, which doesn't happen in the reality. So, these reduction factors should be checked, if they are still conservative to use in high steel classes or even changed for then to be dependent on the properties of the steel used on the joint [15].

The value of these reduction factors depends on the geometrical properties of the joint - end distance e_1 , edge distance e_2 and pitch distance p_1 , as well as the ratio of the ultimate tensile strength of the bolt and of the steel plate.

Concerning the geometrical properties, the reduction factors k_1 and α_d can be represented in linear functions, as it was shown in chapter 2 of this report. In this investigation study, they were extended beyond the edges described in EC3, considering that the minimum distances can change in high strength steel – Figure 5.2.

Key values were chosen to the end, edge and pitch distance of the inner plate and also values beyond the minimum required in EC3. Looking to Figure 5.2, the chosen values were:

$$e_1 = \{1.0; 1.2; 2.0; 3.0; 3.5\} \times d_0$$

$$e_2 = \{1.0; 1.2; 1.5; 2.0\} \times d_0$$

$$p_1 = \{2.0; 2.2; 3.0; 3.75; 4.0\} \times d_0$$

The different combination of these values gave the geometrical properties of each possible test specimen. After calculating the resistance and failure mode of each one of these, it was only tested the ones with bearing failure. The bolt grade, the bolt diameter and the thickness of the plate were chosen in order to have the biggest cases with bearing failure of all the

combination (to cover the maximum cases in each reduction factor) and also to avoid shear on the strongest joint for possible reutilization of the bolts.

As the test specimens have not more than one row, the pitch distance in the perpendicular direction of the load, p_2 wasn't studied.

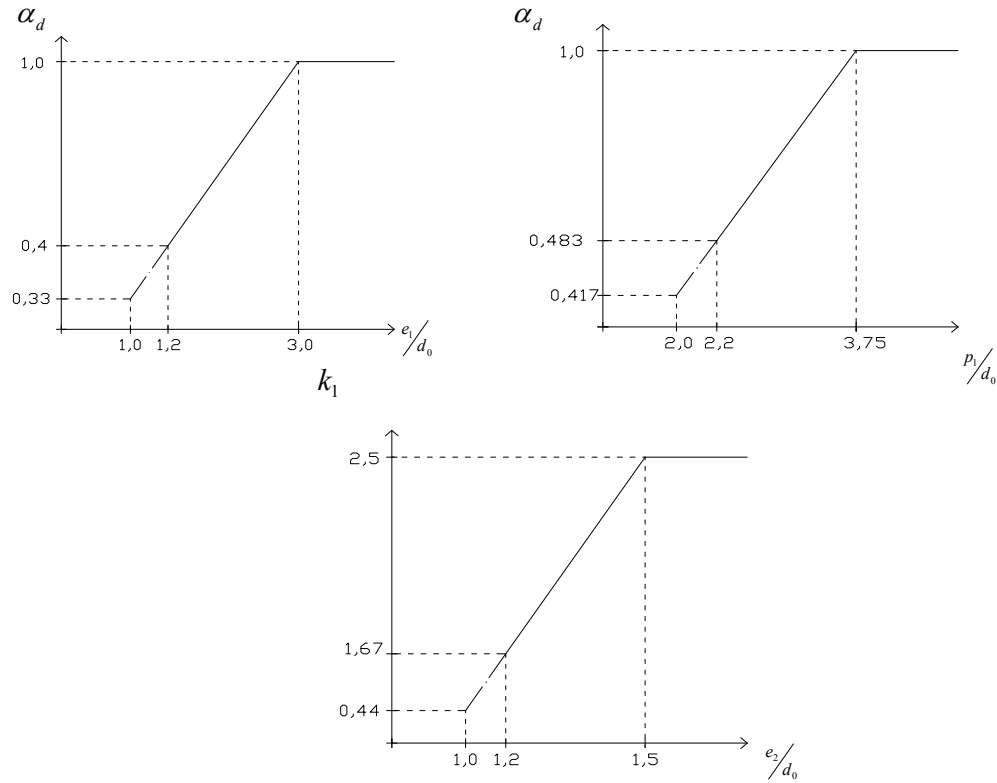


Figure 5.2 – Functions to be validated for high strength steels.

It was also studied the bearing of the bolt which is represented by the ratio between the ultimate tensile strength of the bolt and of the plate, in the reduction factor α_b . The bearing of the bolt only happens when the ratio is less than one and less than α_d . Figure 5.3 shows one example where the bearing of the bolt can happen. The red line represents the cases that have bolt bearing as failure mode.

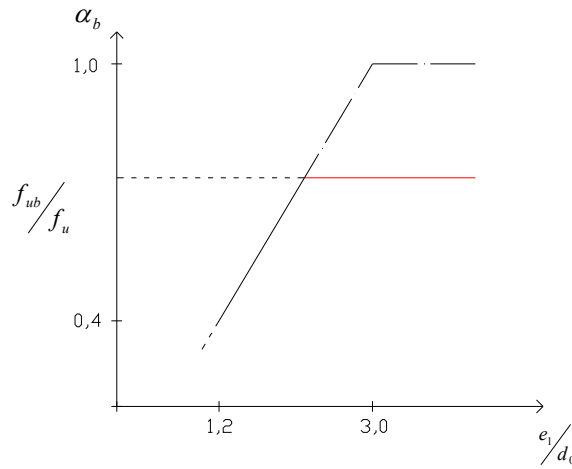


Figure 5.3 – Values of the reduction factor α_b where the bearing of the bolt is the failure mode – red line.

The steel plates used were S690 with 10 mm thickness. The nominal strength values of the steel class S690 used in this investigation are given in Table 5.1. The steel grade was chosen in order to be included in the steel grades up to S700.

Nominal steel grade	f_y (N/mm ²)	lower f_u (N/mm ²)	higher f_u (N/mm ²)
S690	690	770	940

Table 5.1 – Nominal values of the yield strength f_y and the lower and the higher ultimate tensile strength f_u for steel grade S690 [18].

The bolt classes used were 8.8 and 10.9. The nominal strength values used are given in Table 5.2.

Bolt grade	f_{yb} (N/mm ²)	f_{ub} (N/mm ²)
8.8	640	800
10.9	900	1000

Table 5.2 – Nominal values of the yield strength f_{yb} and the ultimate tensile strength f_{ub} for bolts [1].

The bolt diameters used were M24 and M27. Their characteristics are described in Table 5.3.

Bolt diameter	d (mm)	d_0 (mm)	A (mm ²)	A_s (mm ²)
M24	24	26	452	353
M27	27	30	573	459

Table 5.3 – Diameters and areas of bolts used in this investigation.

Concerning the EC3 rules for steels up to S460, they were considered as truth and no test were performed with mild steels. If these calibration tests would have been performed, the test specimens should had the same geometric properties as their similar in high strength steel.

5.1 One bolt test specimens

In the one bolt test specimens two phenomena were studied: bearing of the plate and bearing of the bolt, and two parameters were varied: end distance, e_1 and edge distance, e_2 (pitch distance p_1 is zero).

5.1.1 Bearing of the plate – Series A

The character representing the test specimens with one bolt and with bearing of the plate as failure mechanism is letter A.

To study the bearing of the plate the ratio between the ultimate tensile strength of the bolt and the ultimate tensile strength of the plate must be always bigger then α_d , so we can be shore that bearing of the bolt will not happen. If the ratio is bigger than one we are free to choose any value of the end distance and don't have any limit value for the calibration function of α_d . This is why in these test pieces the bolt class is 10.9. This way the α_b function will be always coincident with α_d function.

$$\frac{f_{ub}}{f_u} = \frac{1000MPa}{940MPa} > 1$$

The combinations of all the values of the end and edge distance make a table in total of 20 possible test specimens. The bolt diameter was M24 in order to have more cases of bearing. If the bolt diameter was less there will be more cases of shear due to the decrease of the strength of the bolts. The reason of choosing 10 mm thickness is that the increase of the thickness would lead to stronger plates and the shear would be critical.

The values used for end and edge distances in the outer plates were so that there weren't any reduction on α_b and k_1 so it wouldn't be critical in the joint (higher resistance than the inner plate).

$$\overbrace{e_1 = 3.8 d_0 = 100\text{mm} \Rightarrow \alpha_b = 1 \quad e_2 = 1.9 d_0 = 50\text{mm} \Rightarrow k_1 = 2.5}^{\text{OUTER PLATES}}$$

Concerning the strongest joint, in order to keep the same width to both inner plates in each test specimen, only the end distance is different. This joint has always higher resistance capacity than the test joint.

Of the 20 possible test specimens 9 had bearing as failure mechanism, so this series had 9 different test specimens. It was excluded for testing the net section failure mechanism, but it would be better to do all the cases and confirm or not the failure mechanism predicted from rules in EC3. In high strength steels, the failure mechanism can be different concerning the possibility of different rules for resistance capacity.

Table 5.4 summarise the essential values of the design of test specimens in this series:

- Resistance of the test joint calculated with equations described in chapter 2.1 of this report;
- Failure mechanism of each test specimen;
- The 9 test specimens tested with bearing failure of the inner plate (blue colour): their resistance and their end and edge distance.
- The resistance of the strongest joint and its end and edge distance on the inner plate (yellow colour in the same column).

$e_1 \backslash e_2 (d_0)$		1.0	1.2	1.5	2
	$e_1 \backslash e_2 (mm)$	25	30	40	50
1.0		Binner	Binner	Binner	Binner
	26	74.6 kN	115.1 kN	188.0 kN	188.0 kN
1.2		Binner	Binner	Binner	Binner
	31	89.5 kN	138.1 kN	225.6 kN	225.6 kN
2.0		net section inner	net section inner	net section inner	Binner
	52	133.1 kN	188.5 kN	299.4 kN	376.0 kN
3.0		net section inner	net section inner	net section inner	net section inner
	78	133.1 kN	188.5 kN	299.4 kN	410.3 kN
3.5		net section inner	net section inner	net section inner	net section inner
	91	133.1 kN	188.5 kN	299.4 kN	410.3 kN
	width [mm]	50	60	80	100

Table 5.4 – Resistance and failure mechanism of test joint (blue) and strongest joint (yellow) in series A.

Note: for each pair of end and edge distance, the upper cell gives the failure mechanism – “Binner” means bearing of the inner plate and “net section inner” means failure of the net section of the inner plate, and the lower gives the calculated resistance of the joint.

The identification of the test specimens uses common matrix notation and mentions always the geometric characteristics of the inner plate of the test joint.

- Example: A2015, cell in the $e_1 = 2.0 d_0$ column and $e_2 = 1.5 d_0$ line - net section of the inner plate as failure mechanism and resistance of $N_{u,R} = 299.4$ kN.

In annex A.1, one example of the calculating procedure on the design of this series is described.

5.1.2 Bearing of the bolt – Series B

The character representing the test specimens with one bolt and with bearing of the bolt as failure mechanism is letter B.

To study the bearing of the bolt the ratio between the ultimate tensile strength of the bolt and the ultimate tensile strength of the plate must be less than one and smaller than α_d factor. In this case α_b factor will be equal to the f_{ub}/f_u , and the ultimate tensile strength of the bolt will be critical – equation (5.1).

In order to obtain these previous results the test specimens were designed.

$$\frac{f_{ub}}{f_u} < \alpha_b \Rightarrow \alpha_b = \frac{f_{ub}}{f_u}$$

$$F_{b,R} = k_1 \alpha_b f_u^h d t \Leftrightarrow F_{b,R} = k_1 \frac{f_{ub}}{f_u^h} f_u^h d t \Leftrightarrow F_{b,R} = k_1 f_{ub} d t \quad (5.1)$$

The bolt class is than 8.8 in order to have $\frac{f_{ub}}{f_u^h} = \frac{800}{940} = 0.85 < 1$.

The bolt diameter was M27. The decreasing of the bolt diameter would lead to shear failure mode instead of bearing.

The value of the end distance was so that $\frac{f_{ub}}{f_u^h} < \alpha_d$ (values on the red part of the graph in Figure 5.4). The value for the end distance was $3.d_0$ and could have been any value higher than $2.6.d_0$ where $\frac{f_{ub}}{f_u^h} = \alpha_d$.

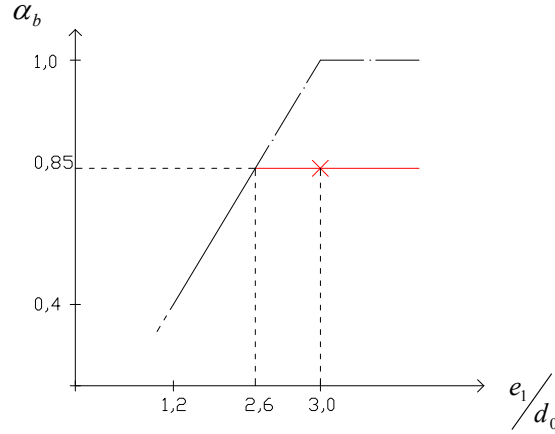


Figure 5.4 – Graph of the reduction factor α_b where the red cross symbolises the test specimen of series B.

The value of the edge distance was both so that k_1 hadn't any reduction (any value bigger than value $1.5 d_0$) and the net section failure wasn't the failure mode. The value for e_2 was $2.5d_0$.

It was decided only to do one test specimen in this series. If we vary the values for end and edge distance beyond those ones, the behaviour of the bearing of the bolt will not vary, as we are changing properties on the plate and not on the bolt – Table 5.5.

		k_1	2.5	2.5	2.5	2.5
	$e_1 \backslash e_2 (d_0)$		1.5	2	2.5	3
α_b		$e_1 \backslash e_2 (mm)$	45	60	75	90
0.33	1		Binner	Binner	Binner	Binner
		30	211.5 kN	211.5 kN	211.5 kN	211.5 kN
0.40	1.2		Binner	Binner	Binner	Binner
		36	253.8 kN	253.8 kN	253.8 kN	253.8 kN
0.67	2		net section inner	Binner	Binner	Binner
		60	332.6 kN	423.0 kN	423.0 kN	423.0 kN
0.85	3		net section inner	net section inner	Binner	Binner
		90	332.6 kN	499.0 kN	540.0 kN	540.0 kN
0.85	3.5		net section inner	net section inner	Binner	Binner
		105	332.6 kN	499.0 kN	540.0 kN	540.0 kN
		width (mm)	90	120	150	180

Table 5.5 - Resistance and failure mechanism of test joint (blue) in the series B.

Note: for each pair of end and edge distance, the upper cell gives the failure mechanism – “Binner” means bearing of the inner plate and “net section inner” means failure of the net section of the inner plate and the lower gives the calculated resistance of the joint.

The end and edge distance in the outer plates had the following values (criterion was the same as in series A):

$$\overbrace{e_1 = 4.0 d_0 = 120mm \Rightarrow \alpha_d = 1 \quad e_2 = 2.5 d_0 = 75mm \Rightarrow k_1 = 2.5}^{\text{OUTER PLATES}}$$

Concerning the strongest joint, the geometrical properties were all the same either in the inner plate or in the outer plate, and only the bolt grade changes. The bolt grade was 10.9 in order to increase the resistance of the joint.

The identification of the test pieces has the same criterion has in series A:

- B3025, $e_1 = 3.0 d_0$ and $e_2 = 2.5 d_0$ – the only test specimen in this series.

In annex A.2 it is described the calculation procedure on the design of this test specimen.

5.2 Two bolts tests specimens – Series D

The test specimens with two bolts were only designed. Due to lack of time they weren't tested. Anyway it was decided to describe all the procedure of design to possible further investigations.

In the test specimens with two bolts, only the bearing of the plate was studied. The behaviour of the bearing of the bolt phenomena would be the same with two bolts or even with more. It is only dependent on each bolt and many bolts have the same behaviour multiplied by the number of bolts and wouldn't have any extra information about that phenomenon.

The parameters varying in these test pieces were e_1 and p_1 . The edge distance was kept constant. The edge distance only influences the net section resistance and that resistance doesn't vary if there is more than one bolt on a row in the direction of the load (net area will keep the same). It would only influence if there were test specimens with more than one bolt in a row in the perpendicular direction of the load, then the net area will be different with one or with two bolts as well as the resistance of it.

The letter representing the test specimens with two bolts is letter D.

The bolt class was 10.9 in order to have bearing of the plate in all the possible combinations ($f_{ub}/f_u > 1$).

The value for the bolt diameter was M20, chosen in order to have the biggest test specimens with bearing as failure mechanism. For smaller diameters the shear would take place

in more cases than bearing, and bigger diameters would only increase the resistance capacity of the joint and kept the same failure mechanism (the plate turn out to be weaker than the bolt).

The edge distance had also the same criterion. As we can see in Figure 5.5 the biggest number of cases with bearing failure on the 25 possible (five values for end distance and five values for pitch distance) is $3.5 d_0$. The increase of the edge distance wouldn't increase the cases in bearing. That is way the value for edge distance was $3.4 d_0$, which has the same cases as $3.5 d_0$.

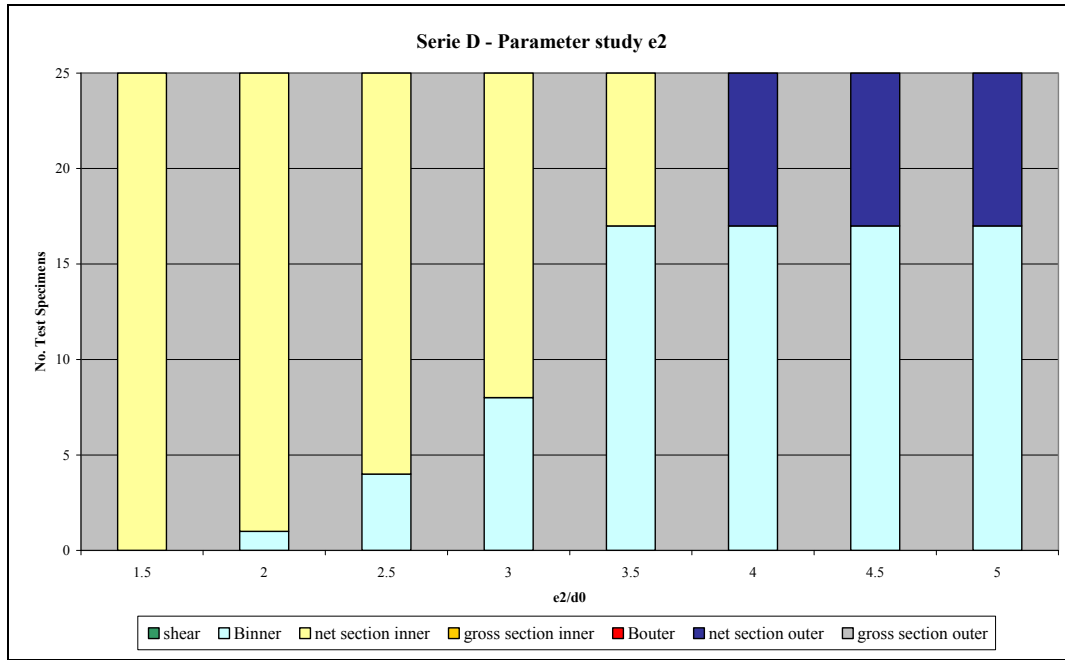


Figure 5.5 – Graph which gives the number of cases in each failure mechanism with different edge distances (e_2).

Reminding the problem which we are studying in the group of fastener. In the test specimens, we concentrate on the behaviour of the bolts in bearing and the resistance of a group of them, if it is possible or not to add all the resistance when all the bolts are in bearing, concerning that high strength steel has less deformation capacity.

As a consequence the test specimens chose of the 25 were also the ones which had the two bolts (end bolt where e_1 is critical and inner bolt where p_1 is critical) with the resistance in shear higher than in bearing ($F_{v,R} > F_{b,R}$) – blue cells in Table 5.6.

e_1 (mm)	end bolt		
	$F_{v,Rd}$ (kN)	$F_{b,Rd}$ (kN)	Failure Mechanism
1	376.8	156.7	Bearing
1.2	376.8	188.0	Bearing
2	376.8	313.3	Bearing
3	376.8	470.0	Shear
3.5	376.8	470.0	Shear
p_1 (mm)	inner bolt		
	$F_{v,Rd}$ (kN)	$F_{b,Rd}$ (kN)	Failure Mechanism
2	376.8	195.8	Bearing
2.2	376.8	227.2	Bearing
3	376.8	352.5	Bearing
3.75	376.8	470.0	Shear
4	376.8	470.0	Shear

Table 5.6 – Resistance of each end and inner bolt varying the end and pitch distance in the joint (yellow – test specimens chose).

The outer plates were design not to be critical in the joint as we are concentrated in bearing of the inner plate. So the values have the same criterion as in the others series A and B:

$$e_1^{outer} = 3.6d_0 = 80mm \Rightarrow \alpha_b = 1.0$$

$$e_2^{outer} = 2.0d_0 = 45mm \Rightarrow k_1 = 2.5$$

$$p_1^{outer} = p_1^{inner}$$

The inner plate of the strongest joint was also design not to be critical in the test specimen. The values of end and pitch distance were chosen in order to have unit values in the reduction factor α_b . The edge distance was the same as for the test joint.

$$e_1 = 3.0d_0 \Rightarrow \alpha_b = 1.0$$

$$p_1 = 3.75d_0 \Rightarrow \alpha_b = 1.0$$

$$e_2 = 3.4d_0 \Rightarrow k_1 = 2.5$$

In Table 5.7, it is summarised the geometric characteristics of the inner plates, test joints – blue, and strongest joints – yellow, as well as their resistance predicted and the correspondent failure mechanism. There were chosen 9 test specimens, both with bearing failure and with the two bolts with bearing resistance being the critical.

$e_1 \backslash p_1 (d_0)$		2	2.2	3	3.75	4
	$e_1 \backslash p_1 (mm)$	44	48	66	83	88
1	22	Binner	Binner	Binner	Binner	Binner
		352.5 kN	383.8 kN	509.2 kN	626.7 kN	626.7 kN
1.2	26	Binner	Binner	Binner	Binner	Binner
		383.8 kN	415.2 kN	540.5 kN	658.0 kN	658.0 kN
2	44	Binner	Binner	Binner	net section inner	net section inner
		509.2 kN	540.5 kN	665.8 kN	709.6 kN	709.6 kN
3	66	Binner	Binner	net section inner	net section inner	net section inner
		665.8 kN	697.2 kN	709.6 kN	709.6 kN	709.6 kN
3.5	77	Binner	Binner	net section inner	net section inner	net section inner
		665.8 kN	697.2 kN	709.6 kN	709.6 kN	709.6 kN

Table 5.7 – Resistance and failure mechanism of test joint (blue) and strongest joint (yellow) in the series D.

Note: for each par of end and pitch distance, the upper cell gives the failure mechanism – “Binner” means bearing of the inner plate and “net section inner” means failure of the net section of the inner plate and the lower gives the calculated resistance of the joint.

In annex A.3 it is described the calculation procedure on the design of this test specimen.

It would be also interesting to have test with bearing failure mechanism but with different resistance on each bolt. Find out what resistance of the group of fasteners if the inner bolt with shear failure and end bolt with bearing failure and the other way around.

6 – Materials, Specimens and Experimental Programme

6.1 – Materials

6.1.1 – Tension tests on the bolts

For the determination of the bolt characteristics, three groups of tension tests were performed, each one with 2 specimens.

Part of the specimen's thread was machined removed. A smaller and constant diameter was obtained in order to have a localization of the bolt rupture - Figure 6.1.



Figure 6.1 – Bolt specimen before testing.

All specimens were tested under tension in a force driven machine with a special test equipment specific for bolts test. The elongation behaviour of the bolt was measured by means of two LVDT (Linear Variable Displacement Transducers) on opposite sides of the test equipment and by a measuring bracket (or horseshoe device). Figure 6.2 (a) and (b) shows pictures of the test set-up.



(a) Test equipment and measuring bracket.



(b) LVDT on opposite sides of the equipment.

Figure 6.2 – Test device for the tension test on the bolts.

Load vs. displacement curves for specimen M24 10.9 are plotted in Figure 6.3. The maximum force – F_u and its corresponding displacement – δ_u can be taken from this graph. In graph of Figure 6.3 is also the data of the measuring bracket up to the elastic range, when it was removed. The results are stiffer in the horse shoe than in the LVDT since the displacements of these also include slippage of the equipment.

The part of the bolt tested in tension is composed of three different sections with three different diameters (total length of unthreaded + total length of machined unthreaded + partial length of thread). A constant area is not available between the measured displacements of the measuring bracket and therefore the determination Young Modulus with the necessary precision is not possible, and this is the reason why the Young modulus is not presented. It was also considered that the correct value of E , is available on the literature and not only very small differences exist in bolt steels but also the value of E is not necessary for the present study.

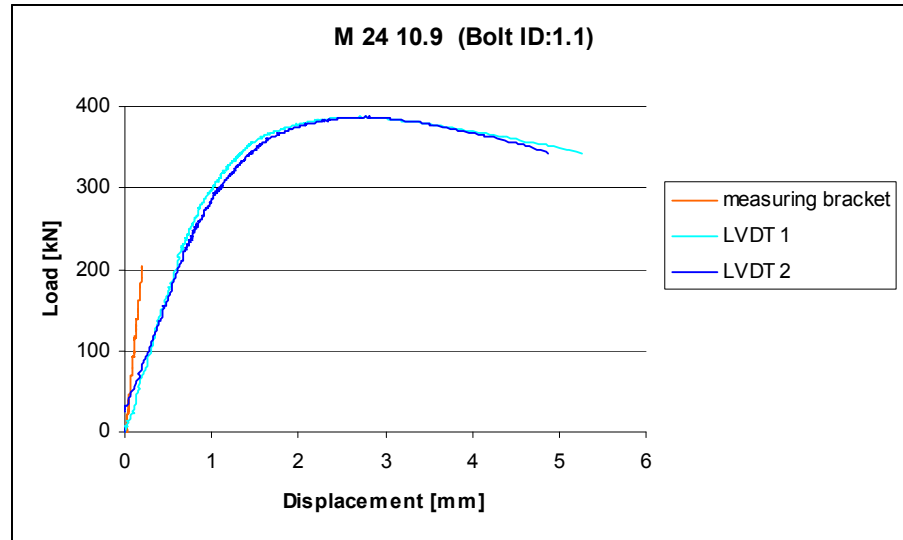


Figure 6.3 – Graph of the tension test on bolt M24 10.9.

The three groups of tests were constituted by:

- Group 1: M24 10.9, Bolt ID 1.1 and 1.2 – Figure 6.4 (a);
- Group 2: M27 8.8, Bolt IB 2.1 and 2.2 – Figure 6.4 (b);
- Group 3: M27 10.9, Bolt ID 3.1 and 3.2 – Figure 6.4 (c).



Figure 6.4 – Bolts specimens.

Five of the six specimens failed by tension on the machined unthreaded part. One bolt M27 10.9 had nut failure and its data was taken off from the average characteristic values.

Table 6.1 summarizes the average relevant characteristics for the tension test on the bolts.

Bolt class	Group	f_u (MPa)	A_u (%)	Z (%)
M24 10.9	1	1229.6	27.5	30.50
M27 8.8	2	974.4	55.5	66.00
M27 10.9	3	1178.8	46.5	55.50

Table 6.1 - Average characteristics values for the bolts.

The percentage elongation after fracture A_u is determined by the permanent elongation of the gauge length after fracture ($L_u - L_0$), expressed as percentage of the original gauge length L_0 [19]. The high values of elongation in group 2 and 3 reveal high ductile material, mainly on group 2 (lowest strength material). This can also be observed in Figure 6.5, looking at the differences of necking on the three different types of bolts and its percentage reduction of area, Z (maximum change in cross sectional area during the test ($S_0 - S_u$) expresses in percentage of the original cross section area (S_0)).



Figure 6.5 – Comparison of the necking on the three groups of specimens (from the left to the right: M24 10.9, M27 8.8, and M27 10.9).

All the data of the tension test on the bolts is in Annex B.1.

6.1.2 – Tension test of the steel plates

For the characterization of the steel plates S690, three tension test were performed in a specialize laboratory. The tests were according to European Norm 10002-1 [19]. All the three specimens were parts of the strips used in the test joints. The average values of the test results are listed in Table 6.2.

	$f_{0.2\%}$	f_u	A_u	Z	f_u/f_y
	N/mm ²	N/mm ²	%	%	-
S 690	769	821	18	75.00	1.07

Table 6.2 - Average characteristics values for the steel plates.

Eurocode 3 indicates requirements for a good material ductility (recommended values up to grade S700) [5]:

- minimum ratio f_u/f_y of 1.05;
- elongation at failure not less than 10 %;
- $\varepsilon_u > \frac{15f_y}{E}$

From the requirements that can be checked (first two), this material verifies in a large range the second and almost verify the first requirement.

All the available data are listed in Annex B.2.

6.2 – Geometrical properties of the specimens

The experimental programme of this study consisted in 30 tests of one bolt connections in bearing. In order to summarize what was described in the previous chapter 5, Table 6.3 lists the general characteristics of the 10 different test specimens (three tests for each - 30 tests in total). Figure 6.6 illustrates an example of test specimen with the notification used.

The values listed in Table 6.3 are nominal values. The actual values of the thirty specimens were measured before testing and are listed in Table C.1 in Annex C.

Test ID	number of tests	Geometry						Bolt			Plate
		e_1/d_0	e_2/d_0	width	t	A_{gross}	A_{net}	d	d_0	Class	Class
				[mm]	[mm]	[mm ²]	[mm ²]	[mm]	[mm]		
A1010	3	1.0	1.0	50	10	500	240	24	26	10.9	S690
A1210	3	1.2	1.0	50	10	500	240	24	26	10.9	S690
A1012	3	1.0	1.2	60	10	600	340	24	26	10.9	S690
A1212	3	1.2	1.2	60	10	600	340	24	26	10.9	S690
A1015	3	1.0	1.5	80	10	800	540	24	26	10.9	S690
A1215	3	1.2	1.5	80	10	800	540	24	26	10.9	S690
A1020	3	1.0	1.9	100	10	1000	740	24	26	10.9	S690
A1220	3	1.2	1.9	100	10	1000	740	24	26	10.9	S690
A2020	3	2.0	1.9	100	10	1000	740	24	26	10.9	S690
B3025	3	3.0	2.5	150	10	1500	1200	27	30	8.8	S690

Table 6.3 – Geometrical characteristics of the specimens (nominal values).

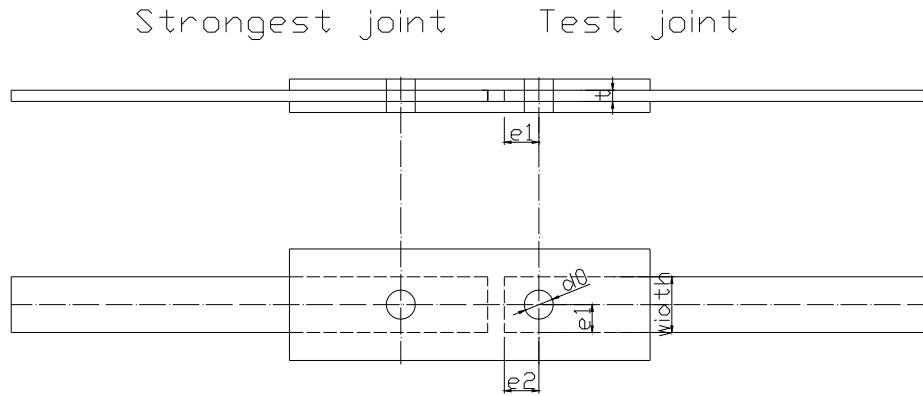


Figure 6.6 – Specimen geometry and notification.

The predicted values for the resistance of the joints with the actual properties of the materials and the actual dimensions of the specimens are listed in Annex C.

The failure mode of series B test specimens changed from bearing of the bolt to bearing of the plate when calculated with the actual strength materials. The ultimate strength actual value of the plate (821MPa) is smaller than the actual ultimate strength of the bolts 8.8 (974 MPa). Therefore, the ratio f_{ub}/f_u of the test joint turns to be bigger than 1.0 when calculated with the values of the material tests. Due to equal geometry of the plates in this series for test joint and strongest joint, both connections have similar loads at failure. Table 6.4 shows the bearing resistance for the series B already corrected with the actual properties of the specimens.

All the other specimens didn't have major changes on their predicted resistance.

Test ID	Geometry		Bolt	Plate	EC3				
	e_1/d_0	e_2/d_0	Class	Class	α_d	f_{ub}/f_u	α_b	k_1	$F_{b,R}$ [kN]
B3025_1T	3.04	2.54	8.8	S690	1.01	1.19	1.00	2.50	560.0
B3025_1S	3.01	2.54	10.9	S690	1.00	1.44	1.00	2.50	576.6
B3025_2T	3.03	2.53	8.8	S690	1.01	1.19	1.00	2.50	560.0
B3025_2S	3.02	2.52	10.9	S690	1.01	1.44	1.00	2.50	576.6
B3025_3T	3.02	2.52	8.8	S690	1.01	1.19	1.00	2.50	560.0
B3025_3S	3.01	2.52	10.9	S690	1.00	1.44	1.00	2.50	562.7

Table 6.4 – Actual properties of Series B test specimens (yellow cells – the design value was $0.85 < 1.0$).

6.3 – Experimental Procedure

The specimens were tested in a force driven testing machine (maximum test load 1000 kN). The tensile force was applied in the inner plates that were clamped to the anchorage devices – Figure 6.7 (a).

The bearing deformation was measured by means of two LVDT (Hewlett-Packard 7DCDT-250):

- LVDT “Hp1”: total elongation of the joint (test + strongest joint).
Measures the displacement of the length between two points as far as possible from the connection - Figure 6.7 (b).
Fixed to the inner plates.
- LVDT “Hp2”: total elongation of the test joint on the opposite side.
Measures the displacement of the length between the bolts and a position approximately 150 mm away - Figure 6.7 (c).
Fixed to the outer plates and inner plates of the test joint.

The measuring devices were already calibrated for previous tests with 25 mm maximum measure.

Figure 6.8 illustrates the measuring instrument’s location on the test specimens.



(a) Test set up



(b) LVDT Hp₁



(c) LVDT Hp₂

Figure 6.7 – Specimen and measuring devices.

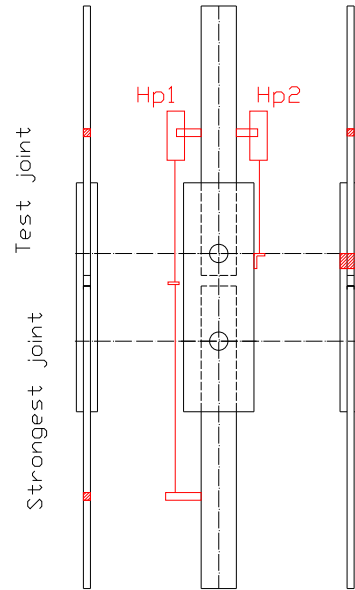


Figure 6.8 – Illustration of the test set-up.

Before installation of the specimens into the testing machine, the dimensions of the plates were measured and the specimen mounted. The specimen was clamped in the upper anchorage device and placed so that all the plates were perfectly aligned. With the specimen self-weight, the bolt gets in contact with the plate before the bolts tight. This way the values measured by the LVDT as well as the load applied during the test are without any initial slip of the plates, since the bolts are already in contact with the plate when the load and measuring begins. After the bolts were hand-tightened, the clamping of the specimen was completed and the LVDT attached. The load was applied up to failure of the test specimen.

The experimental programme had two phases. First, plates were cut and holes were drilled for 10 different test specimens. A regular drilling machine was used and the wire-edge of the hole was taken off. During these first ten tests, the outer plates as well as the inner plates of the strongest joint were observed after failure of the test specimen (that only took place in the inner plate of the test joint). The ones that weren't damage were reused on the other tests which had the same geometry for the outer plates or for inner plate of the strongest joint. In the end, only specimens A2020 and B3025 were tested with all the plates new in their three tests, due to damages not only in the inner plate of the test joint. The same was made with bolts of series A – M24 10.9. Only 4 pairs of bolts (8 in total) were used in the total tests of series A. Therefore our aim to reduce time of preparation of the test specimens was succeeded. On the second phase of 20 tests, the time for drilling holes and cutting plates was reduced a lot.

7 – Results

7.1 – Test Results and Observations

Nine test specimens had bearing as failure mode. One specimen skipped out from the predicted failure mechanism and failed on the net section. This specimen was A1210: end distance $1.2d_0$ and edge distance $1.0d_0$.

Table 7.1 lists the failure mechanism, maximum load, F_u and its displacement δ_u for each test specimen.

Test specimen	F_u	δ_u	Failure mechanism
	[kN]	[mm]	
A1010	178.1	5.4	Bearing
A1012	183.1	5.0	Bearing
A1212	226.2	4.8	Bearing
A1015	192.0	5.7	Bearing
A1215	228.2	5.6	Bearing
A1020	195.3	4.7	Bearing
A1220	240.6	5.1	Bearing
A2020	390.8	11.7	Bearing
B3025	631.4	22.3	Bearing
A1210	209.0	4.1	Net section

Table 7.1 – Average values of the test results for each specimen type.

The values in Table 7.1 are averages for the three tests made for each type of test specimen. These three tests didn't have major deviations between each other. They had always the same failure mechanism and the maximum deviation to the average value of the maximum load is 4%. This way all the following graphs of the test results are representative of the entire three tests for each type of specimen although only one plot of the three test results is presented.

Figure 7.1 plots the load-displacement curves of the two failure mechanisms observed. The displacement values are of the test joint, measured by LVDT Hp2. The curves plotted are from A1212, specimen with bearing failure with the same end distance as the specimen A1210 (net section failure), the other specimen represented. Some differences between these two failures mechanism can be confirmed with this graph.

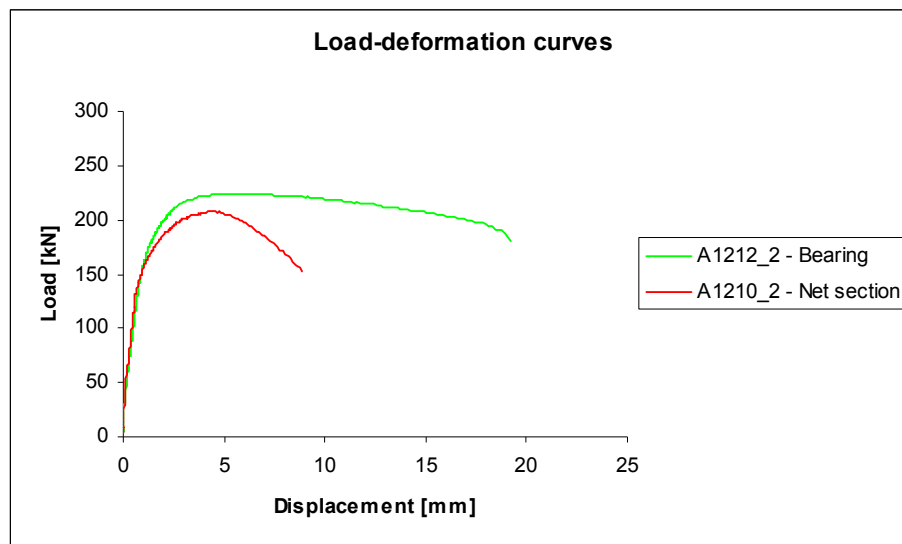


Figure 7.1 – Load-displacement curves for the two different failure mechanisms occurred in the test.

The maximum load is reached approximately at the same displacement. However, the rupture occurs much earlier for the net section failure than for the bearing failure. This reveals a higher ductile behaviour for the bearing than for the net section failure, as was already mentioned in previous chapters.

The allowance of high deformation in ultimate states and the fact that this higher deformation can be reached with bearing failure, lead the resistances formula of bearing to higher values than the ultimate force of the section. The 2.5 value of k_1 is the practical result of these statements.

Figure 7.2 shows photographs of the failure section, of the inner plates of those test specimens.



(a) bearing failure mechanism A1212_2



(b) net section failure mechanism A1210_2

Figure 7.2 – Failure of the inner plates of the test joint of specimens A1212_2 and A1210_2.

The main phenomenon in study is bearing failure, therefore our analyses results will focus in this type of failure mechanism. This way the specimen A1210 will be out of some further analyses.

Figure 7.3 plots load-displacement curves of the tests, with the specimens with constant edge distance and different end distances. Figure 7.4 plots load-displacement curves of the tests with specimens varying the edge distance and keeping constant the end distances.

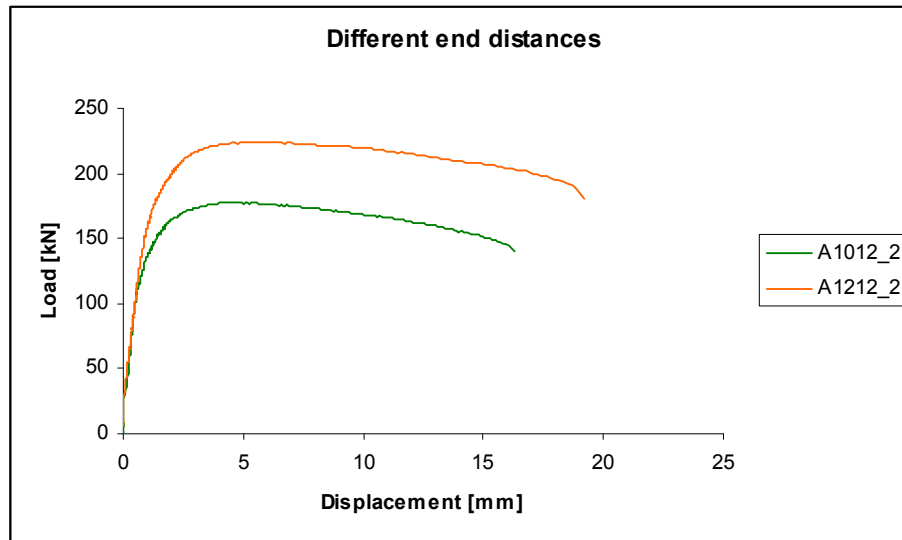


Figure 7.3 – Load-displacement curves of specimens with the same edge distance and different end distance.

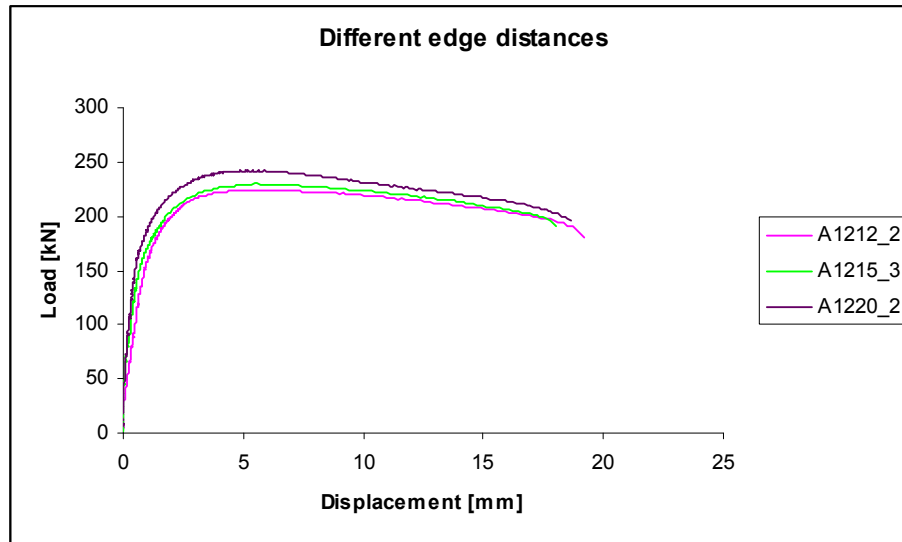


Figure 7.4 – Load-displacement curves of specimens with the same end distance and different edge distance.

As the end distance increases, the deformation at failure (δ_{\max}) increases as well as the ultimate force. For example, δ_{\max} is 16 mm for a specimen with an end distance 1.0 d_0 and an edge distance 1.2 d_0 (A1012) and 19 mm for an end distance 1.2 d_0 and the same edge distance (A1212). Kim and Yura, 1997 [10] reported the same behaviour in steel with lower strength ($f_{y1}=267$ N/mm², $f_{u1}=430$ N/mm², elongation 30% and $f_{y2}=483$ N/mm², $f_{u2}=545$ N/mm², elongation 18%).

On the contrary, as the edge distance increases, δ_{\max} and the ultimate force are approximately the same. Therefore, more deformation capacity and resistance can be achieved by increasing the end distance rather than edge distance. If we add the same distance to the end and to the edge distance, the resistance will increase much more on the bigger end distance than on bigger edge distance.

Kim and Yura [10] used one bolt test specimens with constant edge distance and several end distances. They carried out tests with two steel grades that correspond approximately to S235 and S460. Since no reference tests were made in this study, the results of Kim and Yura investigation will be compared with ours. The test specimens selected to be compared had to have the same geometry properties, edge and end distance when normalized by d_0 .

The only specimens possible to be compared (same end and edge distance) are A1020 and A2020. The only main difference between our test specimens and Kim and Yura test specimens is the thickness. In our case is 10 mm and in their case is 5 mm. Nevertheless, some important comparisons were made.

Table 7.2 summarizes the main properties of the three steel grades to be compared.

Steel Grade	~S235	~S460	S690
f_y [MPa]	263	483	769
f_u [MPa]	430	545	821
A_u [%]	30	18	18

Table 7.2 – Steel grades used in this investigation (S690).and in Kim and Yura investigation (~S235 and ~S460).

Table 7.3 list the average values for the displacement at the maximum force, for the two test specimens in the three steel grades.

δ_u [mm]	~S235	~S460	S690
A1020	5	6	5
A2020	13	12	12

Table 7.3 – Displacement at the maximum force of two test specimens using different steel grades.

As Kim and Yura [10] reported, the specimens have similar deformation capacities. This is contrary to what was expected, especially between specimens made of ~S235 and made of ~S460 or S690. The specimens made of ~S235 were expected to have higher deformation capacity than the others, since the elongation at failure in ~S235 is almost twice the others. Between specimens made of ~S460 and S690 a lower difference was expected, since they have the same elongation at failure (18%).

All specimens had significant bearing deformation. At the far end, the specimens failed either on the plate or on the bolt (exception made to the specimen with net section failure). The shear of the bolt at the far end only occurred in one tests specimen of the B3025, due to small bearing deformation on the bolt 8.8. Figure 7.5 shows these two phases of failure on specimen A1220_3: bearing and then finally shear of the plate

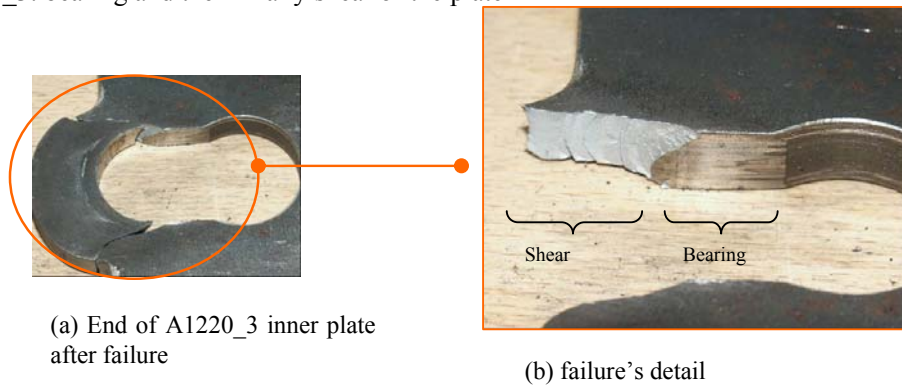


Figure 7.5 – Bearing and shear deformations of the inner plate after failure (A1220_3).

The yield lines shown in Figure 7.6 define the principal stress path that starts from the edge of the hole and continues till the end of the plate. A shear fracture started at the edge of the hole and/ or a tensile fracture started at the end of the plate.

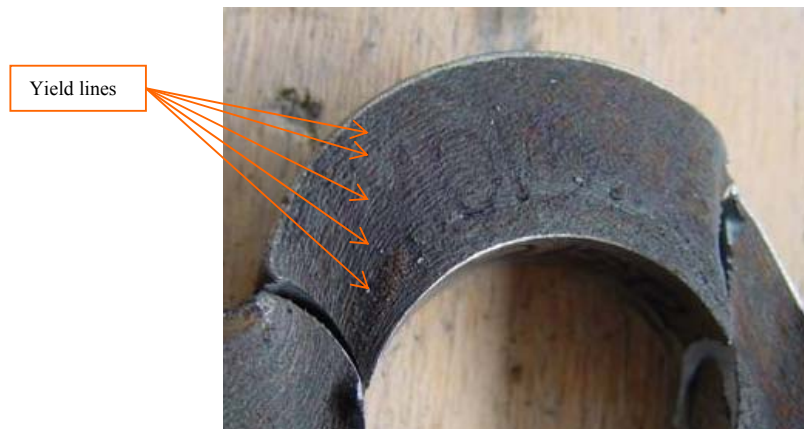


Figure 7.6 – Yield lined in the end of the inner plate of specimen A1015_2.

The specimens with end distance smaller than $2.0 d_0$ failed with shear fracture of the plate. Where shear fracture occurred and specimens had small edge distances ($e_2 \leq 1.2 d_0$), the end of the plate split (A1010, A1012, A1212). For specimens with bigger edge distances, the end of the plate just shears-out without splitting. Figure 7.7 shows the end of the inner plate of test specimens A1010_1 and A1220_1, with shear fracture with splitting and without splitting, respectively.



Figure 7.7 – Shear fracture with splitting and without splitting present on test specimens A1010_1 and A1220_1, respectively.

The test specimen with $2.0 d_0$ end and edge distance (A2020) failed with tensile fracture started at the end of the plate mixed with shear fracture. The tensile fracture at the end of the plate is caused by the transverse tensile stress. As the specimen deforms, the material at the end becomes thinner and becomes susceptible to tensile fracture. In this case, split occurs at the end of the plate. Figure 7.8 shows the mixed tensile fracture and shear fracture on test specimen A2020_1.



Figure 7.8 – Shear and tensile fracture present on test specimen A2020_1

Kim and Yura (1997) [10] also reported in their test specimens these two kinds of fracture, tensile and shear. However the observations are opposite to ours, the tensile fracture is associated with short end distances rather than long end distances. Although the strength of the steels in this study and in Kim and Yura [10] study is different, the elongation is equal in both – 18%. Therefore, the only reason founded to the observations in both tests to be different is the different thickness between the specimens.

Specimen B3025 presented the biggest differences at failure in the three repeated tests. B3025_1 failed at the test joint by shear of the bolt (bolt 8.8). When dismantling the specimen a large bearing deformation was observed in both joints and this is why it was considered bearing and not shear of the bolt as failure mechanism. The only difference is instead of shear of the plate at the end of test, the bolt turn to be weaker than the end of the plate. Observing the bolt 8.8 of the test joint, we can see a small deformation due to bearing of the bolt due to a ratio f_{ub}/f_u close to 1.0 value (1.19). Figure 7.9 shows both bearing deformation (plate and bolt) on test joint of B3025_1.

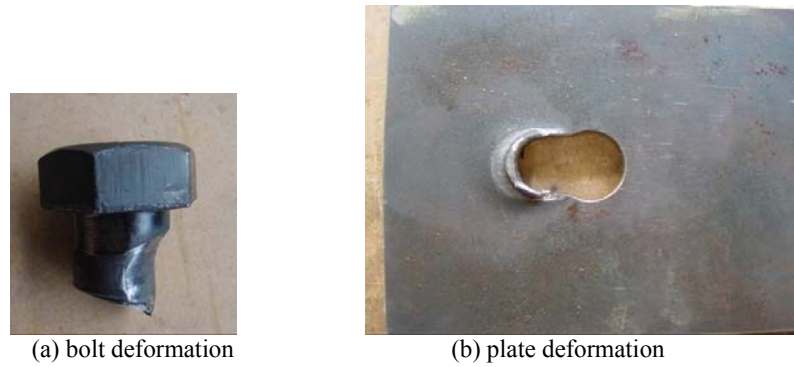


Figure 7.9 – Bearing deformations on B3025_1 test specimen.

B3025_2 and B3025_3 failed at the strongest joint by shear of the plate. Unfortunately, this joint was so damaged that couldn't be dismantled. Therefore no precise observations can be reported. The test joint could be dismantled and bearing deformation was observed both in the plate and in the bolt 8.8 with the approximately the same values as B3025_1. The deformation measured by the LVDT Hp2 includes not only the deformation of the plate, but also the small deformations of the bolt.

7.2 – Comparison with EC3

Table 7.4 lists the maximum load, F_u , as well as the resistance predicted value for each test specimen failed by bearing. Table 7.5 lists the same values for the test specimen that failed by the net section. The reason to split the results is related to further observations that will put apart the net section specimen. The percentage of error also listed in the tables is given by the formula:

$$\%error_i = \frac{r_{ei} - r_{ti}}{r_{ti}} \times 100 \quad (7.1)$$

r_{ei} – experimental value (F_u)

r_{ti} – predicted value ($F_{b,R}$)

Test specimen	F_u	$F_{b,R}$	error
	[kN]	[kN]	%
A1010	178.1	70.5	152.5
A1012	183.1	102.3	79.1
A1212	226.2	124.4	81.8
A1015	192.0	167.7	14.5
A1215	228.2	198.8	14.8
A1020	195.3	166.2	17.5
A1220	240.6	200.4	20.1
A2020	390.8	331.8	17.8
B3025	631.4	566.4	11.5

Table 7.4 – Test results for specimens with bearing failure.

Test specimen	F_u	$N_{u,R} * 1.25$	error'	$F_{b,R}$	error
	[kN]	[kN]	%	[kN]	%
A1210	209.0	186.3	12.2	83.9	149.1

Table 7.5 – Test results for the specimen with net section failure.

On Table 7.5 the percentage of error is also listed to the net section predicted load resistance (error'). On the test specimens design, the formula for the net section resistance, $N_{u,R}$,

included the safety factor $\gamma_{M2}=1.25$, in order to prevent as much as possible the failure of the net section.

$$N_{u,R} = \frac{0,9 A_{net} f_u^I}{\gamma_{M2}}$$

Therefore to calculate the predicted value for failure, $N_{u,R}$ has to be multiplied by γ_{M2} . That is why $N_{u,R}$ is multiplied by $\gamma_{M2}=1.25$ on the table 7.2 and with this value the percentage of error (error') is calculated.

All values for the percentage of error are positive which means that all the predicted values given by EC3 are conservative.

Considering the predicted values for bearing resistance given by EC3, the test results were split in two. Looking at Table 7.4 and 7.3, it is perfectly clear two mean values of errors in the ten test specimens:

- Group I: where edge distance is smaller than 1.2 d_0 , inclusive, the mean value for error is 95%:
 - A1010 152%
 - A1210 149% (considering $F_{b,R}$)
 - A1012 79%
 - A1212 81%
- Group II: where the edge distance is higher than 1.5 d_0 , inclusive, the mean value for error is 15%:
 - A1015 14.5 %
 - A1215 14.8%
 - A1020 17.5%
 - A1220 20.1%
 - A2020 17.8%
 - B3025 11.5%

Of course, it is not a coincidence that the specimen with net section failure is in the first group. The reason for failure of the net section instead of bearing is the excessive conservative values given by EC3 to the bearing resistance for small edge distances.

Figures 7.10 and 7.11 plot the load-displacement curves of the experimental test and the predicted value given by the EC3 for one test specimen for each group. The differences between the distances of the predicted value and experimental value for the maximum bearing load of the connection for each group are clear.

Figure 7.12 plots the same graph but for the specimen A1210. Both the predicted values for the bearing resistance and net section resistance are shown. The different distances between these values and the experimental value reveals the incorrect and correct formula given by the EC3 for bearing and net section resistance of this connection, respectively.

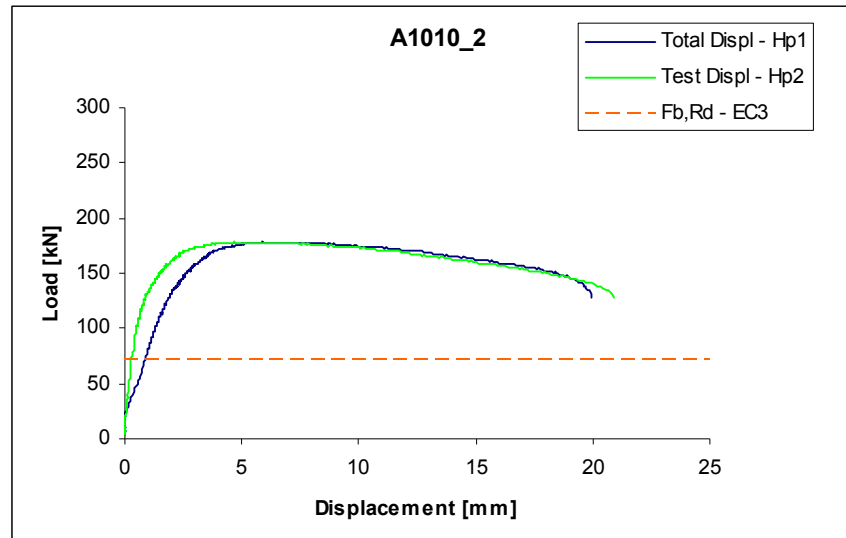


Figure 7.10 – Load-displacement curves for A1010_2 test specimen with high distance between the predicted value and experimental value for the maximum bearing load of the connection.

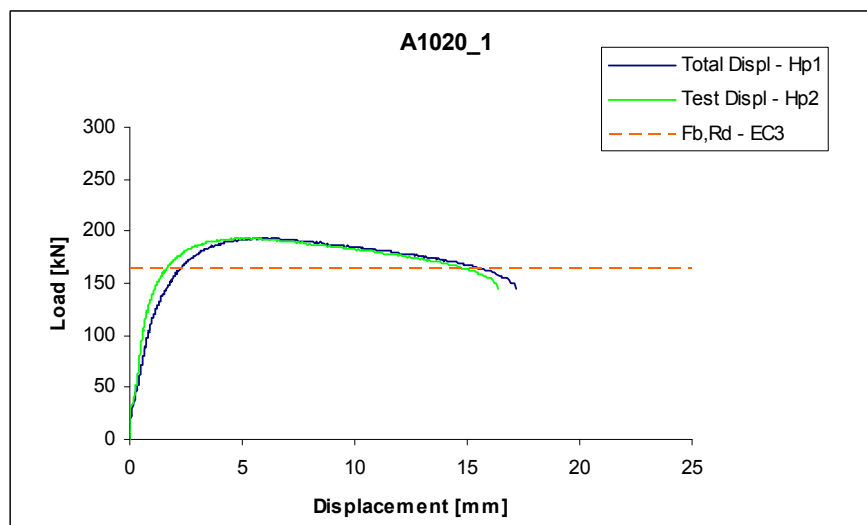


Figure 7.11 – Load-displacement curves for A1020_2 test specimen with low distance between the predicted value and experimental value for the maximum bearing load of the connection.

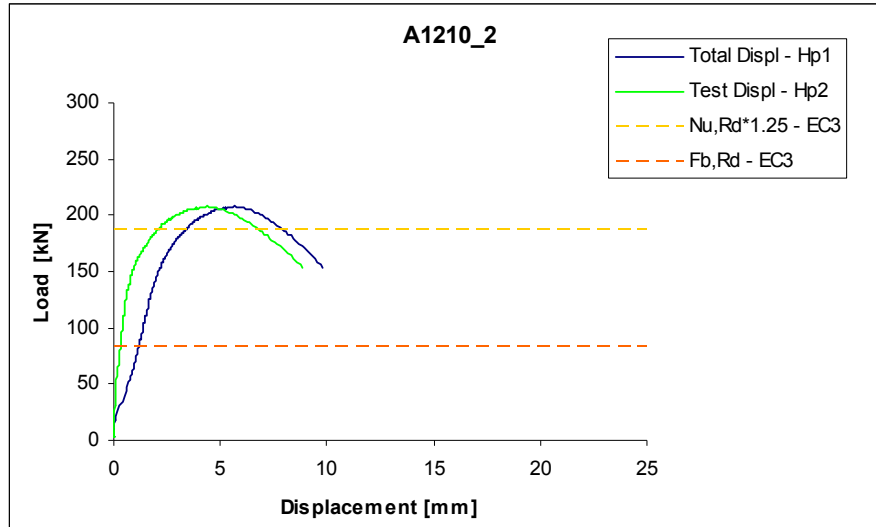


Figure 7.12 – Load-displacement curves for A1210_2 test specimen.

To sum up, the formula for bearing resistance as given in EC3 applied to our test specimens is too much conservative for edge distances $e_2 \leq 1.2 d_0$ and lightly conservative for edge distances $e_2 \geq 1.5 d_0$.

The data of all the thirty tests specimens as well as measurements after failure is presented in Annex D.

8 – Statistical evaluation

Annex Z [20] gives specific guidance on evaluating the tests results according to EC3. This annex describes a standard procedure for determining characteristic values, design values and partial factors for resistance γ_R from the test results.

The efficiency of the resistance function for bearing resistance, $F_{b,R}$ (design model) is checked by means of a statistical interpretation of the available test data. The variation in the prediction of the design model is also determined from the tests and is combined with the variations of the other variables in the resistance function of $F_{b,R}$. These include the variation in material strength and in geometrical properties.

To permit this study to follow the standard evaluation procedure of Annex Z, some assumptions were made:

- The resistance function $F_{b,R}$ is a function of a number of independent variables;

$$F_{b,R} = k_1 \alpha_b f_u d t$$

- 27 test results available for the resistance function are considered sufficient;
- There isn't any correlation (statistical dependence) between the variables in the resistance function;
- All variables follow a log-normal distribution.

Test specimen A1210, with net section failure mechanism, was taken off from this analyses, since it's the bearing resistance function that is going to be evaluated and not the net section resistance.

The test results were split in the same two groups mentioned in the previous chapter: Group I, $e_2 \leq 1.2 d_0$ and Group II, $e_2 \geq 1.5 d_0$. This way we are preventing a wrong influence between those two different results. It was also made the same evaluation with all the test results in one group but as expected the results weren't good. The data of this evaluation is not reported in the body of the report but is available in Annex E.2.

8.1 – Standard Procedure

1. Theoretical resistance, r_t

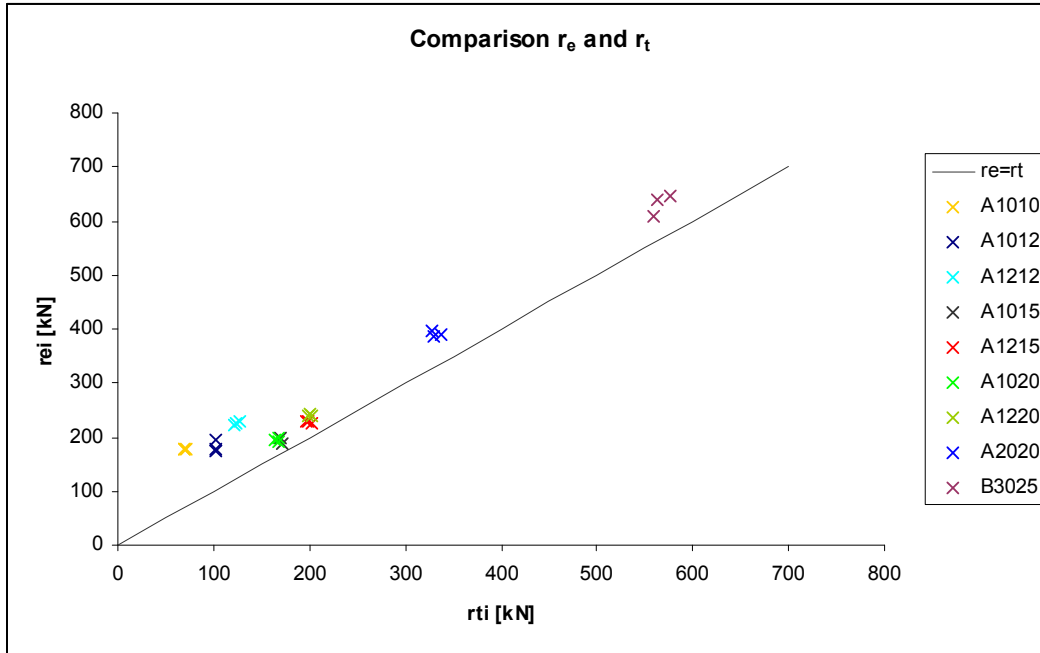
$$r_t = g_{rt}(\underline{X}) = F_{b,R} = k_1 \alpha_b f_u d t \quad (8.1)$$

where \underline{X} - basic variables that affect the resistance

2. Compare experimental values, r_{ei} and theoretical values, r_{ti}

[r_{ti} values are obtained with the actual measured dimensions and material strengths]

The pairs of corresponding values (r_{ti} , r_{ei}) are plotted on a diagram – Figure 8.1. All the points lie above the line $r_t = r_e$, which means that all theoretical values are conservative to the test results.

Figure 8.1 – r_e – r_t diagram.3. Mean value of the correction factor $\bar{b}_{(r)}$

- Probabilistic model of the resistance r : $r = b r_t \delta$ (8.2)

δ - error term, such that the mean value $E(\delta) = 1.0$

- Correction term for each test specimen $b_i = r_{ei} / r_{ti}$ (8.3)

$$\text{Mean correction factor } \bar{b}_{(r)} = \frac{1}{n} \sum_{i=1}^n b_i \quad (n - \text{number of test}) \quad (8.4)$$

Figure 8.2 plots the r_e – r_t diagram where the mean value correction factor $\bar{b}_{(r)}$ is represented by a slope of a straight line passing the origin:

$$r_e = \bar{b}_{(r)} r_t \quad (8.5)$$

(Mean value of the test results as a correction of the theoretical values)

Table 8.1 list the correction factor calculated with the test results of each group as well as the available number of tests.

	Group I $e_2 \leq 1.2 d_0$	Group II $e_2 \geq 1.5 d_0$
$\bar{b}_{(r)}$	2.04	1.16
n	9	18

Table 8.1 – Mean correction factor and number of test results used.

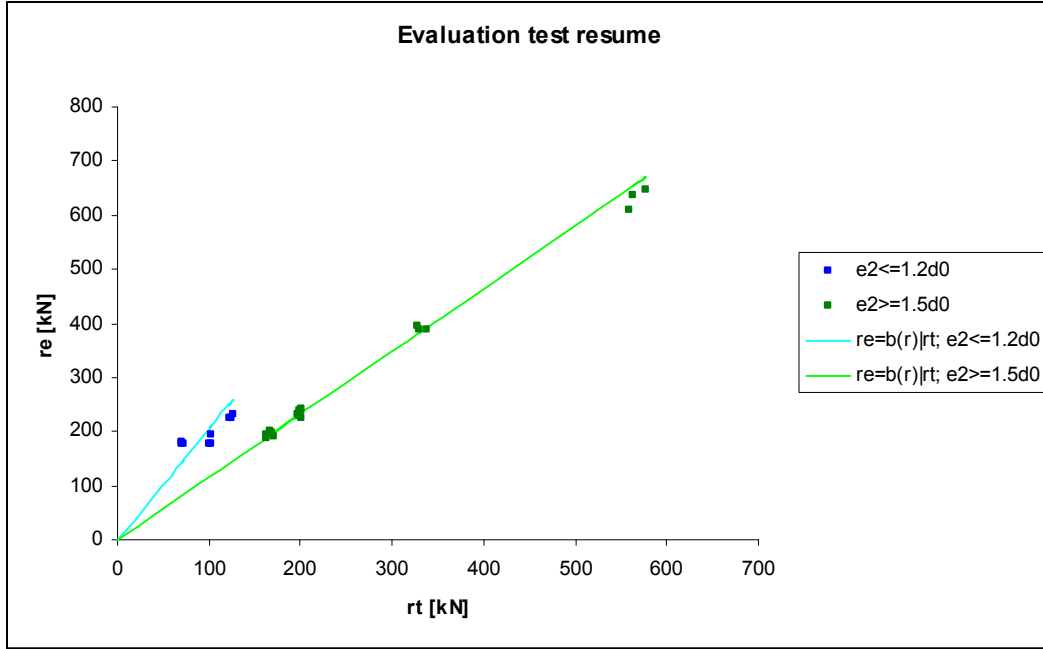


Figure 8.2 – re - rt diagram with the mean value correction line $r_e = \bar{b}_{(r)} r_t$

Note: the evaluation without splitting the test has its main problem in this correlation factor. Since these factors were too different in the first group to the second group, the mean value of the test results calculated as a correction of the theoretical values by mean of the correction factor was too unequal to the real experimental values when using all the data together (the deviations between the mean value and the real value were too high) – see Annex E.2.

4. Coefficient of variation V_{δ} of the error term δ

$$\delta_i = \frac{r_{ei}}{\bar{b} r_{ti}} \text{ for each experimental value for } i=1 \text{ to } n \quad (8.6)$$

$$\Delta_i = \ln(\delta_i); \quad \bar{\Delta} = \frac{1}{n} \sum_{i=1}^n \Delta_i; \quad s_{\Delta}^2 = \frac{1}{n-1} \sum_{i=1}^n (\Delta_i - \bar{\Delta})^2$$

$$\text{Finally, } V_{\delta}^2 = \exp(s_{\Delta}^2) - 1 \quad (8.7)$$

Table 8.2 lists the coefficient of variation V_{δ} calculated for each group of test specimens.

	Group I $e_2 \leq 1.2 d_0$	Group II $e_2 \geq 1.5 d_0$
V_{δ}	0.17	0.03

Table 8.2 - Coefficient of variation V_{δ} for each group.

5. Coefficient of variation V_{X_i} of the basic variables

The coefficients of variation V_{X_i} should be determined on the basis of prior knowledge. The values used were obtained from the example given in Annex Z [20]. The following values have been determined from previous studies:

- $V_{dn}=0.005$
- $V_t=0.05$
- $V_{fu}=0.07$

Considering the formula for the bearing resistance, the basic variables left are the edge and end distance (for the parameters k_1 and α_b , respectively). Since these values are measured dimensions, the value for the coefficient was taken equal to the thickness of the plate, because it is also a measured variable.

- $V_{ab}=V_{e1}=V_t=0.05$
- $V_{k1}=V_{e2}=V_t=0.05$

6. Characteristic value r_k of the resistance

It was considered that the number of test results was limited to a small number - $n = 27 \neq \infty$. In this case the characteristic resistance r_k is given by:

$$r_k = r_m \times \exp\left(-u_{k,\infty}\alpha_{rt}Q_{rt} - u_{k,n}\alpha_{\delta}Q_{\delta} - 0.5Q^2\right) \quad (8.8)$$

where

- $r_m = \bar{b}_{(r)}r_t(X_m)$, the mean value of the test results as a correction of the theoretical values calculated using mean values X_m of the basic variables.
- $u_{k,n}$ is the characteristic fractile factor, that for 27 total number of results is equal to 1.74 (obtained from linear interpolation from the values for $n=20$ and $n=30$).
- $u_{k,\infty}$ is the value for $u_{k,n}$ for $n \rightarrow \infty$ and is equal to 1.64.
- $Q = \sigma_{\ln(r)} = \sqrt{\ln(V_r^2 + 1)}$
- $Q_{rt} = \sqrt{\ln(V_{rt}^2 + 1)}$
- $Q_{\delta} = \sqrt{\ln(V_{\delta}^2 + 1)}$
- $\alpha_{rt} = \frac{Q_{rt}}{Q}$
- $\alpha_{\delta} = \frac{Q_{\delta}}{Q}$

$\sigma_{\ln(r)}$ is the standard deviation of the variable $\ln(r)$.

V_r is the coefficient of variation of the variable r and for small values of V_{δ}^2 and

V_{Xi}^2 :

$$V_r^2 = V_{\delta}^2 + V_{rt}^2 \quad \text{with} \quad V_{rt}^2 = \sum_{i=1}^j V_{Xi}^2, \quad j - \text{number of basic variables}$$

Table 8.3 lists the values calculated for the two groups of tests results.

	Group I	Group II
V_{δ}^2	0.03	0.001
V_{rt}^2	0.01	0.01
V_r^2	0.04	0.01
$u_{k,n} (n=27)^{(*)}$	1.74	
$u_{k,\infty}$	1.64	
Q	0.20	0.12
Q_{rt}	0.11	0.11
Q_{δ}	0.17	0.03
α_{rt}	0.55	0.97
α_{δ}	0.84	0.26

Table 8.3 – Values for the calculation of r_k .

(*) In Annex Z is stated that the fractile factors u_k may be determined on the basis of the total number of the tests in the original series, $n=27$, since the phenomena in all tests is the same.

7. Design value r_d of the resistance

The procedure for determining the characteristic value r_k is extended to obtain the design value of the resistance r_d , replacing the characteristic fractile factor u_k by the design fractile factor u_d .

$$r_d = r_m \times \exp(-u_{d,\infty} \alpha_{rt} Q_{rt} - u_{d,n} \alpha_{\delta} Q_{\delta} - 0.5 Q^2) \quad (8.9)$$

where

- $u_{d,n}$ is the design fractile factor, that for 27 total number of tests results is equal to 3.50 (obtained from linear interpolation from the values for $n=20$ and $n=30$).
- $u_{d,\infty}$ is the value for $u_{d,n}$ for $n \rightarrow \infty$ and is equal to 3.04.

An initial estimative for the partial factor γ_R is calculated by the formula $\gamma_R = r_k / r_d$ and is listed in Table 8.4.

	Group I	Group II
γ_R	1.40	1.18

Table 8.4 – Initial estimative for the partial safety factor.

8. Partial safety factor γ_R

Ratio k_c is calculated between the nominal resistance r_n and characteristic resistance r_k . The nominal resistance is calculated using the nominal values of the material strength ($f_u=770$ MPa) and the nominal values for the geometrical variables (d and t).

$$k_c = r_n / r_k$$

Therefore, a corrected partial safety factor is calculated by:

$$\gamma_R^* = k_c \gamma_R = (r_n / r_k) (r_k / r_d) = r_n / r_d \quad (8.10)$$

To keep the same value of the safety factor in the formula of bearing resistance $\gamma_{M2}=1.25$, this resistance function should be modified:

$$F_{b,Rd}^{new} = \frac{\alpha_b k_1 f_u dt}{\gamma_R^*} \times \frac{\gamma_{M2}}{\gamma_{M2}} = \frac{\alpha_b k_1 f_u dt \times \gamma_{M2} / \gamma_R^*}{\gamma_{M2}} = F_{b,Rd} \times \underbrace{\frac{\gamma_{M2}}{\gamma_R^*}}_{\text{correction factor } [CF]} \quad (8.11)$$

Table 8.5 lists the values of this correction factor as well as k_c and γ_R^* for each group of test specimens.

	Group I $e_2 \leq 1.2 d_0$	Group II $e_2 \geq 1.5 d_0$
k_c	0.66	0.98
γ_R^*	0.93	1.16
$CF = \gamma_{M2} / \gamma_R^*$	1.34	1.08

Table 8.5 – Values of k_c , γ_R^* , γ_{M2} / γ_R^* obtained for each Group I and II.

As expected the correction factors are bigger than 1.0, due to excessive conservative values of resistance obtained from the bearing formula given by EC3.

All the data of this statistical evaluation is available in Annex E.1.

8.3 – Proposed correction for the k_I factor

The correction factor obtained was attached to the k_I factor since the split of tests results was based on the edge distance of each test specimen. There fore, a new function for k_I is proposed for steel grade S690 based on the statistical evaluation.

$$F_{b,Rd}^p = \frac{\alpha_b (CF \times k_I) f_u dt}{\gamma_{M2}} = \frac{\alpha_b k_I^p f_u dt}{\gamma_{M2}} \quad (8.12)$$

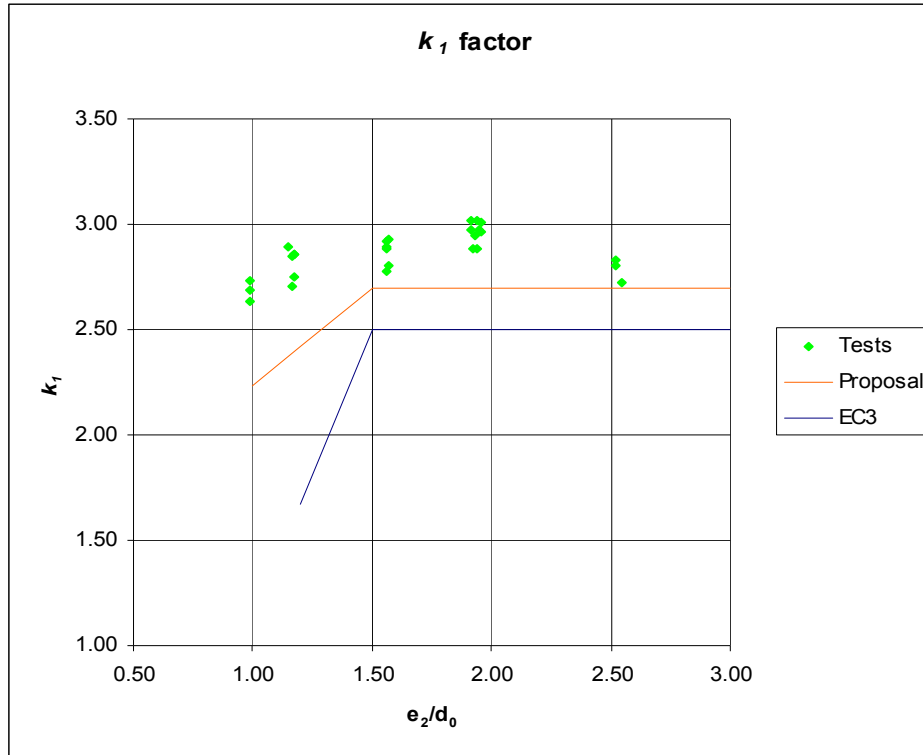
The minimum distance required in the EC3 for edge distance and end distance is also to sever. According to our test results a significant resistance can be achieved even for $e_2 < 1.2d_0$ and $e_1 < 1.2d_0$ (minimum distances required by EC3). There fore, these minimum distances required in the EC3 can both be reduced to $1.0d_0$.

Table 8.6 lists the present rules in the EC3 and the correspondent proposed modification for each one.

	EC3		Proposal	
Bearing resistance, $F_{b,Rd}$	$k_I = \chi_{red} \times 2.5$		$k_I = \chi_{red}^p \times 2.5$	
	$e_2 = 1.2d_0$	$\chi_{red} = \frac{2}{3}$	$e_2 = 1.0d_0$	$\chi_{red}^p = CF^{GroupI} \times \chi_{red} = 1.34 \times \frac{2}{3}$
	$e_2 \geq 1.5d_0$	$\chi_{red} = 1.0$	$e_2 \geq 1.5d_0$	$\chi_{red}^p = CF^{GroupII} \times \chi_{red} = 1.08 \times 1.0$
	$1.2d_0 < e_2 < 1.5d_0$	Linear interpolation	$1.2d_0 < e_2 < 1.5d_0$	Linear interpolation
Minimum distances	$e_2^{\min} = 1.2d_0$		$e_2^{\min} = 1.0d_0$	
	$e_1^{\min} = 1.2d_0$		$e_1^{\min} = 1.0d_0$	

Table 8.6 – Comparison between the present rules in EC3 and the proposed ones.

Figure 8.3 plots the function k_I given in EC3, its proposal modification and the k_I values for the 27 tests results.

Figure 8.3 – Values for the factor k_1 .

The comparison to k_1 function suggested by Puthli [6] is presented in Figure 8.4. Although both proposal functions are less conservative than EC3 functions, the values don't seem to be similar.

Puthli [6] corrections functions is based on plate S460, and it wasn't made by a statistical evaluation. Besides that, the data used for this function hadn't only bearing as failure mechanism, it was also included data with net section failure. This can induce wrong conclusions in the corrections of the bearing resistance.

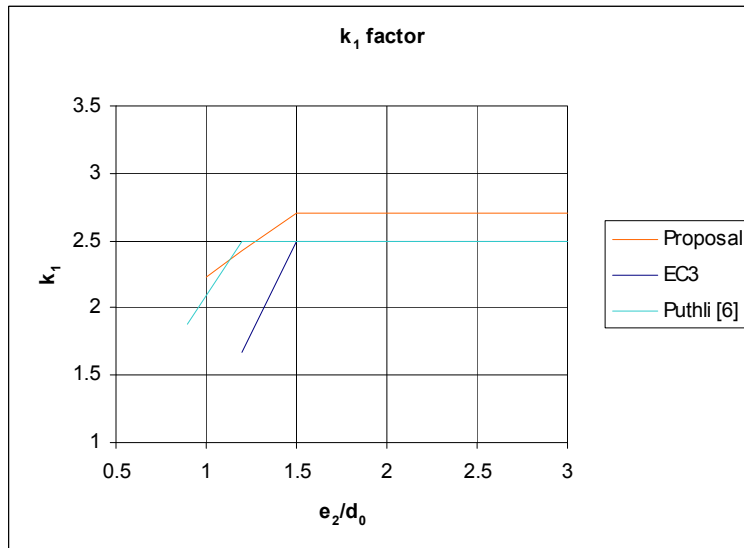


Figure 8.4 – Comparison with previous corrections available in literature.

9 - Conclusions

The rules described in EC3 for bolts in bearing dependent on end-distance, edge-distance and pitch for 8.8 and 10.9 bolt classes are allowed to be used in plates of steel grade up to S700. A series of tests were carried out using specimens designed according to the rules of EC3, in order to investigate whether or not those rules are adequate to high strength steels.

Thirty test specimens of one bolt joints made with steel grade S690 were tested. The end and edge distance varied.

The test results showed that the rules given by EC3 are conservative using steel grade S690:

- For small edge distances $e_2 \leq 1.2 d_0$, the experimental values are 95% higher than the theoretical values.
- For higher edge distances $e_2 \geq 1.5 d_0$, the difference falls to 15%.
- Tests specimens with edge/end distances smaller than the minimums allowed by EC - $1.0 d_0$, had significant resistance.

In order to present a correction to EC3 bearing resistance formula using the available test data from this experimental programme, a statistical evaluation according to EC was carried out (27 tests results). The statistical evaluations gave the following corrections:

- For edge distances $e_2 \leq 1.2 d_0$, the bearing resistance values given by the EC3 rules can be 34% higher.
- For edge distances $e_2 \geq 1.5 d_0$, the bearing resistance values given by the EC3 rules can be 8% higher.

This correction was made in k_1 factor, since the main differences between experimental values/theoretical values were found in tests specimens with different edge distances. There fore a new k_1 functions is suggested for the steel grade S690. The minimum values to edge and end distances can also be reduced from $1.2 d_0$ to $1.0 d_0$.

Concerning deformation capacity, comparing tests data available in the literature [10], specimens with the same geometry properties but with different steel grades (S235, S460, S690) had similar values of deformation at the maximum load. This was not expected.

The steel used in this experimental programme had a significant elongation of 18%, a high value for high strength steel. This can explain the unexpected high deformation

Regarding the definition of “deformation capacity”, some clarification seems appropriate: “Which criterion should be considered to define deformation capacity?” The definition taken in this study corresponds to the deformation level at maximum load. In all the tests, there is a long plateau in load-deformation curve where the maximum load occurs. All the deformation after the maximum load is being disregarded and could be useful in ultimate states. Then, some guidelines are necessary.

The corrections suggested are based only in 10 different tests specimens made of S690. Further investigations to see if all steel grades (from S235 to S700) can be included in such revision would be useful. It should be also reported in those tests the deformation capacity, so it can be compared with high or low steel grades.

This study is based in a limited number of geometries properties, there fore more test should be carried out, even with the same steel grade, in order to have a higher range of end and edge distance.

A statistical analysis should be then followed using all the test data available and adjust the suggested k_1 factor for all the steel grades and geometry properties of one-bolt joints.

Test with the two-bolts joints already designed would be also useful and a perfect following of this study.

10 - References

- [1] European Committee for Standardisation. Eurocode 3: Design of steel Structures. Part 1.8: Design of joints. EN 1993-1-8: 200, Stage 49 draft, June 2004.
- [2] Ed Moore D. B., Wald F., “Design of Structural Connections to Eurocode 3 – Frequently asked questions”, Building research Establishment, Watford, September 2003.
- [3] Bjorhovde, R., Brozzetti, J., Colson, A., “Connections in steel structures: Behaviour, Strength and Design”, Elsevier applied science, 1987, pp. 8-17.
- [4] McCormac, J., Nelson J. K., “Structural Steel Design: LRFD Method”, Third edition, Pearson Education, 2003.
- [5] European Committee for Standardisation. Eurocode 3: Design of steel Structures. Part 1.12: Additional rules for extension of EN 1993 up to steel grades S 700. prEN 1993-1-12: 2005, Stage 49 draft, 8 December 2004.
- [6] Puthli, R., Fleisher, O., “Investigations on bolted connections for high strength steel members”, Journal of Constructional Steel Research, Elsevier, 2001, pp.313-326.
- [7] Kato, B., “Role of strain Hardening of steel in Structural Performance”, ISIJ International, Vol. 30, N°. 11, 1990, pp. 1003-1009.
- [8] Ohashi, M. et al, “Development of New Steel Plates for Building Structural Use”, Nippon Steel Technical Report No. 44, January 1990, pp. 8-20.
- [9] Kulak, G.L., Fisher, J. W., and Struik J. H. A., “Guide to Design Criteria for Bolted and Riveted Joints”, John Wiley and Sons, NY, NY, 1987.
- [10] Kim, H., Yura, J., “The effect of the ultimate-to-yield ratio on the bearing strength of bolted connections”, Journal of Constructional Steel Research 49, 1999, pp.255-269.
- [11] Ju, S., Fan, C., Wu, G., “Three-dimensional finite elements of steel bolted connections”, Engineering Structures 26, 2004, pp. 403-413.
- [12] Aceti R., Ballio, G., Capsoni, A., Corradi, L., “A limit analysis study to interpret the ultimate behavior of bolted joints”, Journal of Constructional Steel Research 60, 2004, pp. 1333-1351.
- [13] Rogers, C., Hancock, G., “Bolted Connection Tests of Thin G550 and G300 Sheet Steels”, Journal of Structural Engineering, July 1998, pp. 798-808.
- [14] Rogers, C., Hancock, G., “Failure Modes of Bolted-Sheet-Steel Connections Loaded in Shear”, Journal of Structural Engineering, March 2000, pp. 288-296.
- [15] Chung, K., Ip K., “Finite element investigation on the structural behaviour of cold-formed steel bolted connections”, Engineering Structures 23, 2001, pp. 1115-1125.
- [16] European Committee for Standardisation. Eurocode 3: Design of steel structures. Part 1.1: General rules and rules for buildings. ENV 1993-1-1, February 1992.
- [17] Shigley, J. E., Mischke, C. R., Budynas, R. G., “Mechanical Engineering Design” Seventh Ed. McGraw-Hill, 2003.

- [18] European Committee for Standardization. EN 10137-2:1996.
- [19] European Committee for Standardisation. EN 10002-1. Metallic Materials – Tensile Testing - Part 1: Method of test at ambiante temperature, July 2001.
- [20] European Committee for Standardisation. Eurocode 3: Design of steel structures. Annex Z [informative]: Determinations of design resistance from tests. ENV 1993-1-1, 1992.

11 - Bibliography

Akbar R. Tamboli, "Handbook of Structural Steel Connection Design and Details", McGraw-Hill, 1999

Bickford, J., "An introduction to the design and behavior of bolted joints", second edition, Marcel Dekker, New York, 1990

ESDEP Lectures

ANNEX A – Design calculation procedure of test specimens

A.1 – Series A

Test Specimen A1215

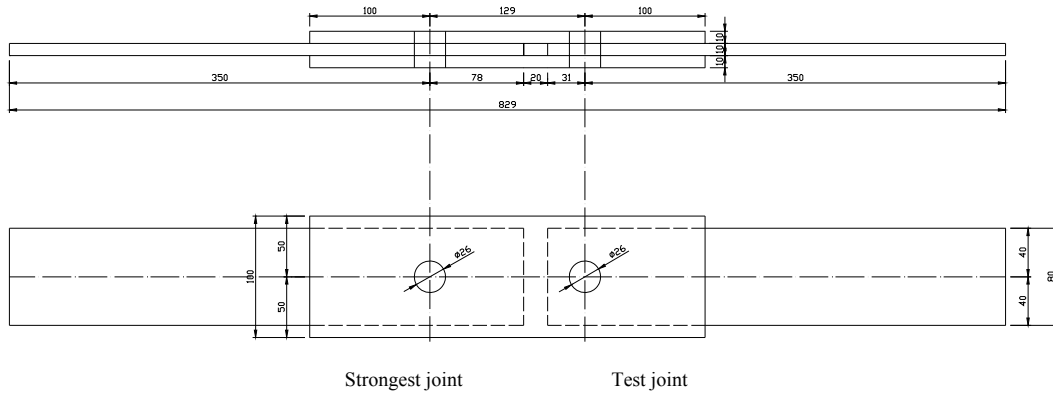


Figure A.1 – Drawing of test specimen A1215 of series A.

	Material properties	Geometric properties
Plates	S690	thickness $t = 10 \text{ mm}$
	$f_y = 690 \text{ N/mm}^2$ $f_{u, \text{lower}} = 770 \text{ N/mm}^2$ $f_{u, \text{higher}} = 940 \text{ N/mm}^2$	
Bolts	10.9	M24
	$f_{yb} = 900 \text{ N/mm}^2$ $f_{ub} = 1000 \text{ N/mm}^2$	$d = 24 \text{ mm}$ $d_0 = 26 \text{ mm}$ $A = 452 \text{ mm}^2$ $A_s = 353 \text{ mm}^2$

Figure A.2 – Table of constituent's properties of the test specimen.

Test joint

$$\text{Inner plate} \begin{cases} e_1 = 1,2 d_0 = 31 \text{ mm} \\ e_2 = 1,5 d_0 = 40 \text{ mm} \\ \text{width} = 2 \times e_2 = 80 \text{ mm} \end{cases} \quad \text{Outer plate} \begin{cases} e_1 = 3,8 d_0 = 100 \text{ mm} \\ e_2 = 1,9 d_0 = 50 \text{ mm} \\ \text{width} = 2 \times e_2 = 100 \text{ mm} \end{cases}$$

i. Shear resistance

per fastener and shear plane: $F_{v,R} = \alpha_v f_{ub} A$

joint $2 F_{v,R} = 2 \times 0,6 \times 1000 \times 452 \times 10^{-3} = 2 \times 271,2 \text{ kN} = 542,4 \text{ kN}$

ii. Bearing resistance

per fastener $F_{b,R} = k_1 \alpha_b f_u^h d t$

- Inner plate

$$\alpha_b = 0,4 \quad \begin{cases} e_1 = 1,2 d_0 = 31 \text{ mm} \Rightarrow \alpha_d = e_1 / 3 d_0 = 0,4 \\ f_{ub} / f_u = \frac{1000}{940} = 1,06 > 1,0 \end{cases}$$

$$k_1 = 2,5 \quad \begin{cases} e_2 = 1,5 d_0 = 40 \text{ mm} \Rightarrow \frac{2,8 e_2}{d_0} - 1,7 = 2,5 \end{cases}$$

$$F_{b,R}^{inner} = 2,5 \times 0,4 \times 940 \times 24 \times 10 \times 10^{-3} = 225,6 \text{ kN}$$

- Outer plates

$$\alpha_b = 1,0 \quad \begin{cases} e_1 = 3,8 d_0 = 100 \text{ mm} \Rightarrow \alpha_d = e_1 / 3 d_0 = 1,3 > 1,0 \\ f_{ub} / f_u = \frac{1000}{940} = 1,06 > 1,0 \end{cases}$$

$$k_1 = 2,5 \quad \begin{cases} e_2 = 1,9 d_0 = 50 \text{ mm} \Rightarrow \frac{2,8 e_2}{d_0} - 1,7 = 3,6 > 2,5 \end{cases}$$

$$F_{b,R}^{outers} = 2 \times (2,5 \times 1,0 \times 940 \times 24 \times 10 \times 10^{-3}) = 1128 \text{ kN}$$

iii. Net cross section resistance

$$N_{u,R} = \frac{0,9 A_{net} f_u^I}{1,25}$$

- Inner plate

$$A_{net} = (width - d_0) t = (80 - 26) \times 10 = 540 \text{ mm}^2$$

$$N_{u,R}^{inner} = \frac{0,9 \times 540 \times 770}{1,25} \times 10^{-3} = 299,4 \text{ kN}$$

- Outer plates

$$A_{net} = (width - d_0) t = (100 - 26) \times 10 = 740 \text{ mm}^2$$

$$N_{u,R}^{outers} = 2 \times \left(\frac{0,9 \times 740 \times 770}{1,25} \times 10^{-3} \right) = 820,5 \text{ kN}$$

iv. Gross section resistance

$$N_{pl,R} = \frac{A_{gross} f_y}{1,0}$$

- Inner plate

$$A_{gross} = width \times t = 80 \times 10 = 800 \text{ mm}^2$$

$$N_{pl,R}^{inner} = \frac{800 \times 690}{1,0} \times 10^{-3} = 552 \text{ kN}$$

- Outer plates

$$A_{gross} = width \times t = 100 \times 10 = 1000 \text{ mm}^2$$

$$N_{pl,R}^{outers} = 2 \times \left(\frac{1000 \times 690}{1,0} \times 10^{-3} \right) = 1380 \text{ kN}$$

$$F_R^{test joint} = \min \{ F_{v,R}; F_{b,R}^{inner}; F_{b,R}^{outers}; N_{u,R}^{inner}; N_{u,R}^{outers}; N_{pl,R}^{inner}; N_{pl,R}^{outers} \} = F_{b,R}^{inner} = 225,6 \text{ kN}$$

Strongest joint

The only different in this test specimen between the test joint and the strongest joint is the end distance in the inner plate. Due to that, it will just be shown the values that are different from the test joint.

$$\text{Inner plate } \{e_1 = 3,0 d_0 = 78 \text{ mm}\}$$

- i. Shear resistance – see test joint
- ii. Bearing resistance

$$\text{per fastener } F_{b,R} = k_1 \alpha_b f_u^h d t$$

- Inner plate

$$\alpha_b = 1,0 \quad \left\{ \begin{array}{l} e_1 = 3,0 d_0 = 78 \text{ mm} \Rightarrow \alpha_d = \frac{e_1}{3 d_0} = 1 \\ f_{ub}/f_u = \frac{1000}{940} = 1,06 > 1,0 \end{array} \right.$$

$$k_1 = 2,5 \quad \left\{ \begin{array}{l} e_2 = 1,5 d_0 = 40 \text{ mm} \Rightarrow \frac{2,8 e_2}{d_0} - 1,7 = 2,5 \end{array} \right.$$

$$F_{b,R}^{inner} = 2,5 \times 1,0 \times 940 \times 24 \times 10 \times 10^{-3} = 564 \text{ kN}$$

- Outer plates – see test joint

- iii. Net cross section resistance – see test joint
- iv. Gross section resistance – see test joint

$$F_R^{strongest joint} = \min \{ F_{v,R}; F_{b,R}^{inner}; F_{b,R}^{outers}; N_{u,R}^{inner}; N_{u,R}^{outers}; N_{pl,R}^{inner}; N_{pl,R}^{outers} \} = N_{u,R}^{inner} = 299,4 \text{ kN}$$

A.2 – Series B

Test Specimen B3025

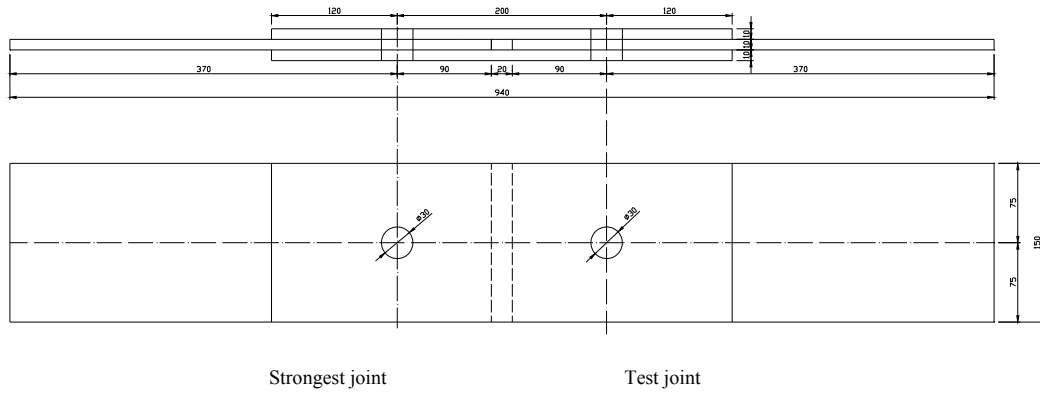


Figure A.3 – Drawing of test specimen B3025 of series B.

	Material properties		Geometric properties
Plates	S690		thickness t = 10 mm
	$f_y = 690 \text{ N/mm}^2$ $f_u^{\text{lower}} = 770 \text{ N/mm}^2$ $f_u^{\text{higher}} = 940 \text{ N/mm}^2$		
Bolts	Test joint: 8.8	Strongest joint: 10.9	M27
	$f_{yb} = 640 \text{ N/mm}^2$ $f_{ub} = 800 \text{ N/mm}^2$	$f_{yb} = 900 \text{ N/mm}^2$ $f_{ub} = 1000 \text{ N/mm}^2$	d = 27 mm d ₀ = 30 mm A = 573 mm ² A _s = 459 mm ²

Figure A.4 – Table of constituent's properties of the test specimen.

Test joint

$$\begin{array}{lcl}
 \text{Inner plate} & \left\{ \begin{array}{l} e_1 = 3,0 d_0 = 90 \text{ mm} \\ e_2 = 2,5 d_0 = 75 \text{ mm} \\ \text{width} = 2 \times e_2 = 150 \text{ mm} \end{array} \right. & \text{Outer plate} \left\{ \begin{array}{l} e_1 = 4,0 d_0 = 120 \text{ mm} \\ e_2 = 2,5 d_0 = 75 \text{ mm} \\ \text{width} = 2 \times e_2 = 150 \text{ mm} \end{array} \right.
 \end{array}$$

i. Shear resistance

per fastener and shear plane: $F_{v,R} = \alpha_v f_{ub} A$

$$\text{joint } 2 F_{v,R} = 2 \times (0,6 \times 800 \times 573 \times 10^{-3}) = 550,1 \text{ kN}$$

ii. Bearing resistance

per fastener $F_{b,R} = k_1 \alpha_b f_u^h d t$

- Inner plate

$$\alpha_b = 0,85 \quad \begin{cases} e_1 = 3,0 d_0 = 90 \text{ mm} \Rightarrow \alpha_d = e_1 / 3 d_0 = 1,0 \\ f_{ub} / f_u = \frac{800}{940} = 0,85 \end{cases}$$

$$k_1 = 2,5 \quad \begin{cases} e_2 = 2,5 d_0 = 75 \text{ mm} \Rightarrow \frac{2,8 e_2}{d_0} - 1,7 > 2,5 \end{cases}$$

$$F_{b,R}^{inner} = 2,5 \times 0,85 \times 940 \times 27 \times 10 \times 10^{-3} = 540 \text{ kN}$$

- Outer plates

$$\alpha_b = 0,85 \quad \begin{cases} e_1 = 4,0 d_0 = 120 \text{ mm} \Rightarrow \alpha_d = e_1 / 3 d_0 = 1,3 > 1,0 \\ f_{ub} / f_u = \frac{800}{940} = 0,85 \end{cases}$$

$$k_1 = 2,5 \quad \begin{cases} e_2 = 2,5 d_0 = 75 \text{ mm} \Rightarrow \frac{2,8 e_2}{d_0} - 1,7 > 2,5 \end{cases}$$

$$F_{b,R}^{outers} = 2 \times (2,5 \times 0,85 \times 940 \times 27 \times 10 \times 10^{-3}) = 1080 \text{ kN}$$

iii. Net cross section resistance

$$N_{u,R} = \frac{0,9 A_{net} f_u^l}{1,25}$$

- Inner plate

$$A_{net} = (width - d_0) t = (150 - 30) \times 10 = 1200 \text{ mm}^2$$

$$N_{u,R}^{inner} = \frac{0,9 \times 1200 \times 770}{1,25} \times 10^{-3} = 665,3 \text{ kN}$$

- Outer plates

$$A_{net} = (width - d_0) t = (150 - 30) \times 10 = 1200 \text{ mm}^2$$

$$N_{u,R}^{outers} = 2 \times \left(\frac{0,9 \times 1200 \times 770}{1,25} \times 10^{-3} \right) = 1330,6 \text{ kN}$$

iv. Gross section resistance

$$N_{pl,R} = \frac{A_{gross} f_y}{1,0}$$

- Inner plate

$$A_{gross} = width \times t = 150 \times 10 = 1500 \text{ mm}^2$$

$$N_{pl,R}^{inner} = \frac{1500 \times 690}{1,0} \times 10^{-3} = 1035 \text{ kN}$$

- Outer plates

$$A_{gross} = width \times t = 150 \times 10 = 1500 \text{ mm}^2$$

$$N_{pl,R}^{outers} = 2 \times \left(\frac{1500 \times 690}{1,0} \times 10^{-3} \right) = 2070 \text{ kN}$$

$$F_R^{test joint} = \min \{ F_{v,R}; F_{b,R}^{inner}; F_{b,R}^{outers}; N_{u,R}^{inner}; N_{u,R}^{outers}; N_{pl,R}^{inner}; N_{pl,R}^{outers} \} = F_{b,R}^{inner} = 540 \text{ kN}$$

Strongest joint

The only different in this test specimen between the test joint and the strongest joint is the class of the bolt. Due to that, it will just be shown the values that are different from the test joint.

i. Shear resistance

$$\text{per fastener and shear plane: } F_{v,R} = \alpha_v f_{ub} A$$

$$\text{joint } 2 F_{v,R} = 2 \times (0,6 \times 1000 \times 573 \times 10^{-3}) = 687,6 \text{ kN}$$

ii. Bearing resistance

$$\text{per fastener } F_{b,R} = k_1 \alpha_b f_u^h d t$$

- Inner plate

$$\alpha_b = 1,0 \quad \begin{cases} e_1 = 3,0 d_0 = 90 \text{ mm} \Rightarrow \alpha_d = e_1 / 3 d_0 = 1 \\ f_{ub} / f_u = \frac{1000}{940} = 1,06 > 1,0 \end{cases}$$

$$k_1 = 2,5 \quad \begin{cases} e_2 = 2,5 d_0 = 75 \text{ mm} \Rightarrow \frac{2,8 e_2}{d_0} - 1,7 > 2,5 \end{cases}$$

$$F_{b,R}^{inner} = 2,5 \times 1,0 \times 940 \times 27 \times 10 \times 10^{-3} = 634,5 \text{ kN}$$

- Outer plates

$$\alpha_b = 1,0 \quad \left\{ \begin{array}{l} e_1 = 4,0 d_0 = 120 \text{ mm} \Rightarrow \alpha_d = e_1 / 3 d_0 > 1 \\ f_{ub} / f_u = \frac{1000}{940} = 1,06 > 1,0 \end{array} \right.$$

$$k_1 = 2,5 \quad \left\{ e_2 = 2,5 d_0 = 75 \text{ mm} \Rightarrow \frac{2,8 e_2}{d_0} - 1,7 > 2,5 \right.$$

$$F_{b,R}^{outers} = 2 \times (2,5 \times 1,0 \times 940 \times 27 \times 10 \times 10^{-3}) = 2 \times 634,5 \text{ kN} = 1269 \text{ kN}$$

iii. Net cross section resistance – see test joint

iv. Gross section resistance – see test joint

$$F_R^{strongest joint} = \min \{ F_{v,R} ; F_{b,R}^{inner} ; F_{b,R}^{outers} ; N_{u,R}^{inner} ; N_{u,R}^{outers} ; N_{pl,R}^{inner} ; N_{pl,R}^{outers} \} = F_{b,R}^{inner} = 634,5 \text{ kN}$$

A.3 – Series D

Test Specimen D2030

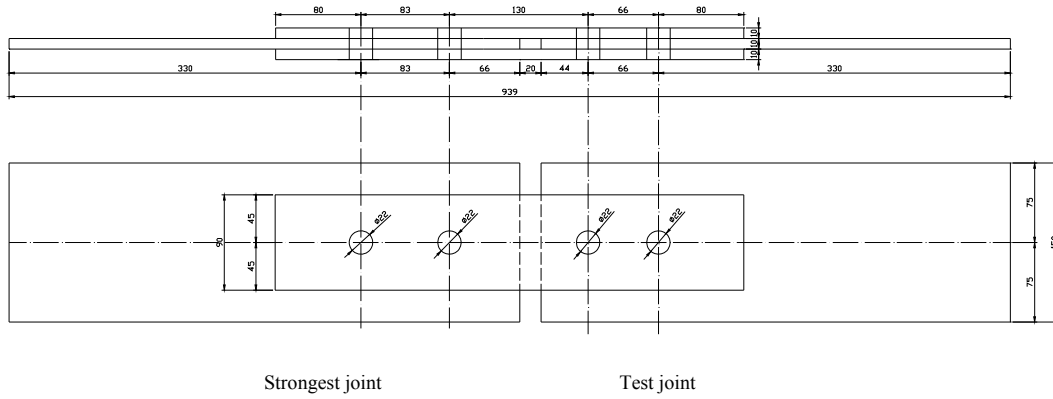


Figure A.5 – Drawing of test specimen D2030 of series D.

	Material properties	Geometric properties
Plates	S690	thickness $t = 10 \text{ mm}$
	$f_y = 690 \text{ N/mm}^2$ $f_u^{\text{lower}} = 770 \text{ N/mm}^2$ $f_u^{\text{higher}} = 940 \text{ N/mm}^2$	
Bolts	10.9	M20
	$f_{yb} = 900 \text{ N/mm}^2$ $f_{ub} = 1000 \text{ N/mm}^2$	$d = 20 \text{ mm}$ $d_0 = 22 \text{ mm}$ $A = 314 \text{ mm}^2$ $A_s = 245 \text{ mm}^2$

Figure A.6 – Table of constituent's properties of the test specimen.

Test joint

$$\begin{array}{lcl}
 \text{Inner plate} & \left\{ \begin{array}{l} e_1 = 2,0 d_0 = 44 \text{ mm} \\ p_1 = 3,0 d_0 = 66 \text{ mm} \\ e_2 = 3,4 d_0 = 75 \text{ mm} \\ \text{width} = 150 \text{ mm} \end{array} \right. & \text{Outer plate} \left\{ \begin{array}{l} e_1 = 3,6 d_0 = 80 \text{ mm} \\ p_1 = p_1^{\text{inner}} \\ e_2 = 2,0 d_0 = 45 \text{ mm} \\ \text{width} = 2 \times e_2 = 90 \text{ mm} \end{array} \right.
 \end{array}$$

- i. Shear resistance

per fastener and shear plane: $F_{v,R} = \alpha_v f_{ub} A$

$$\text{joint } 2 \times 2 \times F_{v,R} = 4 \times (0,6 \times 1000 \times 314 \times 10^{-3}) = 2 \times 376,8 \text{ kN} = 753,6 \text{ kN}$$

$$L_j = 66 \text{ mm} = 3,3 d < 15 d \Rightarrow \text{short joint } \beta_{L_f} = 1,0$$

ii. Bearing resistance

per fastener $F_{b,R} = k_1 \alpha_b f_u^h d t$

- Inner plate

• End bolt

$$\alpha_b = 0,67 \quad \left\{ \begin{array}{l} e_1 = 2,0 d_0 = 44 \text{ mm} \Rightarrow \alpha_d = e_1 / 3 d_0 = 0,67 \\ f_{ub} / f_u = \frac{1000}{940} = 1,06 > 1,0 \end{array} \right.$$

$$k_1 = 2,5 \quad \left\{ e_2 = 3,4 d_0 = 75 \text{ mm} \Rightarrow \frac{2,8 e_2}{d_0} - 1,7 > 2,5 \right.$$

$$F_{b,R}^{inner, endb} = 2,5 \times 0,67 \times 940 \times 20 \times 10 \times 10^{-3} = 313,3 \text{ kN}$$

• Inner bolt

$$\alpha_b = 0,75 \quad \left\{ \begin{array}{l} p_1 = 3,0 d_0 = 66 \text{ mm} \Rightarrow \alpha_d = p_1 / 3 d_0 - \frac{1}{4} = 0,75 \\ f_{ub} / f_u = \frac{1000}{940} = 1,06 > 1,0 \end{array} \right.$$

$$k_1 = 2,5 \quad \left\{ e_2 = 3,4 d_0 = 75 \text{ mm} \Rightarrow \frac{2,8 e_2}{d_0} - 1,7 > 2,5 \right.$$

$$F_{b,R}^{inner, innerb} = 2,5 \times 0,75 \times 940 \times 20 \times 10 \times 10^{-3} = 352,5 \text{ kN}$$

- Outer plates

• End bolt

$$\alpha_b = 1,0 \quad \left\{ \begin{array}{l} e_1 = 3,6 d_0 = 80 \text{ mm} \Rightarrow \alpha_d = e_1 / 3 d_0 > 1,0 \\ f_{ub} / f_u = \frac{1000}{940} = 1,06 > 1,0 \end{array} \right.$$

$$k_1 = 2,5 \quad \left\{ e_2 = 2,0 d_0 = 45 \text{ mm} \Rightarrow \frac{2,8 e_2}{d_0} - 1,7 > 2,5 \right.$$

$$F_{b,R}^{outers, endb} = 2 \times (2,5 \times 1,0 \times 940 \times 20 \times 10 \times 10^{-3}) = 2 \times 470 \text{ kN} = 940 \text{ kN}$$

• Inner bolt

$$\alpha_b = 0,75 \quad \left\{ \begin{array}{l} p_1 = 3,0 d_0 = 66 \text{ mm} \Rightarrow \alpha_d = p_1 / 3 d_0 - \frac{1}{4} = 0,75 \\ f_{ub} / f_u = \frac{1000}{940} = 1,06 > 1,0 \end{array} \right.$$

$$k_1 = 2,5 \quad \left\{ e_2 = 2,0 d_0 = 45 \text{ mm} \Rightarrow \frac{2,8 e_2}{d_0} - 1,7 > 2,5 \right.$$

$$F_{b,R}^{outers, innerb} = 2 \times (2,5 \times 0,75 \times 940 \times 20 \times 10 \times 10^{-3}) = 2 \times 352,5 \text{ kN} = 705 \text{ kN}$$

Group of fasteners:

- Inner plate

$$(a) F_{v,R,i} \geq F_{b,R,i} \forall i \Rightarrow F_R = \sum_i F_{b,R,i} \text{ - True}$$

$$F_{v,R} > F_{b,R}^i \forall i \Rightarrow F_R^{inner} = \sum_i F_{b,R}^{inner,i} = 314,9 + 352,5 = 665,8 kN$$

- Outer plates

$$(a) F_{v,R,i} \geq F_{b,R,i} \forall i \Rightarrow F_R = \sum_i F_{b,R,i} \text{ - False}$$

$$(b) otherwise \Rightarrow F_R = n \times \min \{F_{v,R,i}; F_{b,R,i}\}, n - \text{number of fasteners}$$

$$F_R^{outers} = 2 \times F_{v,R} = 2 \times 376,8 = 753,6 kN$$

iii. Net cross section resistance

$$N_{u,R} = \frac{0,9 A_{net} f_u^l}{1,25}$$

- Inner plate

$$A_{net} = (width - d_0) t = (150 - 22) \times 10 = 1280 mm^2$$

$$N_{u,R}^{inner} = \frac{0,9 \times 1280 \times 770}{1,25} \times 10^{-3} = 709,6 kN$$

- Outer plates

$$A_{net} = (width - d_0) t = (90 - 22) \times 10 = 680 mm^2$$

$$N_{u,R}^{outers} = 2 \times \left(\frac{0,9 \times 680 \times 770}{1,25} \times 10^{-3} \right) = 754 kN$$

iv. Gross section resistance

$$N_{pl,R} = \frac{A_{gross} f_y}{1,0}$$

- Inner plate

$$A_{gross} = width \times t = 150 \times 10 = 1500 mm^2$$

$$N_{pl,R}^{inner} = \frac{1500 \times 690}{1,0} \times 10^{-3} = 1035 kN$$

- Outer plates

$$A_{gross} = width \times t = 90 \times 10 = 900 mm^2$$

$$N_{pl,R}^{outers} = 2 \times \left(\frac{900 \times 690}{1,0} \times 10^{-3} \right) = 1242 kN$$

$$F_R^{test joint} = \min \{F_R^{inner}, F_R^{outers}, N_{u,R}^{inner}, N_{u,R}^{outers}, N_{pl,R}^{inner}, N_{pl,R}^{outers}\} = F_R^{inner} = 665,8 kN$$

Strongest joint

The only different in this test specimen between the test joint and the strongest joint is the end distance and pitch distance in the inner plate. Due to that, it will just be shown the values that are different from the test joint.

$$\text{Inner plate} \begin{cases} e_1 = 3,0 d_0 = 66 \text{ mm} \\ p_1 = 3,75 d_0 = 83 \text{ mm} \end{cases}$$

- i. Shear resistance – see test joint
- ii. Bearing resistance

$$\text{per fastener } F_{b,R} = k_1 \alpha_b f_u^h d t$$

- Inner plate

• End bolt

$$\alpha_b = 1,0 \begin{cases} e_1 = 3,0 d_0 = 66 \text{ mm} \Rightarrow \alpha_d = e_1 / 3 d_0 = 1,0 \\ f_{ub} / f_u = \frac{1000}{940} = 1,06 > 1,0 \end{cases}$$
$$k_1 = 2,5 \begin{cases} e_2 = 3,4 d_0 = 75 \text{ mm} \Rightarrow \frac{2,8 e_2}{d_0} - 1,7 > 2,5 \end{cases}$$

$$F_{b,R}^{inner, endb} = 2,5 \times 1,0 \times 940 \times 20 \times 10 \times 10^{-3} = 470 \text{ kN}$$

• Inner bolt

$$\alpha_b = 1,0 \begin{cases} p_1 = 3,75 d_0 = 83 \text{ mm} \Rightarrow \alpha_d = p_1 / 3 d_0 - \frac{1}{4} = 1,0 \\ f_{ub} / f_u = \frac{1000}{940} = 1,06 > 1,0 \end{cases}$$
$$k_1 = 2,5 \begin{cases} e_2 = 3,4 d_0 = 75 \text{ mm} \Rightarrow \frac{2,8 e_2}{d_0} - 1,7 > 2,5 \end{cases}$$

$$F_{b,R}^{inner, innerb} = 2,5 \times 1,0 \times 940 \times 20 \times 10 \times 10^{-3} = 470 \text{ kN}$$

- Outer plates – see test joint

Group of fasteners:

- Inner plate

(a) $F_{v,R,i} \geq F_{b,R,i} \quad \forall i \Rightarrow F_R = \sum_i F_{b,R,i}$ - False

(b) *otherwise* $\Rightarrow F_R = n \times \min\{F_{v,R,i}; F_{b,R,i}\}, n - \text{number of fasteners}$

$$F_R^{inner} = 2 \times F_{v,R} = 2 \times 376 = 753,6 \text{ kN}$$

- Outer plates – see test joint

iii. Net cross section resistance – see test joint

iv. Gross section resistance – see test joint

$$F_R^{strongest\ joint} = \min\{F_R^{inner}; F_R^{outers}; N_{u,R}^{inner}; N_{u,R}^{outers}; N_{pl,R}^{inner}; N_{pl,R}^{outers}\} = N_{u,R}^{inner} = 709,6 \text{ kN}$$

ANNEX B: Material Tests

B.1 - Tension test on the bolts

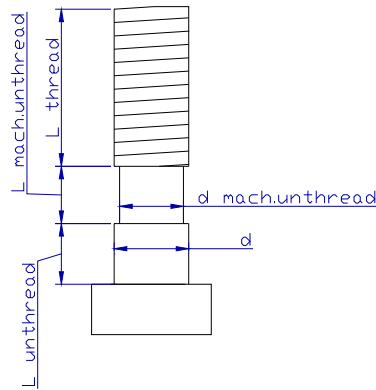


Figure B.1 - Notation of the specimen's measures.

B.1.1 – Group 1: M24 10.9

	Initial (o)	Final (u)	A _u / Z [%]	Initial (o)	Final (u)	A _u / Z [%]	Average values
Bolt ID	1.1			1.2			
Class	10.9			10.9			
Geometry	M24.80			M24.80			
d_{mach.unthreaded} [mm]	19.65	17.00		19.80	15.80		
d_{Mthread} [mm]	23.55			23.80			
d_{mthread} [mm]	20.20			20.50			
d [mm]	24.00			24.00			
L_{mach.unthreaded} [mm]	19.80	24.25	22.50	19.60	25.90	32.00	27.50
L_{thread} [mm]	40.00			40.10			
L_{unthread} [mm]	20.35			20.30			
A_{mach.unthreaded} [mm²]	303.26	226.98	25.00	307.91	196.07	36.50	30.50
F_u [kN]	387.3			364.0			
f_u [N/mm²]	1277.2			1182.1			1229.6
δ_u LVDT1 [mm]	2.69			2.05			
δ_u LVDT2 [mm]	1.77			2.30			
δ_u average [mm]	2.23			2.18			2.21

Table B.1 – Resume table of measures and results of tension test on the bolts of Group 1.

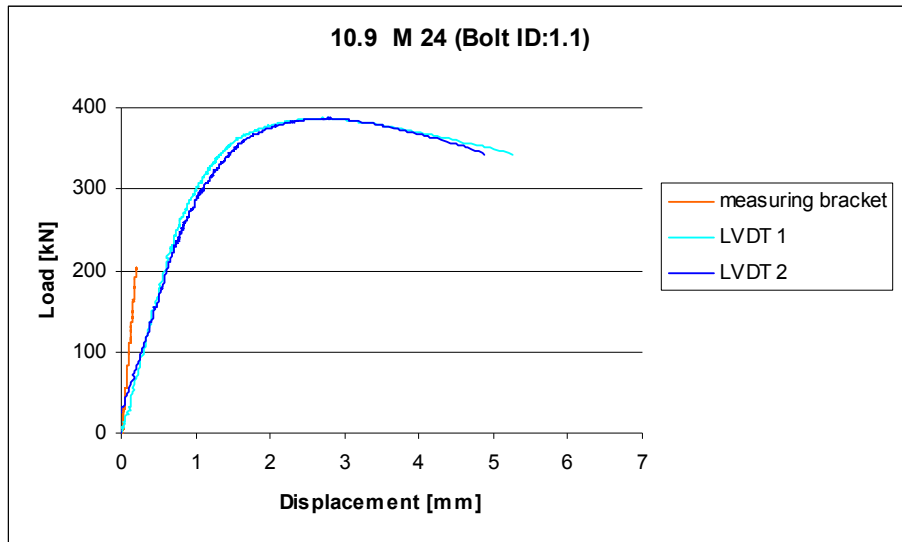


Figure B.2 – Graph result of tension test on bolt 1.1.

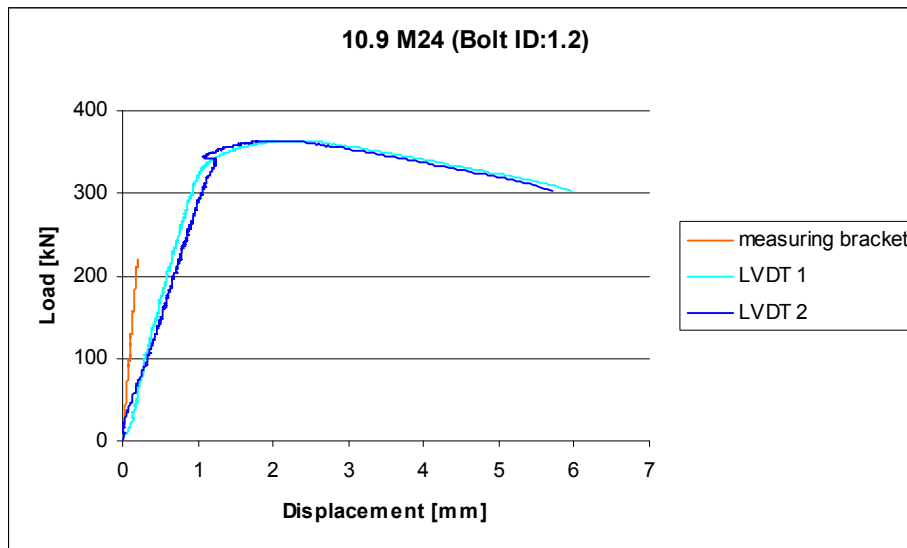


Figure B.3 – Graph result of tension test on bolt 1.2.

B.1.2 – Group 2: M27 8.8

	Initial (o)	Final (u)	A_u / Z [%]	Initial (o)	Final (u)	A_u / Z [%]	Average values
Bolt ID	2.1			2.2			
Class	8.8			8.8			
Geometry	M27.90			M27.90			
d_{mach.unthreaded} [mm]	22.85	13.30		22.70	13.30		
d_{Mthread} [mm]	26.90			27.20			
d_{mthread} [mm]	23.30			23.45			
d [mm]	26.80			26.80			
L_{mach.unthreaded} [mm]	19.80	30.70	55.00	19.90	31.10	56.50	55.50
L_{thread} [mm]	51.40			48.55			
L_{unthread} [mm]	18.45			20.75			
A_{mach.unthreaded} [mm²]	410.07	138.93	66.00	404.71	138.93	65.50	66.00
F_u [kN]	397.6			396.3			
f_u [N/mm²]	969.6			979.1			974.4
δ_u LVDT1 [mm]	2.67			2.17			
δ_u LVDT2 [mm]	2.47			1.80			
δ_u average [mm]	2.57			1.99			2.28

Table B.2 – Resume table of measures and results of tension test on the bolts of Group 2.

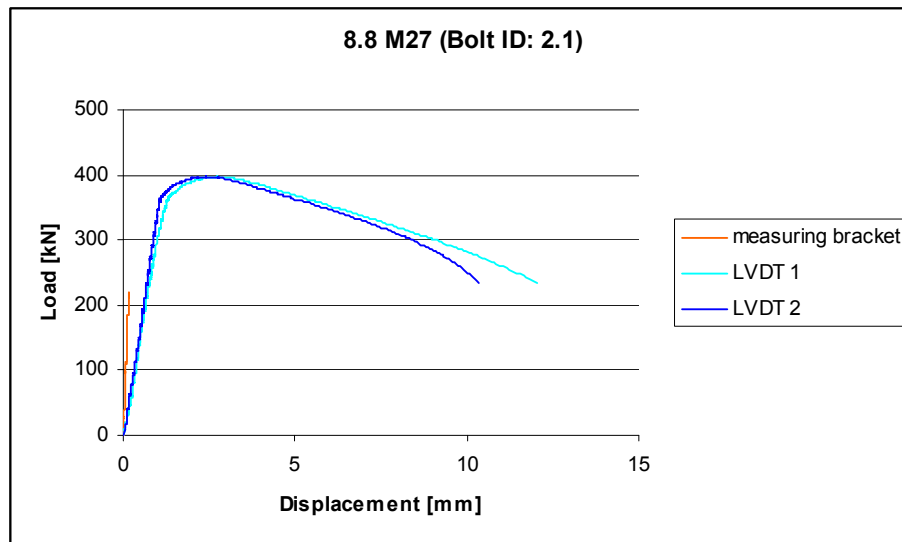
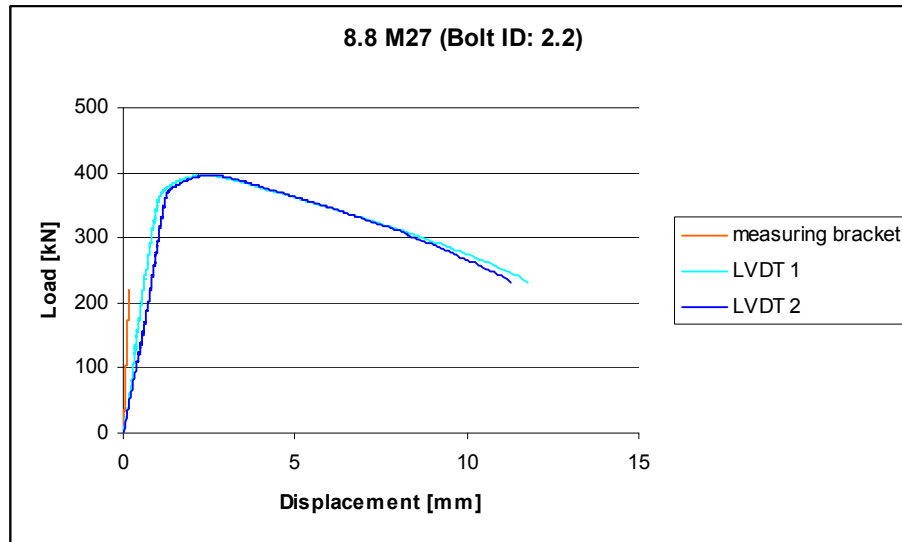


Figure B.4 – Graph result of tension test on bolt 2.1.



B.1.3 – Group 3: M27 10.9

	Initial (o)		Final (u)	A _u / Z [%]	Initial (o)		Final (u)	A _u / Z [%]	Average values
Bolt ID	3.1				3.2				
Class	10.9				10.9				
Geometry	M27.90				M27.90				
d _{mach.unthreaded} [mm]	22.9 15.25				22.9				
d _{Mthread} [mm]	26.85				26.8				
d _{mthread} [mm]	23.2				23.3				
d [mm]	26.85				27				
L _{mach.unthreaded} [mm]	19.85	29.10	46.50	19.75	—		—		46.50
L _{thread} [mm]	48.95			41.85					
L _{unthread} [mm]	21.20			22.2					
A _{mach.unthreaded} [mm ²]	411.87	182.65	55.50	411.87	—		—		55.50
F _u [kN]	485.53			495.14		Nut Failure			
f _u [N/mm ²]	1178.84			1202.18				1178.84	
δ _u LVDT1 [mm]	2.79			1.22					
δ _u LVDT2 [mm]	2.62			3.89					
δ _u average [mm]	2.70			2.55				2.70	

Table B.3 – Resume table of measures and results of tension test on the bolts of Group 3.

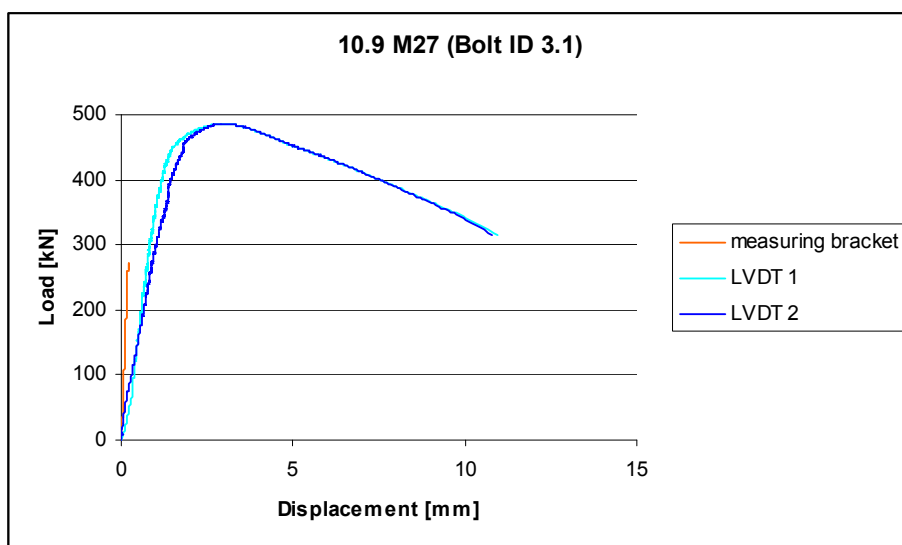


Figure B.6 – Graph result of tension test on bolt 3.1.

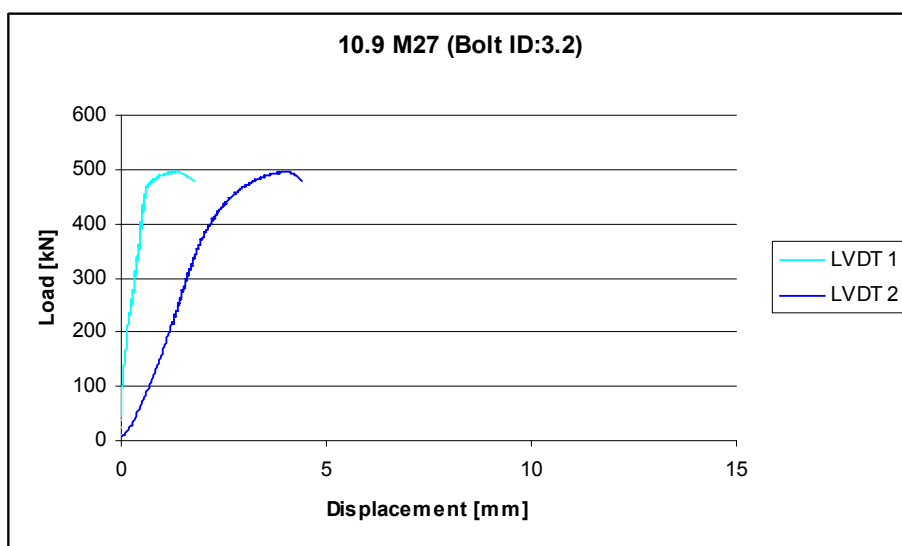


Figure B.7 – Graph result of tension test on bolt 3.2 – nut failure.

B.2 – Tension tests of the steel plates

Test n°.	$f_{0.2\%}$	f_u	strain	Z	f_u/f_y
	N/mm ²	N/mm ²	%	%	
1	775	836	18	75	1.08
2	764	815	18.3	75	1.07
3	769	813	18.3	75	1.06
Average values	769.3	821.3	18.2	75.0	1.07

Table B.4 – Results of the three tension test on the steel plates.

ANNEX C: Actual properties of the test specimens

Test ID	number of tests	Geometry								Bolt		Plate	EC3							
		e ₁ /d ₀	e ₁	e ₂ /d ₀	e ₂	width	t	A _{gross}	A _{net}	d ₀	Class	Class	α _d	f _{ub} /f _u	α _b	k _t	F _{b,R}	F _{v,R}	N _{u,R}	N _{p,R}
			[mm]		[mm]	[mm]	[mm]	[mm ²]	[mm ²]	[mm]							[kN]	[kN]	[kN]	[kN]
A1010 1	1	1.00	25.81	0.99	25.51	51.20	10.00	512.0	253.8	25.83	10.9	S690	0.33	1.50	0.33	1.07	70.0	667.0	150.1	393.9
A1010 2	1	1.01	26.13	0.99	25.53	51.10	10.20	521.2	257.6	25.85	10.9	S690	0.34	1.50	0.34	1.06	72.1	667.0	152.3	401.0
A1010 3	1	1.00	26.00	0.98	25.60	51.10	10.00	511.0	251.0	26.00	10.9	S690	0.33	1.50	0.33	1.06	69.4	667.0	148.4	393.1
A1210 1	1	1.19	31.03	0.98	25.58	51.00	10.00	510.0	249.5	26.05	10.9	S690	0.40	1.50	0.40	1.05	82.1	667.0	147.5	392.4
A1210 2	1	1.19	30.85	0.99	25.65	51.30	10.00	513.0	253.0	26.00	10.9	S690	0.40	1.50	0.40	1.06	82.8	667.0	149.6	394.7
A1210 3	1	1.22	31.43	0.99	25.68	51.10	10.05	513.6	253.8	25.85	10.9	S690	0.41	1.50	0.41	1.08	86.8	667.0	150.1	395.1
A1012 1	1	1.03	27.60	1.15	30.80	60.65	10.00	512.0	338.5	26.80	10.9	S690	0.34	1.50	0.34	1.52	102.7	667.0	200.2	393.9
A1012 2	1	0.98	25.40	1.17	30.28	60.35	10.00	603.5	345.5	25.80	10.9	S690	0.33	1.50	0.33	1.59	102.6	667.0	204.3	464.3
A1012 3	1	0.98	25.45	1.17	30.30	60.60	10.10	612.1	349.5	26.00	10.9	S690	0.33	1.50	0.33	1.56	101.5	667.0	206.7	470.9
A1212 1	1	1.21	31.25	1.17	30.30	60.65	10.15	615.6	352.7	25.90	10.9	S690	0.40	1.50	0.40	1.58	126.8	667.0	208.6	473.6
A1212 2	1	1.18	30.48	1.17	30.18	60.45	10.10	610.5	350.5	25.75	10.9	S690	0.39	1.50	0.39	1.58	124.2	667.0	207.3	469.7
A1212 3	1	1.20	31.15	1.16	30.20	60.45	10.00	604.5	344.5	26.00	10.9	S690	0.40	1.50	0.40	1.55	122.2	667.0	203.7	465.1
A1015 1	1	0.99	25.70	1.56	40.53	81.00	10.00	810.0	550.0	26.00	10.9	S690	0.33	1.50	0.33	2.50	162.4	667.0	325.2	623.2
A1015 2	1	1.03	26.65	1.56	40.48	80.95	10.05	813.5	553.3	25.90	10.9	S690	0.34	1.50	0.34	2.50	169.9	667.0	327.2	625.9
A1015 3	1	1.03	26.75	1.56	40.50	81.10	10.10	819.1	556.5	26.00	10.9	S690	0.34	1.50	0.34	2.50	170.7	667.0	329.1	630.2
A1215 1	1	1.21	31.20	1.57	40.50	81.10	10.15	823.2	561.3	25.80	10.9	S690	0.40	1.50	0.40	2.50	201.6	667.0	331.9	633.3
A1215 2	1	1.17	30.37	1.56	40.45	81.00	10.30	834.3	567.5	25.90	10.9	S690	0.39	1.50	0.39	2.50	198.4	667.0	335.6	641.9
A1215 3	1	1.18	30.48	1.57	40.30	81.00	10.10	818.1	558.0	25.75	10.9	S690	0.39	1.50	0.39	2.50	196.4	667.0	330.0	629.4
A1020 1	1	0.99	25.85	1.95	50.78	101.40	10.00	1014.0	754.0	26.00	10.9	S690	0.33	1.50	0.33	2.50	163.3	667.0	445.9	780.1
A1020 2	1	1.01	26.15	1.92	49.85	100.00	10.15	1015.0	751.1	26.00	10.9	S690	0.34	1.50	0.34	2.50	167.7	667.0	444.2	780.9
A1020 3	1	1.01	26.25	1.93	50.05	100.20	10.10	1012.0	749.4	26.00	10.9	S690	0.34	1.50	0.34	2.50	167.5	667.0	443.2	778.6
A1220 1	1	1.20	31.30	1.95	50.65	101.30	10.20	1033.3	768.1	26.00	10.9	S690	0.40	1.50	0.40	2.50	201.7	667.0	454.2	794.9
A1220 2	1	1.21	31.15	1.94	49.80	99.85	10.10	1008.5	748.9	25.70	10.9	S690	0.40	1.50	0.40	2.50	201.1	667.0	442.9	775.9
A1220 3	1	1.21	31.40	1.92	49.83	99.90	10.00	999.0	739.0	26.00	10.9	S690	0.40	1.50	0.40	2.50	198.4	667.0	437.0	768.6
A2020 1	1	2.00	51.75	1.95	50.60	100.25	10.00	1002.5	743.5	25.90	10.9	S690	0.67	1.50	0.67	2.50	328.2	667.0	439.7	771.3
A2020 2	1	2.01	51.95	1.93	50.10	100.10	10.00	1001.0	742.0	25.90	10.9	S690	0.67	1.50	0.67	2.50	329.5	667.0	438.8	770.1
A2020 3	1	2.02	52.00	1.94	49.98	100.05	10.20	1020.5	757.4	25.80	10.9	S690	0.67	1.50	0.67	2.50	337.7	667.0	447.9	785.1
B3025 1T	1	3.04	90.00	2.54	75.25	150.50	10.10	1520.1	1221.1	29.60	8.8	S690	1.01	1.19	1.00	2.50	559.9	667.0	722.1	1169.4
B3025 1S	1	3.01	89.21	2.54	75.21	150.00	10.40	1560.0	1251.9	29.63	10.9	S690	1.00	1.44	1.00	2.50	576.6	667.0	740.3	1200.2
B3025 2T	1	3.03	89.85	2.53	75.15	150.60	10.10	1521.1	1221.1	29.70	8.8	S690	1.01	1.19	1.00	2.50	559.9	667.0	722.1	1170.2
B3025 2S	1	3.02	90.28	2.52	75.30	150.60	10.40	1566.2	1255.8	29.85	10.9	S690	1.01	1.44	1.00	2.50	576.6	667.0	742.6	1205.0
B3025 3T	1	3.02	90.50	2.52	75.60	151.00	10.10	1525.1	1222.1	30.00	8.8	S690	1.01	1.19	1.00	2.50	559.9	667.0	722.7	1173.3
B3025 3S	1	3.01	90.15	2.52	75.55	151.00	10.15	1532.7	1228.2	30.00	10.9	S690	1.00	1.44	1.00	2.50	562.7	667.0	726.3	1179.1

Table C.1 – Actual dimensions and resistances of the test specimens.

ANNEX D: Test results

D.1 – Test specimen A1010

Test No.			A1010_1		A1010_2		A1010_3	
			initial	final	initial	final	initial	final
Geometry	C_1	[mm]	12.90	11.00	13.20	10.75	13.00	11.1
	C_2 average	[mm]	12.60		12.60		12.60	
	d_0 average	[mm]	25.83	51.80	25.85	50.80	26.00	50.1
	e_1	[mm]	25.81		26.13		26.00	
	e_1/d_0		1.00		1.01		1.00	
	e_2	[mm]	25.51		25.53		25.60	
	e_2/d_0		0.99		0.99		0.98	
	width	[mm]	51.20	58.80	51.10	58.55	51.10	59
	t	[mm]	10.00		10.20		10.00	
	A_{gross}	[mm ²]	512.00		521.22		511.00	
	A_{net}	[mm ²]	253.75		257.55		251.00	
EC3	α_d		0.33		0.34		0.33	
	f_{ub}/f_u		1.50		1.50		1.50	
	α_b		0.33		0.34		0.33	
	k_1		1.07		1.06		1.06	
	$F_{b,Rd}$	[kN]	70.0		72.1		69.4	
	$F_{v,Rd}$	[kN]	667.0		667.0		667.0	
	$N_{u,Rd}$	[kN]	150.1		152.3		148.4	
	$N_{pL,Rd}$	[kN]	393.9		401.0		393.1	
	Failure mechanism		Bearing inner plate		Bearing inner plate		Bearing inner plate	
Test Results	F_u	[kN]	176.5		178.6		179.2	
	δ_u	[mm]	7.1		4.7		4.5	
	Failure mechanism		Bearing inner plate		Bearing inner plate		Bearing inner plate	
Error		%	152.1		147.6		158.1	

Table D.1 – Test results of the three test specimens A1010.

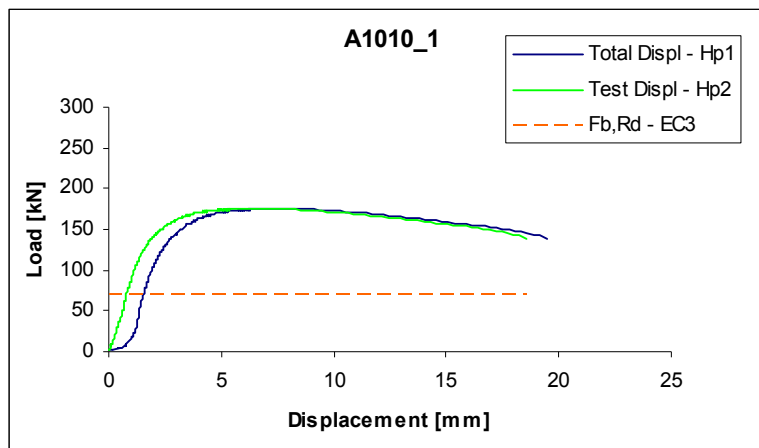


Figure D.1 – Load-displacement curve and predicted value for A1010_1 test specimen.

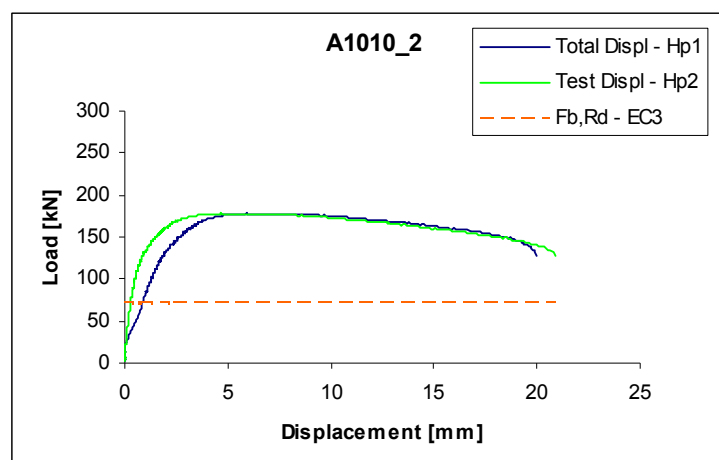


Figure D.2 – Load-displacement curve and predicted value for A1010_2 test specimen.

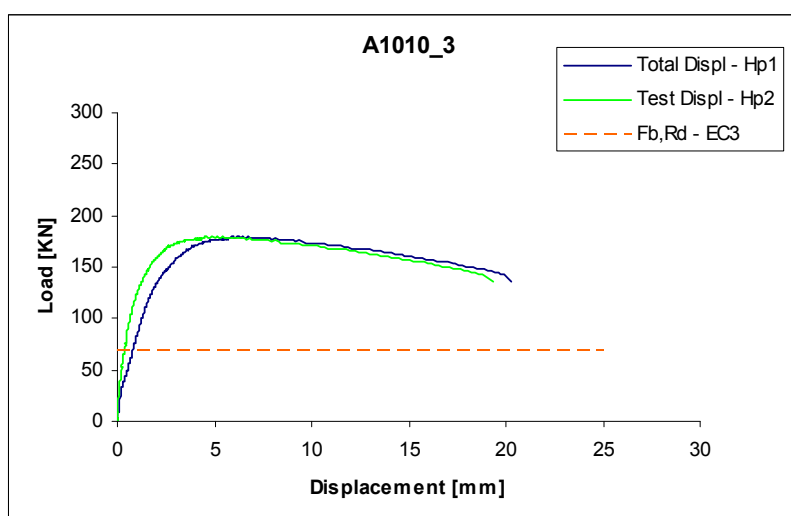


Figure D.3 – Load-displacement curve and predicted value for A1010_3 test specimen.

Specimen	Failure Plate	Failure's detail	Bolt position at failure	Specimen's plates after failure
A1010_1				
A1010_2				
A1010_3				

Table D.2 – Pictures of Specimens A1010.

D.2 – Test specimen A1210

Test No.			A1210_1		A1210_2		A1210_3	
			initial	final	initial	final	initial	final
Geometry	C ₁	[mm]	18.00	17.70	17.85	17.65	18.50	18.3
	C ₂	[mm]	12.55	9,25/11,75	12.65	8,3/9,8	12.75	7,7/12,8
	average							
	d ₀	[mm]	26.05	38.70	26.00	41.90	25.85	36
	average							
	e ₁	[mm]	31.03		30.85		31.43	
	e ₁ /d ₀		1.19		1.19		1.22	
	e ₂	[mm]	25.58		25.65		25.68	
	e ₂ /d ₀		0.98		0.99		0.99	
	width	[mm]	51.00	48.15	51.30	46.00	51.10	48.2
	t	[mm]	10.00	8.00	10.00	5.70	10.05	7
	A _{gross}	[mm ²]	510.00		513.00		513.56	
	A _{net}	[mm ²]	249.50		253.00		253.76	
EC3	α _d		0.40		0.40		0.41	
	f _{ub} /f _u		1.50		1.50		1.50	
	α _b		0.40		0.40		0.41	
	k ₁		1.05		1.06		1.08	
	F _{b,Rd}	[kN]	82.1		82.8		86.8	
	F _{v,Rd}	[kN]	667.0		667.0		667.0	
	N _{u,Rd}	[kN]	184.4		187.0		187.6	
	N _{pl,Rd}	[kN]	392.4		394.7		395.1	
	Failure mechanism		Bearing inner plate		Bearing inner plate		Bearing inner plate	
Test Results	F _u	[kN]	212.2		208.1		206.7	
	δ _u	[mm]	4.3		4.4		3.6	
	Failure mechanism		Net section		Net section		Net section	
Error' (net section)		%	15.1		11.3		10.2	

Table D.3 – Test results of the three test specimens A1210.

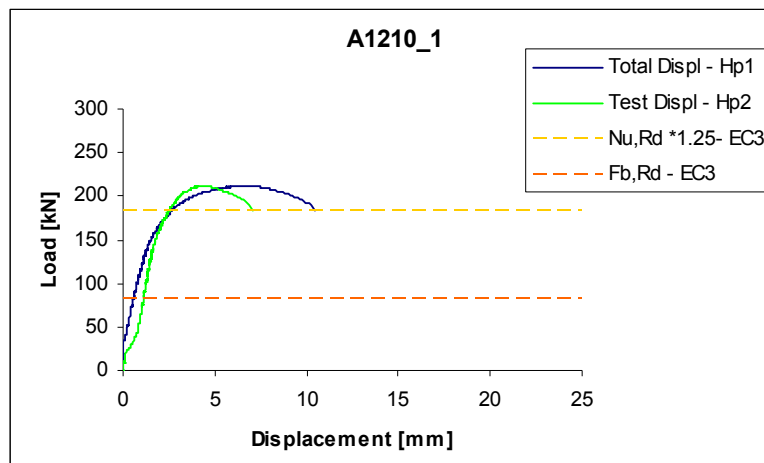


Figure D.4 – Load-displacement curve and predicted value for A1210_1 test specimen.

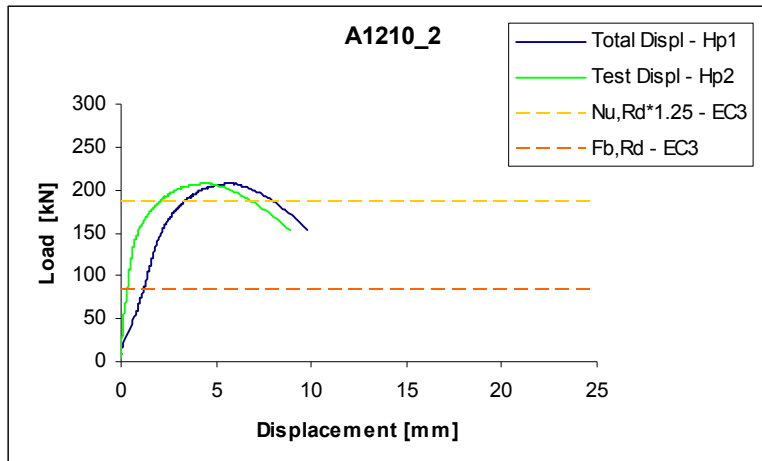


Figure D.5 – Load-displacement curve and predicted value for A1210_2 test specimen.

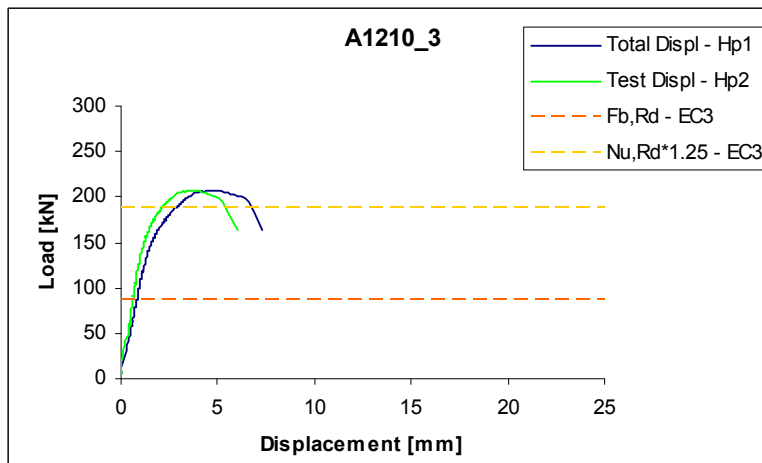


Figure D.6 – Load-displacement curve and predicted value for A1210_3 test specimen.











Specimen	Failure Plate	Failure's detail	Bolt position at failure	Specimen's plates after failure
A1210_1				
A1210_2			NOT AVAILABLE	
A1210_3			NOT AVAILABLE	

Table D.4 – Pictures of Specimens A1210.

D.3 – Test specimen A1012

Test No.			A1012 1		A1012 2		A1012 3	
			initial	final	initial	final	initial	final
Geometry	C ₁	[mm]	14.20	12.40	12.50	11.30	12.45	11.2
	C ₂ average	[mm]	17.40		17.38		17.30	
	d ₀ average	[mm]	26.80	45.35	25.80	47.00	26.00	44.7
	e ₁	[mm]	27.60		25.40		25.45	
	e ₁ /d ₀		1.03		0.98		0.98	
	e ₂	[mm]	30.80		30.28		30.30	
	e ₂ /d ₀		1.15		1.17		1.17	
	width	[mm]	60.65	67.00	60.35	64.30	60.60	64.2
	t	[mm]	10.00		10.00		10.10	
	A _{gross}	[mm ²]	606.50		603.50		612.06	
	A _{net}	[mm ²]	338.50		345.50		349.46	
EC3	α _d		0.34		0.33		0.33	
	f _{ub} /f _u		1.50		1.50		1.50	
	α _b		0.34		0.33		0.33	
	k ₁		1.52		1.59		1.56	
	F _{b,Rd}	[kN]	102.7		102.6		101.5	
	F _{v,Rd}	[kN]	667.0		667.0		667.0	
	N _{u,Rd}	[kN]	200.2		204.3		206.7	
	N _{pl,Rd}	[kN]	466.6		464.3		470.9	
	Failure mechanism		Bearing inner plate		Bearing inner plate		Bearing inner plate	
Test Results	F _u	[kN]	195.7		177.9		175.8	
	δ _u	[mm]	5.4		4.5		5.0	
	Failure mechanism		Bearing inner plate		Bearing inner plate		Bearing inner plate	
Error		%	90.6		73.4		73.1	

Table D.5 – Test results of the three test specimens A1012.

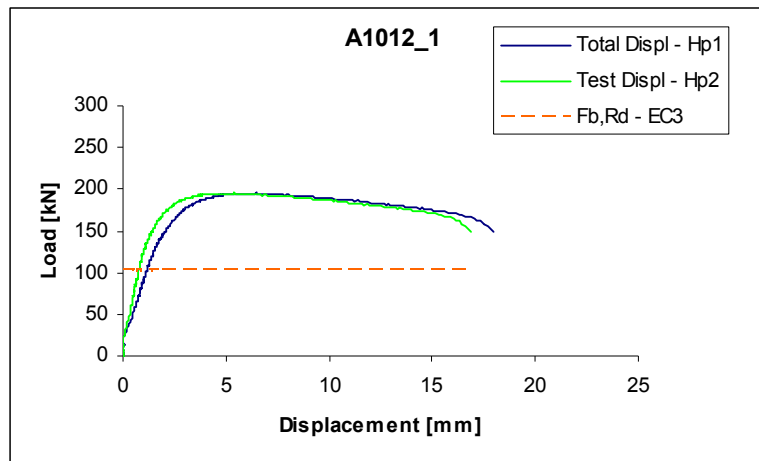


Figure D.7 – Load-displacement curve and predicted value for A1012_1 test specimen.

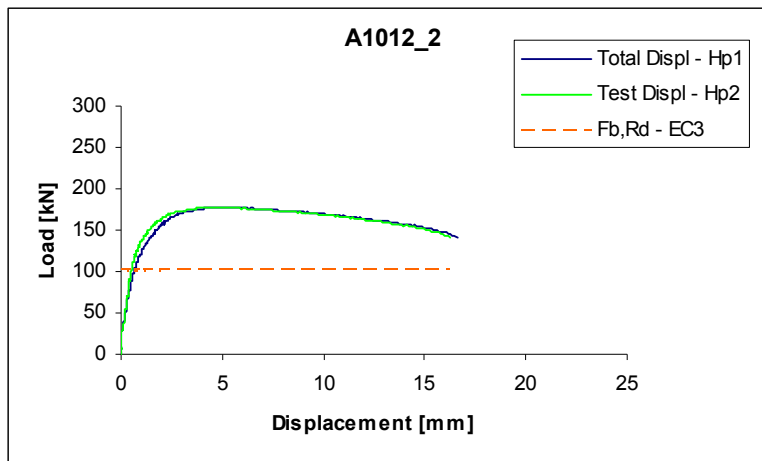


Figure D.8 – Load-displacement curve and predicted value for A1012_2 test specimen.

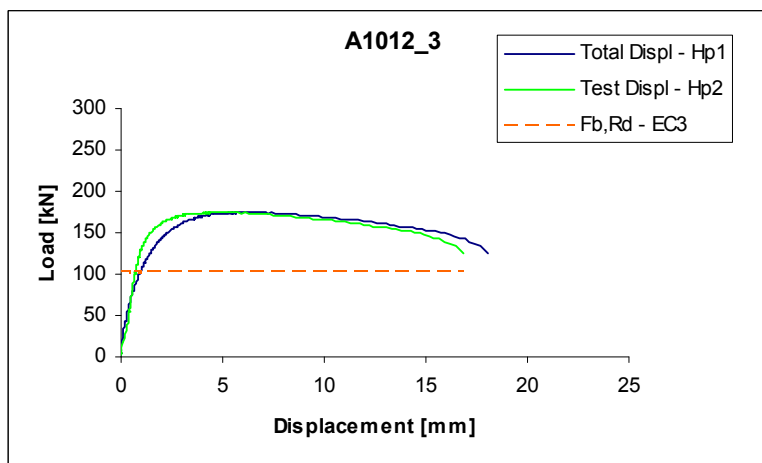


Figure D.9 – Load-displacement curve and predicted value for A1012_3 test specimen.

Specimen	Failure Plate	Failure's detail	Bolt position at failure	Specimen's plates after failure
A1012_1				
A1012_2				
A1012_3			NOT AVAILABLE	

Table D.6 – Pictures of Specimens A1012.

D.4 – Test specimen A1212

Test No.			A1212_1		A1212_2		A1212_3	
			initial	final	initial	final	initial	final
Geometry	C_1	[mm]	18.30	12.70	17.60	14.35	18.15	12.7
	C_2 average	[mm]	17.35		17.30		17.20	
	d_0 average	[mm]	25.90	56.40	25.75	48.90	26.00	50.65
	e_1	[mm]	31.25		30.48		31.15	
	e_1/d_0		1.21		1.18		1.20	
	e_2	[mm]	30.30		30.18		30.20	
	e_2/d_0		1.17		1.17		1.16	
	width	[mm]	60.65	71.30	60.45	67.50	60.45	71.3
	t	[mm]	10.15		10.10		10.00	
	A_{gross}	[mm ²]	615.60		610.55		604.50	
	A_{net}	[mm ²]	352.71		350.47		344.50	
EC3	α_d		0.40		0.39		0.40	
	f_{ub}/f_u		1.50		1.50		1.50	
	α_b		0.40		0.39		0.40	
	k_1		1.58		1.58		1.55	
	$F_{b,Rd}$	[kN]	126.8		124.2		122.2	
	$F_{v,Rd}$	[kN]	667.0		667.0		667.0	
	$N_{u,Rd}$	[kN]	208.6		207.3		203.7	
	$N_{pl,Rd}$	[kN]	473.6		469.7		465.1	
Test Results	Failure mechanism		Bearing inner plate		Bearing inner plate		Bearing inner plate	
	F_u	[kN]	230.1		224.6		223.9	
	δ_u	[mm]	4.5		5.2		4.8	
	Failure mechanism		Bearing inner plate		Bearing inner plate		Bearing inner plate	
Error		%	81.4		80.8		83.2	

Table D.7 – Test results of the three test specimens A1212.

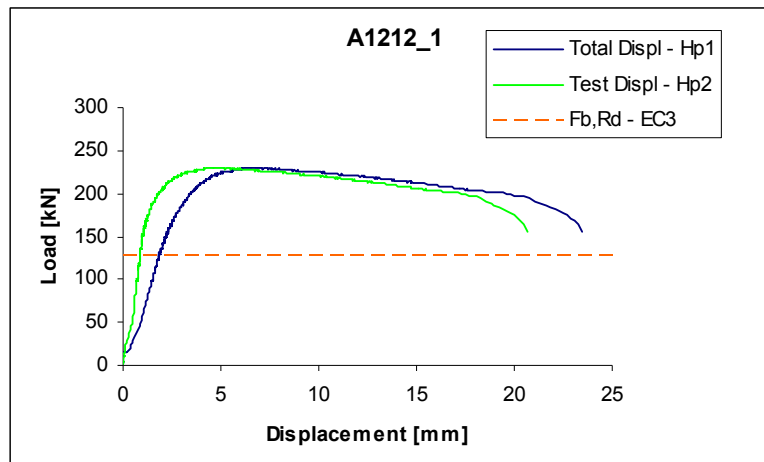


Figure D.10 – Load-displacement curve and predicted value for A1212_1 test specimen.

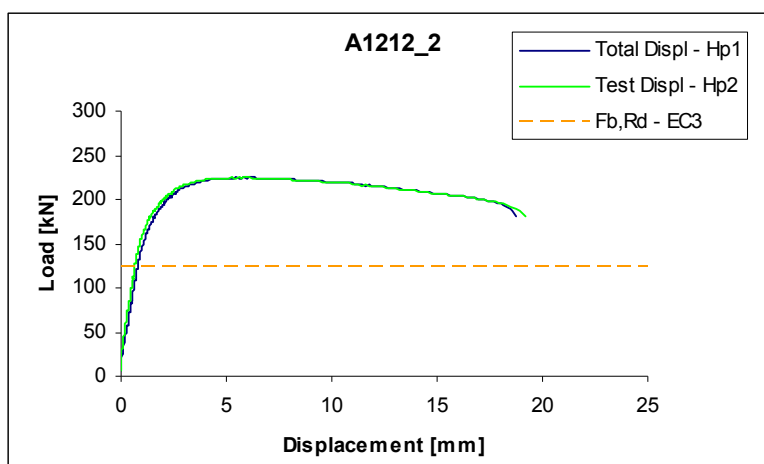


Figure D.11 – Load-displacement curve and predicted value for A1212_2 test specimen.

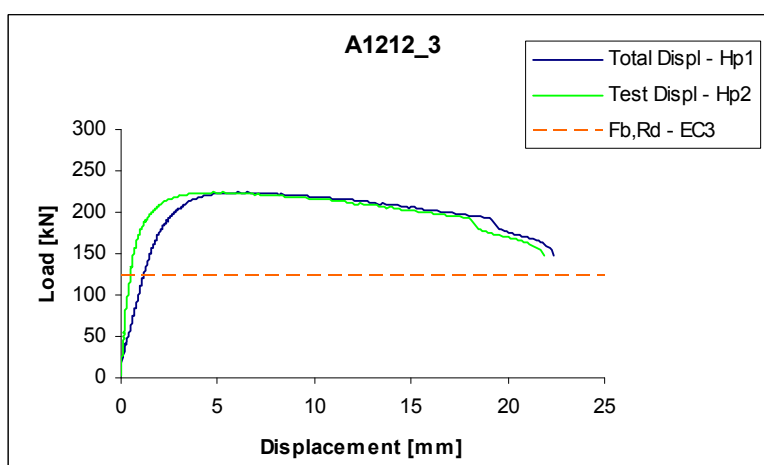


Figure D.12 – Load-displacement curve and predicted value for A1212_3 test specimen.


Specimen	Failure Plate	Failure's detail	Bolt position at failure	Specimen's plates after failure
A1212_1			NOT AVAILABLE	
A1212_2				
A1212_3				

Table D.8 – Pictures of Specimens A1212.

D.5 – Test specimen A1015

Test No.			A1015_1		A1015_2		A1015_3	
			initial	final	initial	final	initial	final
Geometry	C_1	[mm]	12.70	12.00	13.70	12.60	13.75	12.70
	C_2 average	[mm]	27.53		27.53		27.50	
	d_0 average	[mm]	26.00	47.35	25.90	45.15	26.00	44.95
	e_1	[mm]	25.70		26.65		26.75	
	e_1/d_0		0.99		1.03		1.03	
	e_2	[mm]	40.53		40.48		40.50	
	e_2/d_0		1.56		1.56		1.56	
	width	[mm]	81.00	81.75	80.95	81.90	81.10	82.00
	t	[mm]	10.00		10.05		10.10	
	A_{gross}	[mm ²]	810.00		813.55		819.11	
	A_{net}	[mm ²]	550.00		553.25		556.51	
EC3	α_d		0.33		0.34		0.34	
	f_{ub}/f_u		1.50		1.50		1.50	
	α_b		0.33		0.34		0.34	
	k_1		2.50		2.50		2.50	
	$F_{b,Rd}$	[kN]	162.4		169.9		170.7	
	$F_{v,Rd}$	[kN]	667.0		667.0		667.0	
	$N_{u,Rd}$	[kN]	325.2		327.2		329.1	
	$N_{pl,Rd}$	[kN]	623.2		625.9		630.2	
	Failure mechanism		Bearing inner plate		Bearing inner plate		Bearing inner plate	
Test Results	F_u	[kN]			198.5		189.5	
	δ_u	[mm]			5.8		5.7	
	Failure mechanism		Bearing inner plate		Bearing inner plate		Bearing inner plate	
Error		%			16.8		11.0	

Table D.9 – Test results of the three test specimens A1015.

Both LVDT Hp1 and Hp2 were lost during the test of A1015_1, that is why no data is available of this test – green cells in table D.5

A1015_2 and A1015_3 had also problems with the measurements. Due to misalignment of the plates at the beginning of the test, the measurements of the two LVDT have deviations to the real values – yellow cells in table D.5.

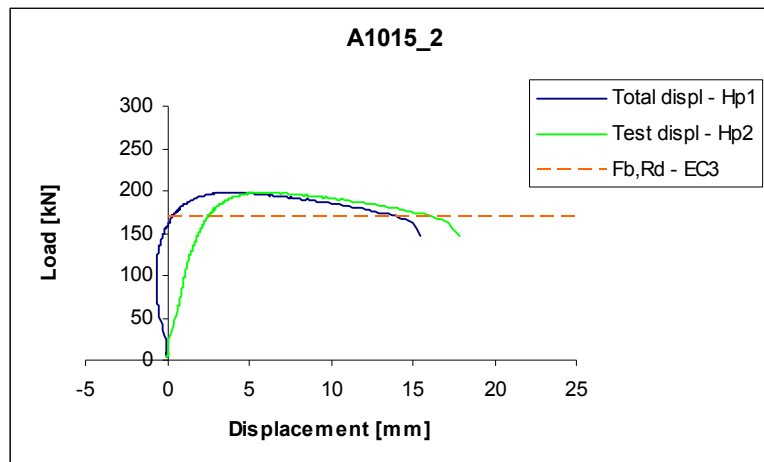


Figure D.13 – Load-displacement curve and predicted value for A1015_2 test specimen.

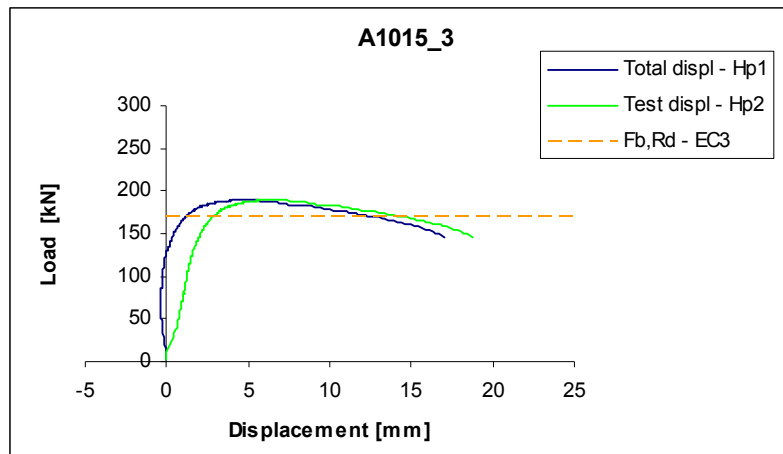


Figure D.14 – Load-displacement curve and predicted value for A1015_3 test specimen.


Specimen	Failure Plate	Failure's detail	Bolt position at failure	Specimen's plates after failure
A1015_1				
A1015_2				
A1015_3			NOT AVAILABLE	

Table D10 – Pictures of Specimens A1015.

D.6 – Test specimen A1215

Test No.			A1215_1		A1215_2		A1215_3	
			initial	final	initial	final	initial	final
Geometry	C_1	[mm]	18.30	15.70	17.42	15.60	17.60	15.5
	C_2 average	[mm]	27.60		27.50		27.43	
	d_0 average	[mm]	25.80	48.75	25.90	43.45	25.75	48.9
	e_1	[mm]	31.20		30.37		30.48	
	e_1/d_0		1.21		1.17		1.18	
	e_2	[mm]	40.50		40.45		40.30	
	e_2/d_0		1.57		1.56		1.57	
	width	[mm]	81.10	83.05	81.00	83.30	81.00	83.35
	t	[mm]	10.15		10.30		10.10	
	A_{gross}	[mm ²]	823.17		834.30		818.10	
	A_{net}	[mm ²]	561.30		567.53		558.03	
EC3	α_d		0.40		0.39		0.39	
	f_{ub}/f_u		1.50		1.50		1.50	
	α_b		0.40		0.39		0.39	
	k_1		2.50		2.50		2.50	
	$F_{b,Rd}$	[kN]	201.6		198.4		196.4	
	$F_{v,Rd}$	[kN]	667.0		667.0		667.0	
	$N_{u,Rd}$	[kN]	331.9		335.6		330.0	
	$N_{pl,Rd}$	[kN]	633.3		641.9		629.4	
Test Results	Failure mechanism		Bearing inner plate		Bearing inner plate		Bearing inner plate	
	F_u	[kN]	225.9		228.7		230.1	
	δ_u	[mm]	6.0		5.4		5.5	
Error	Failure mechanism		Bearing inner plate		Bearing inner plate		Bearing inner plate	
		%	12.1		15.3		17.2	

Table D.11 – Test results of the three test specimens A1215.

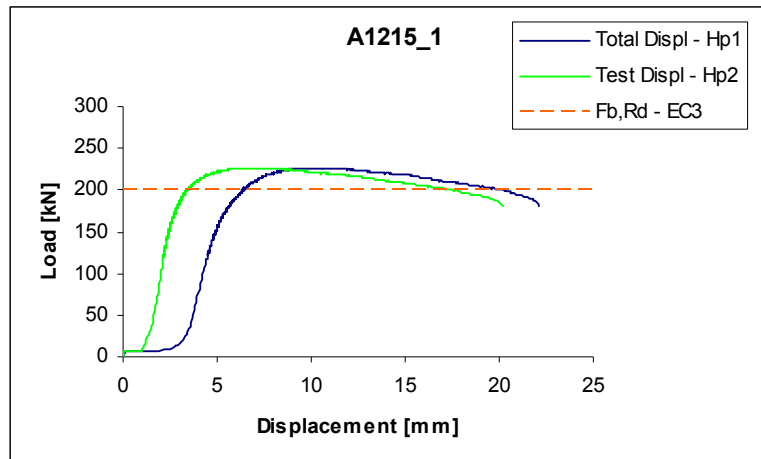


Figure D.15 – Load-displacement curve and predicted value for A1215_1 test specimen.

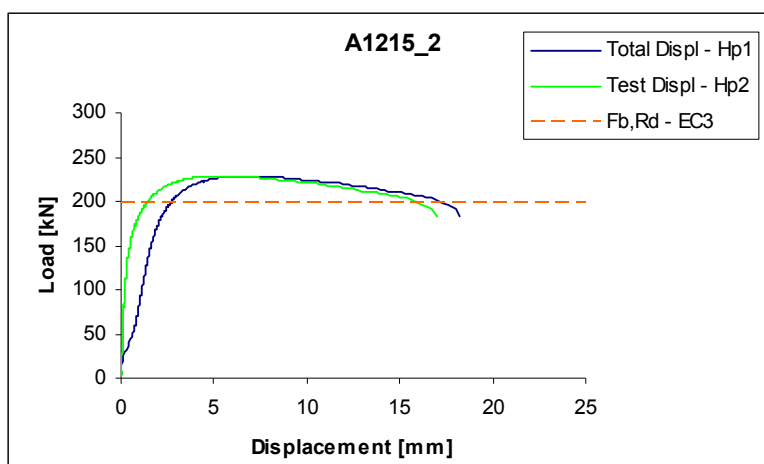


Figure D.16 – Load-displacement curve and predicted value for A1215_2 test specimen.

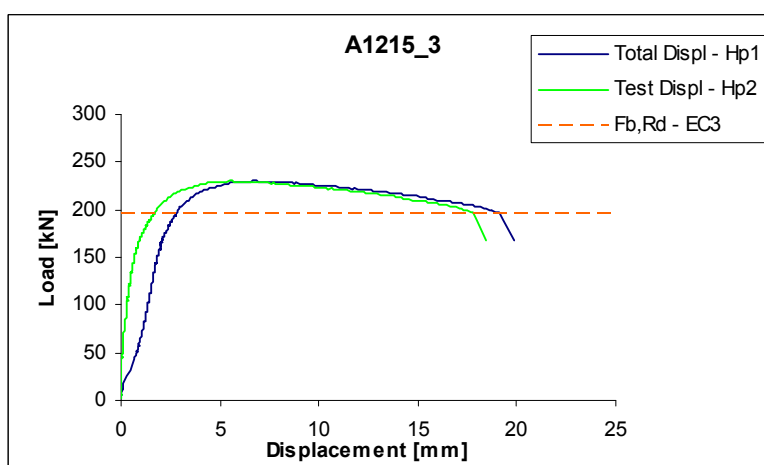


Figure D.17 – Load-displacement curve and predicted value for A1215_3 test specimen.












Specimen	Failure Plate	Failure's detail	Bolt position at failure	Specimen's plates after failure
A1215_1				
A1215_2			NOT AVAILABLE	
A1215_3				

Table D.12 – Pictures of Specimens A1215.

D.7 – Test specimen A1020

Test No.			A1020_1		A1020_2		A1020_3	
			initial	final	initial	final	initial	final
Geometry	C_1	[mm]	12.85	12.20	13.15	12.45	13.25	12.6
	C_2 average	[mm]	37.78		36.85		37.05	
	d_0 average	[mm]	26.00	45.20	26.00	46.20	26.00	46.4
	e_1	[mm]	25.85		26.15		26.25	
	e_1/d_0		0.99		1.01		1.01	
	e_2	[mm]	50.78		49.85		50.05	
	e_2/d_0		1.95		1.92		1.93	
	width	[mm]	101.40	101.50	100.00	100.00	100.20	100.2
	t	[mm]	10.00		10.15		10.10	
	A_{gross}	[mm ²]	1014.00		1015.00		1012.02	
	A_{net}	[mm ²]	754.00		751.10		749.42	
EC3	α_d		0.33		0.34		0.34	
	f_{ub}/f_u		1.50		1.50		1.50	
	α_b		0.33		0.34		0.34	
	k_1		2.50		2.50		2.50	
	$F_{b,Rd}$	[kN]	163.3		167.7		167.5	
	$F_{v,Rd}$	[kN]	667.0		667.0		667.0	
	$N_{u,Rd}$	[kN]	445.9		444.2		443.2	
	$N_{pl,Rd}$	[kN]	780.1		780.9		778.6	
	Failure mechanism		Bearing inner plate		Bearing inner plate		Bearing inner plate	
Test Results	F_u	[kN]	193.7		199.2		193.0	
	δ_u	[mm]	4.8		4.5		4.6	
	Failure mechanism		Bearing inner plate		Bearing inner plate		Bearing inner plate	
Error		%	18.6		18.8		15.2	

Table D.13 – Test results of the three test specimens A1020.

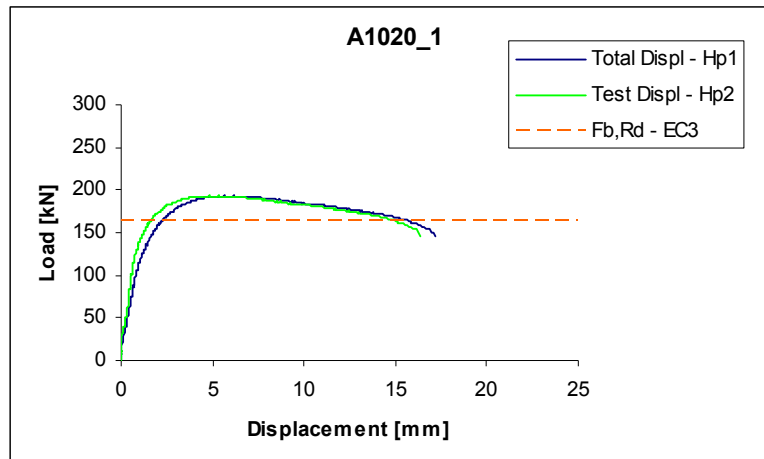


Figure D.18 – Load-displacement curve and predicted value for A1020_1 test specimen.

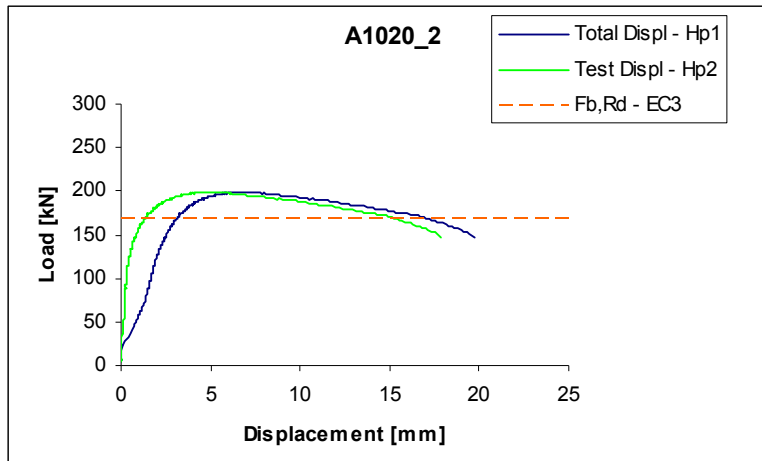


Figure D.19 – Load-displacement curve and predicted value for A1020_2 test specimen.

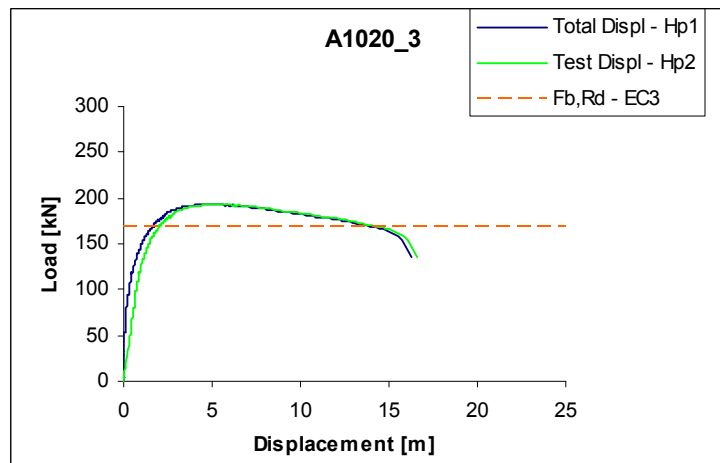


Figure D.20 – Load-displacement curve and predicted value for A1020_3 test specimen.











Specimen	Failure Plate	Failure's detail	Bolt position at failure	Specimen's plates after failure
A1020_1			NOT AVAILABLE	
A1020_2			NOT AVAILABLE	
A1020_3				

Table D.14 – Pictures of Specimens A1020.

D.8 – Test specimen A1220

Test No.			A1220_1		A1220_2		A1220_3	
			initial	final	initial	final	initial	final
Geometry	C ₁	[mm]	18.30	15.80	18.30	16.10	18.40	15.9
	C ₂ average	[mm]	37.65		36.95		36.83	
	d ₀ average	[mm]	26.00	49.65	25.70	46.80	26.00	45.55
	e ₁	[mm]	31.30		31.15		31.40	
	e ₁ /d ₀		1.20		1.21		1.21	
	e ₂	[mm]	50.65		49.80		49.83	
	e ₂ /d ₀		1.95		1.94		1.92	
	width	[mm]	101.30	101.70	99.85	100.55	99.90	100.6
	t	[mm]	10.20		10.10		10.00	
	A _{gross}	[mm ²]	1033.26		1008.49		999.00	
	A _{net}	[mm ²]	768.06		748.92		739.00	
EC3	α _d		0.40		0.40		0.40	
	f _{ub} /f _u		1.50		1.50		1.50	
	α _b		0.40		0.40		0.40	
	k ₁		2.50		2.50		2.50	
	F _{b,Rd}	[kN]	201.7		201.1		198.4	
	F _{v,Rd}	[kN]	667.0		667.0		667.0	
	N _{u,Rd}	[kN]	454.2		442.9		437.0	
	N _{pl,Rd}	[kN]	794.9		775.9		768.6	
	Failure mechanism		Bearing inner plate		Bearing inner plate		Bearing inner plate	
Test Results	F _u	[kN]	239.7		242.4		239.7	
	δ _u	[mm]			4.9		5.2	
	Failure mechanism		Bearing inner plate		Bearing inner plate		Bearing inner plate	
Error		%	18.8		20.6		20.8	

Table D.15 – Test results of the three test specimens A1220.

The LVDT Hp2 on the test A1220_1 only measured till a certain point before the maximum force. Afterwards it failed. This is why the value for δ_u for this test is not available – green cell.

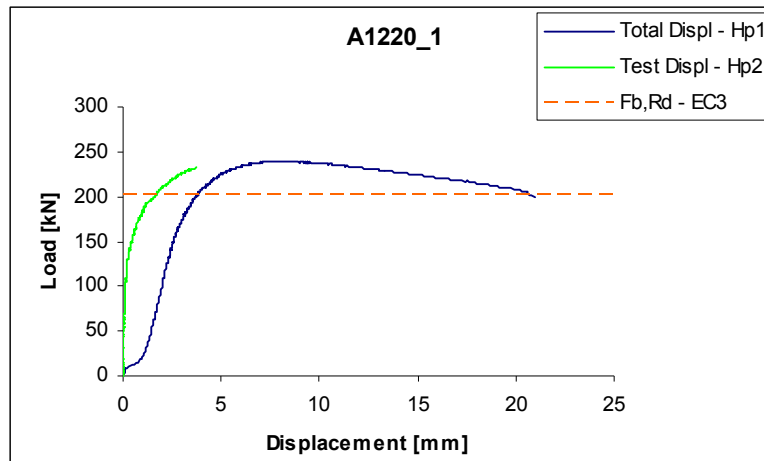


Figure D.21 – Load-displacement curve and predicted value for A1220_1 test specimen.

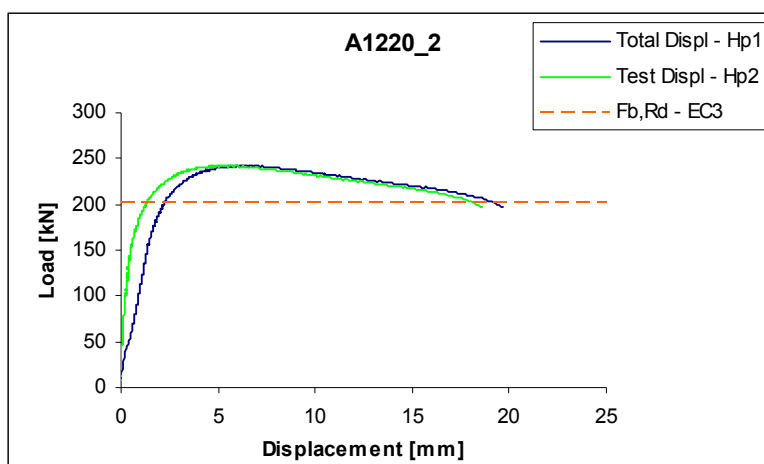


Figure D.22 – Load-displacement curve and predicted value for A1220_2 test specimen.

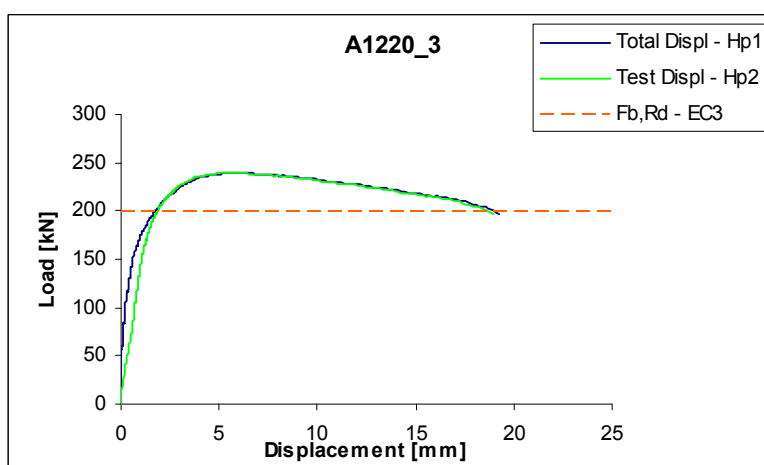


Figure D.23 – Load-displacement curve and predicted value for A1220_3 test specimen.










Specimen	Failure Plate	Failure's detail	Bolt position at failure	Specimen's plates after failure
A1220_1				NOT AVAILABLE
A1220_2			NOT AVAILABLE	
A1220_3			NOT AVAILABLE	

Table D.16 – Pictures of Specimens A1220.

D.9 – Test specimen A2020

Test No.			A2020_1		A2020_2		A2020_3	
			initial	final	initial	final	initial	final
Geometry	C_1	[mm]	38.80	22.00	39.00	18.60	39.10	25.95
	C_2 average	[mm]	37.65		37.15		37.08	
	d_0 average	[mm]	25.90	55.05	25.90	69.20	25.80	54.45
	e_1	[mm]	51.75		51.95		52.00	
	e_1/d_0		2.00		2.01		2.02	
	e_2	[mm]	50.60		50.10		49.98	
	e_2/d_0		1.95		1.93		1.94	
	width	[mm]	100.25	113.90	100.10	115.50	100.05	113.15
	t	[mm]	10.00		10.00		10.20	
	A_{gross}	[mm ²]	1002.50		1001.00		1020.51	
	A_{net}	[mm ²]	743.50		742.00		757.35	
EC3	α_d		0.67		0.67		0.67	
	f_{ub}/f_u		1.50		1.50		1.50	
	α_b		0.67		0.67		0.67	
	k_1		2.50		2.50		2.50	
	$F_{b,Rd}$	[kN]	328.2		329.5		337.7	
	$F_{v,Rd}$	[kN]	667.0		667.0		667.0	
	$N_{u,Rd}$	[kN]	439.7		438.8		447.9	
	$N_{pl,Rd}$	[kN]	771.3		770.1		785.1	
Test Results	Failure mechanism		Bearing inner plate		Bearing inner plate		Bearing inner plate	
	F_u	[kN]	394.9		388.0		389.4	
	δ_u	[mm]	10.9		12.0		12.3	
Error	Failure mechanism		Bearing inner plate		Bearing inner plate		Bearing inner plate	
	%		20.3		17.8		15.3	

Table D.17 – Test results of the three test specimens A2020.

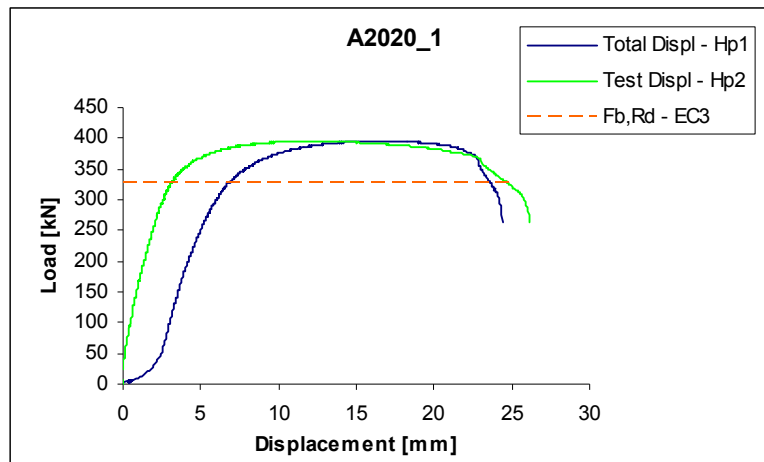


Figure D.24 – Load-displacement curve and predicted value for A2020_1 test specimen.

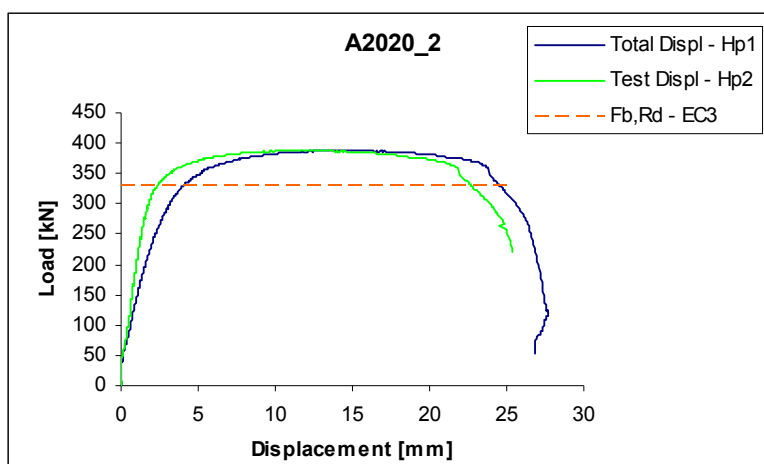


Figure D.25 – Load –displacement curve and predicted value for A2020_2 test specimen.

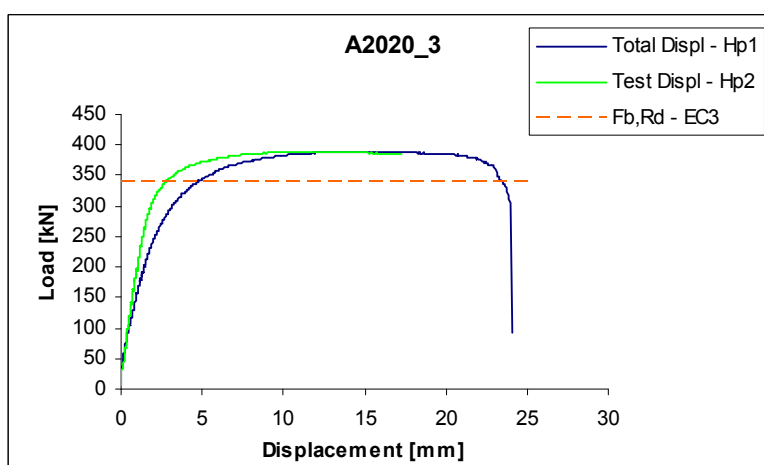


Figure D.26 – Load-displacement curve and predicted value for A2020_3 test specimen.












Specimen	Failure Plate	Failure's detail	Bolt position at failure	Specimen's plates after failure
A2020_1				NOT AVAILABLE
A2020_2				
A2020_3				

Table D.18 – Pictures of Specimens A2020.

D.10 – Test specimen B3025

Test No.			B3025_1				B3025_2				B3025_3			
			B3025_i1	8.8	B3025_i2	10.9	B3025_i5	8.8	B3025_i6	10.9	B3025_i8	8.8	B3025_i7	10.9
			initial	final	initial	final	initial	final	initial	final	initial	final	initial	final
Geometry	C ₁	[mm]	75.20	59.75	74.40	62.40	75.00	57.25	75.35		75.50	57.65	75.15	
	C ₂ average	[mm]	60.45		60.40		60.30		60.38		60.60		60.55	
	d ₀ average	[mm]	29.60	46.10	29.63	42.75	29.70	49.65	29.85		30.00	49.6	30.00	
	e ₁	[mm]	90.00		89.21		89.85		90.28		90.50		90.15	
	e ₁ /d ₀		3.04		3.01		3.03		3.02		3.02		3.01	
	e ₂	[mm]	75.25		75.21		75.15		75.30		75.60		75.55	
	e ₂ /d ₀		2.54		2.54		2.53		2.52		2.52		2.52	
	width	[mm]	150.50	150.50	150.00	150.00	150.60	152.5	150.60		151.00	152	151.00	
	t	[mm]	10.10		10.40		10.10		10.40		10.10		10.15	
	A _{gross}	[mm ²]	1520.05		1560.00		1521.06		1566.24		1525.10		1532.65	
	A _{net}	[mm ²]	1221.09		1251.90		1221.09		1255.80		1222.10		1228.15	
EC3	α _d		1.01		1.00		1.01		1.01		1.01		1.00	
	f _{ub} /f _u		1.19		1.44		1.19		1.44		1.19		1.44	
	α _b		1.00		1.00		1.00		1.00		1.00		1.00	
	k ₁		2.50		2.50		2.50		2.50		2.50		2.50	
	F _{b,Rd}	[kN]	559.9		576.6		559.9		576.6		559.9		562.7	
	F _{v,Rd}	[kN]	670.0		810.6		670.0		810.6		670.0		810.6	
	N _{u,Rd}	[kN]	722.1		740.3		722.1		742.6		722.7		726.3	
	N _{pl,Rd}	[kN]	1169.4		1200.2		1170.2		1205.0		1173.3		1179.1	
	Failure mechanism		Bearing inner plate		Bearing inner plate		Bearing inner plate		Bearing inner plate		Bearing inner plate		Bearing inner plate	
Test Results	F _u	[kN]	609.1						646.9				638.0	
	δ _u	[mm]	22.2											
	Failure mechanism		Bearing inner plate						Bearing inner plate				Bearing inner plate	
Error	%		8.8						12.2				13.4	

Table D.19 – Test results of the three test specimens B3025.

The values for δ_u for B3025_2 and B3025_3 (green cells) are not available because, as they failed to the strongest joint, no LVDT was measuring its displacement. Also some dimensions after failure in these specimens are not available, since it was impossible to dismount the joint and measure those dimensions.

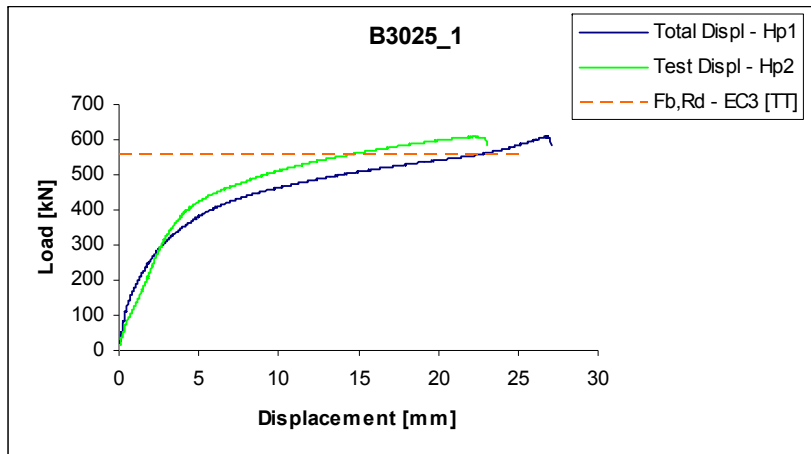


Figure D.27 – Load-displacement curve and predicted value for B3025_1.

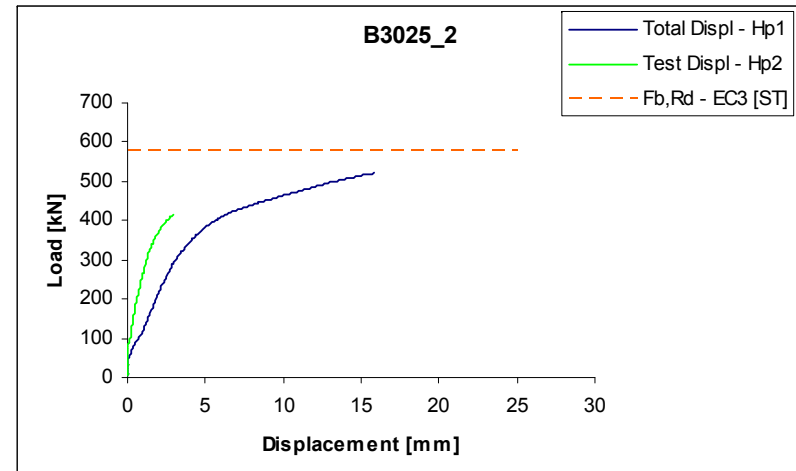


Figure D.28 – Load-displacement curve and predicted value for B3025_2.

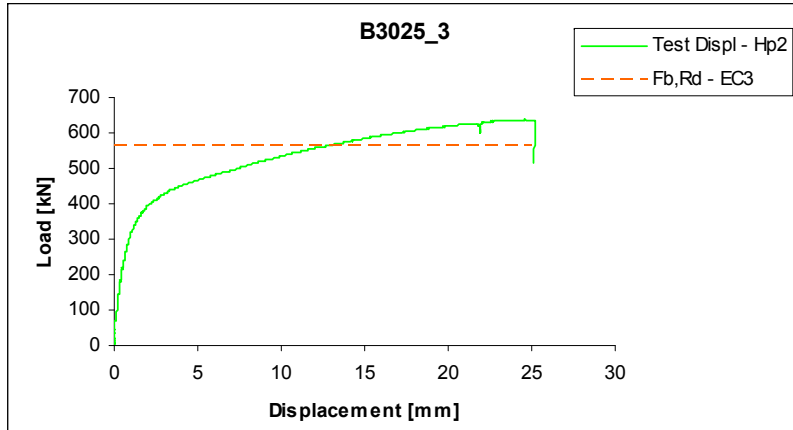


Figure D.29 – Load-displacement curve and predicted value for B3025_3.

Note: Both LVDTs in specimen B3025_2 failed after a certain point. The same happened with the LVDT Hp1 in specimen B3025_3.


Specimen	Test Joint (8.8)		Strongest Joint (10.9)		Specimen's plates after failure
	Plate	Bolt	Plate	Bolt	
B3025_1					NOT AVAILABLE
B3025_2			NOT AVAILABLE	NOT AVAILABLE	
B3025_3			NOT AVAILABLE	NOT AVAILABLE	

Table D.20 – Pictures of Specimens B3025.

ANNEX E: Statistical evaluation

E.1 – Two groups of tests results: Group I $e_2 \leq 1.2d_0$ and Group II $e_2 \geq 1.5d_0$

	Theoretical value		Experimental value			% error							Characteristic value	Design value	Nominal value
Test no.	r_{ti}	r_{ti}^2	r_{ei}	r_{ei}^2	$r_{ei} \cdot r_{ti}$		$b_i = r_{ei}/r_{ti}$	$r_{ei} = b_i(r_{ti})$	$\delta_i = r_{ei}/(b_i \cdot r_{ti})$		$\Delta_i = LN(\delta_i)$	$(\Delta_i - \Delta)^2$	r_k	r_d	r_n
	[kN]		[kN]					[kN]					[kN]	[kN]	[kN]
	0.00							0.00					0.00	0.00	0.00
A1010_1	70.02	4902.40	176.49	31149.78	12357.54	152.07	2.52	143.17	1.23		0.21	0.05	98.80	70.40	65.64
A1010_2	72.12	5201.69	178.55	31881.17	12877.73	147.57	2.48	147.48	1.21		0.19	0.04	101.77	72.52	67.62
A1010_3	69.45	4822.87	179.24	32126.98	12447.66	158.10	2.58	142.00	1.26		0.23	0.06	97.99	69.83	65.11
A1012_1	102.71	10550.18	195.72	38307.10	20103.40	90.55	1.91	210.03	0.93		-0.07	0.00	144.94	103.28	96.29
A1012_2	102.57	10521.23	177.87	31636.67	18244.36	73.41	1.73	209.74	0.85		-0.16	0.02	144.74	103.13	96.16
A1012_3	101.54	10309.82	175.81	30907.75	17850.87	73.14	1.73	207.62	0.85		-0.17	0.02	143.28	102.09	95.19
A1212_1	126.79	16076.26	230.06	52927.14	29169.69	81.45	1.81	259.26	0.89		-0.12	0.01	178.91	127.49	118.87
A1212_2	124.19	15422.29	224.57	50429.44	27887.95	80.83	1.81	253.94	0.88		-0.12	0.01	175.24	124.87	116.42
A1212_3	122.20	14932.89	223.88	50121.36	27357.94	83.21	1.83	249.87	0.90		-0.11	0.01	172.43	122.87	114.56
sum	891.59	92739.64	1762.18	349487.39	178297.13			18.40		9.00		2.20			
mean value	99.07		195.80				$b $	2.04	$\delta $	1.00	$\Delta $	-0.01			
standard deviation	22.15		22.25								s_{Δ}^2	0.03			
											V_{δ}^2	0.03			
											V_{δ}	0.17			

Table E.1 – Statistical evaluation values for the Group I $e_2 \leq 1.2d_0$

	V_{xi}	V_{xi}^2	Q_{rt}	0.11	$u_{k,n} (n=27)$	1.74	γ_r	1.40
V_{dn}	0.005	0.000025	Q_{δ}	0.17	$u_{k,\infty}$	1.64	k_c	0.66
V_t	0.05	0.0025	Q	0.20	exp,k	0.69	γ_r^*	0.93
V_{fu}	0.07	0.0049	α_{rt}	0.55	$u_{d,n} (n=27)$	3.50	γ_{rt}/γ_r^*	1.34
V_{ab}	0.05	0.0025	α_{δ}	0.84	$u_{d,\infty}$	3.04		
V_{k1}	0.05	0.0025			exp, d	0.49		
V_{rt}^2	0.01							
V_r^2	0.04							
V_r	0.21							

Table E.2 – (cont.) Statistical evaluation values for the Group I $e_2 \leq 1.2d_0$

	Theoretical value		Experimental value			% error							Characteristic value	Design value	Nominal value
Test no.	r_{ti}	r_{ti}^2	r_{ei}	r_{ei}^2	$r_{ei} \cdot r_{ti}$		$b_i = r_{ei}/r_{ti}$	$r_e = b_{[i]}/r_{ti}$	$\delta_i = r_{ei}/(b_i \cdot r_{ti})$		$\Delta_i = LN(\delta_i)$	$(\Delta_i - \Delta)^2$	r_k	r_d	r_n
	[kN]		[kN]					[kN]					[kN]	[kN]	[kN]
	0.00							0.00					0.00	0.00	0.00
A1015_1	162.37	26364.43	188.00	35344.00	30525.80	15.78	1.16	188.41	1.00		0.00	0.00	154.82	131.39	152.22
A1015_2	169.87	28855.32	198.47	39389.94	33713.64	16.84	1.17	197.11	1.01		0.01	0.00	161.97	137.46	159.25
A1015_3	170.70	29136.84	189.54	35925.79	32353.74	11.04	1.11	198.07	0.96		-0.04	0.00	162.76	138.13	160.03
A1215_1	201.63	40653.76	225.94	51048.43	45555.58	12.06	1.12	233.96	0.97		-0.03	0.00	192.26	163.16	189.03
A1215_2	198.40	39360.75	228.69	52297.29	45370.26	15.27	1.15	230.21	0.99		-0.01	0.00	189.17	160.54	186.00
A1215_3	196.35	38554.46	230.06	52927.14	45172.75	17.17	1.17	227.84	1.01		0.01	0.00	187.23	158.89	184.08
A1020_1	163.32	26673.09	193.66	37504.97	31628.68	18.58	1.19	189.51	1.02		0.02	0.00	155.73	132.16	153.11
A1020_2	167.69	28120.80	199.16	39663.11	33396.98	18.76	1.19	194.58	1.02		0.02	0.00	159.90	135.70	157.21
A1020_3	167.50	28057.80	192.98	37239.35	32324.20	15.21	1.15	194.36	0.99		-0.01	0.00	159.72	135.55	157.04
A1220_1	201.71	40685.65	239.67	57443.63	48343.88	18.82	1.19	234.05	1.02		0.02	0.00	192.33	163.22	189.10
A1220_2	201.09	40438.17	242.42	58767.94	48749.03	20.55	1.21	233.34	1.04		0.04	0.00	191.75	162.72	188.52
A1220_3	198.38	39356.05	239.67	57443.63	47547.39	20.81	1.21	230.19	1.04		0.04	0.00	189.16	160.53	185.98
A2020_1	328.22	107725.88	394.88	155928.63	129605.36	20.31	1.20	380.85	1.04		0.04	0.00	312.96	265.59	307.70
A2020_2	329.48	108560.16	388.01	150551.76	127843.35	17.76	1.18	382.32	1.01		0.01	0.00	314.17	266.62	308.89
A2020_3	337.70	114042.44	389.38	151619.90	131495.64	15.30	1.15	391.85	0.99		-0.01	0.00	322.01	273.27	316.60
B3025_1	559.94	313537.28	609.14	371053.98	341085.41	8.79	1.09	649.73	0.94		-0.06	0.00	533.92	453.11	524.95
B3025_2	576.58	332439.88	646.91	418495.14	372993.93	12.20	1.12	669.03	0.97		-0.03	0.00	549.78	466.57	540.54
B3025_3	562.72	316649.30	637.99	407024.86	359004.37	13.38	1.13	652.95	0.98		-0.02	0.00	536.56	455.35	527.55
sum	4893.65	1699212.07	5634.57	2209669.49	1936710.00	16.03		20.89	18.00		-0.01	0.02			
mean value	271.87		313.03				b_i	1.16	δ_i	1.00	Δ_i	0.00			
standard deviation	143.14		157.39								s_{Δ}^2	0.00			
											v_{δ}^2	0.001			
											v_{δ}	0.03			

Table E.3 – Statistical evaluation values for the Group II $e_2 \geq 1.5d_0$

	V_{xi}	V_{xi}^2	Q_{rt}	0.11	γ_r	1.18
V_{dn}	0.01	0.000025	Q_{δ}	0.03	k_c	0.98
V_t	0.05	0.0025	Q	0.12	γ_r^*	1.16
V_{fu}	0.07	0.0049	α_{rt}	0.97	γ_{ri}/γ_r^*	1.08
V_{ab}	0.05	0.0025	α_{δ}	0.26		
V_{k1}	0.05	0.0025	$u_{k,n} (n=27)$	1.74		
V_{rt}^2	0.01		$u_{k,\infty}$	1.64		
V_r^2	0.01		\exp, k	0.82		
V_r	0.12		$u_{d,n} (n=27)$	3.50		
			$u_{d,\infty}$	3.04		
			\exp, d	0.70		

Table E.4 – (cont.) Statistical evaluation values for the Group II

E.2 – One group of tests results

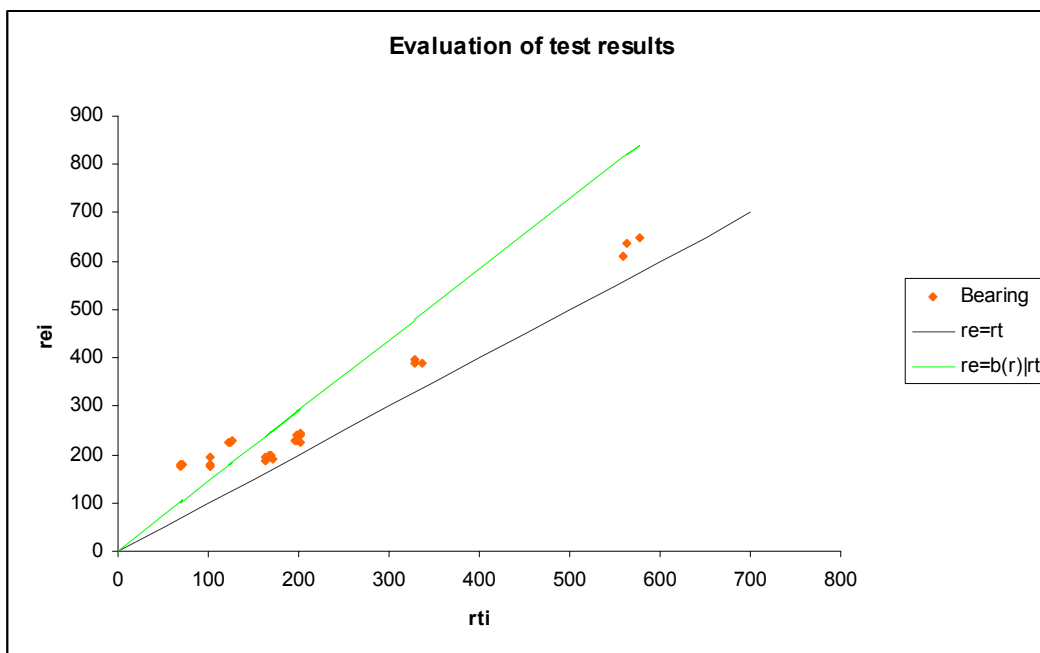


Figure E.1 - r_e - r_t diagram with the mean value correction line $r_e = \bar{b}_{(r)} r_t$

	V_{xi}	V_{xi}^2	Q_{rt}	0.11	γ_r	1.69
V_{dn}	0.01	0.000025	Q_{δ}	0.28	k_c	1.14
V_t	0.05	0.0025	Q	0.30	γ_r^*	1.93
V_{fu}	0.07	0.0049	α_{rt}	0.37	γ_{ri}/γ_r^*	0.65
V_{ab}	0.05	0.0025	α_{δ}	0.94		
V_{k1}	0.05	0.0025	$u_{k,n} (n=27)$	1.74		
	V_{rt}^2	0.012425	$u_{k,\infty}$	1.64		
	V_r^2	0.10	\exp, k	0.56		
	V_r	0.31	$u_{d,n} (n=27)$	3.50		
			$u_{d,\infty}$	3.04		
			\exp, d	0.33		

Table E.5 - Statistical evaluation values.

	Theoretical value		Experimental value			% error							Charact eristic value	Design value	Nominal value
Test no.	r_{ti}	r_{ti}^2	r_{ei}	r_{ei}^2	$r_{ei} \cdot r_{ti}$		$b_i = r_{ei}/r_{ti}$	$r_e = b_{(ij)} r_{ti}$	$\delta_i = r_{ei}/(b_i \cdot r_{ti})$		$\Delta_i = LN(\delta_i)$	$(\Delta_i - \Delta_j)^2$	r_k	Test no.	r_{ti}
	[kN]		[kN]					[kN]					[kN]		[kN]
	0.00							0.00					0.00	0.00	
A1010_1	70.02	4902.40	176.49	31149.78	12357.54	152.07	2.52	101.89	1.73		0.55	0.35	57.39	33.98	65.64
A1010_2	72.12	5201.69	178.55	31881.17	12877.73	147.57	2.48	104.95	1.70		0.53	0.33	59.12	35.00	67.62
A1010_3	69.45	4822.87	179.24	32126.98	12447.66	158.10	2.58	101.06	1.77		0.57	0.38	56.92	33.70	65.11
A1012_1	102.71	10550.18	195.72	38307.10	20103.40	90.55	1.91	149.47	1.31		0.27	0.10	84.19	49.85	96.29
A1012_2	102.57	10521.23	177.87	31636.67	18244.36	73.41	1.73	149.26	1.19		0.18	0.05	84.08	49.78	96.16
A1012_3	101.54	10309.82	175.81	30907.75	17850.87	73.14	1.73	147.75	1.19		0.17	0.05	83.23	49.28	95.19
A1212_1	126.79	16076.26	230.06	52927.14	29169.69	81.45	1.81	184.50	1.25		0.22	0.07	103.93	61.53	118.87
A1212_2	124.19	15422.29	224.57	50429.44	27887.95	80.83	1.81	180.71	1.24		0.22	0.07	101.79	60.27	116.42
A1212_3	122.20	14932.89	223.88	50121.36	27357.94	83.21	1.83	177.82	1.26		0.23	0.07	100.17	59.30	114.56
A1015_1	162.37	26364.43	188.00	35344.00	30525.80	15.78	1.16	236.28	0.80		-0.23	0.03	133.09	78.80	152.22
A1015_2	169.87	28855.32	198.47	39389.94	33713.64	16.84	1.17	247.19	0.80		-0.22	0.03	139.24	82.44	159.25
A1015_3	170.70	29136.84	189.54	35925.79	32353.74	11.04	1.11	248.39	0.76		-0.27	0.05	139.92	82.84	160.03
A1215_1	201.63	40653.76	225.94	51048.43	45555.58	12.06	1.12	293.40	0.77		-0.26	0.05	165.27	97.85	189.03
A1215_2	198.40	39360.75	228.69	52297.29	45370.26	15.27	1.15	288.70	0.79		-0.23	0.04	162.62	96.28	186.00
A1215_3	196.35	38554.46	230.06	52927.14	45172.75	17.17	1.17	285.73	0.81		-0.22	0.03	160.95	95.29	184.08
A1020_1	163.32	26673.09	193.66	37504.97	31628.68	18.58	1.19	237.66	0.81		-0.20	0.03	133.87	79.26	153.11
A1020_2	167.69	28120.80	199.16	39663.11	33396.98	18.76	1.19	244.02	0.82		-0.20	0.03	137.46	81.38	157.21
A1020_3	167.50	28057.80	192.98	37239.35	32324.20	15.21	1.15	243.75	0.79		-0.23	0.04	137.30	81.29	157.04
A1220_1	201.71	40685.65	239.67	57443.63	48343.88	18.82	1.19	293.52	0.82		-0.20	0.03	165.34	97.89	189.10
A1220_2	201.09	40438.17	242.42	58767.94	48749.03	20.55	1.21	292.62	0.83		-0.19	0.02	164.83	97.59	188.52
A1220_3	198.38	39356.05	239.67	57443.63	47547.39	20.81	1.21	288.68	0.83		-0.19	0.02	162.61	96.28	185.98
A2020_1	328.22	107725.88	394.88	155928.63	129605.36	20.31	1.20	477.61	0.83		-0.19	0.02	269.03	159.29	307.70
A2020_2	329.48	108560.16	388.01	150551.76	127843.35	17.76	1.18	479.45	0.81		-0.21	0.03	270.07	159.90	308.89
A2020_3	337.70	114042.44	389.38	151619.90	131495.64	15.30	1.15	491.41	0.79		-0.23	0.04	276.81	163.89	316.60
B3025_1	559.94	313537.28	609.14	371053.98	341085.41	8.79	1.09	814.81	0.75		-0.29	0.06	458.98	271.75	524.95

	Theoretical value		Experimental value			% error							Charact eristic value	Design value	Nominal value
Test no.	r_{ti}	r_{ti}^2	r_{ei}	r_{ei}^2	$r_{ei} \cdot r_{ti}$		$b_i = r_{ei}/r_{ti}$	$r_e = b_{(j)} r_t$	$\delta_i = r_{ei}/(b_i \cdot r_t)$		$\Delta_i = LN(\delta_i)$	$(\Delta_i - \Delta)^2$	r_k	Test no.	r_{ti}
	[kN]		[kN]					[kN]					[kN]		[kN]
B3025_2	576.58	332439.88	646.91	418495.14	372993.93	12.20	1.12	839.01	0.77		-0.26	0.05	472.61	279.82	540.54
B3025_3	562.72	316649.30	637.99	407024.86	359004.37	13.38	1.13	818.84	0.78		-0.25	0.04	461.25	273.09	527.55
sum	5785.24	1791951.71	7396.75	2559156.88	2115007.13		39.29		27.00		-1.14	2.09			
mean value	214.27		273.95				$ b $	1.46	$ \delta $	1.00	Δ	-0.04			
standard deviation	143.03		140.47								s_{Δ}^2	0.08			
											V_{δ}^2	0.08			
											V_{δ}	0.29			

Table E.6 – (cont.) Statistical evaluation values.